

Dr. Michael Sarnthein, Prof. emer.
Institut für Geowissenschaften
University of Kiel
Olshausenstr. 40
24098 K i e l, Germany
<michael.sarnthein@ifg.uni-kiel.de>

13/26 March 2020

Dear Dr. Paul / Dear André,

Below you will find our point-to-point response to the critique raised by two referees, that were constructive and very helpful. Inversely, we regret not having an opportunity yet to include a response to the “extended comment” that Bard & Heaton recently announced to submit to C.P.

Following the advice of Ref. #1 and #2 we have carefully revised and streamlined many sections of our manuscript either following directly the comments of the two referees and/or taking care of their legitimate critique by broadening our empirical evidence and arguments in support of our strategy, interpretations, and conclusions, as outlined in detail below. For a better insight we submit a revised version of both our merged manuscript and the Supplementary Materials, where our recent changes are marked in RED.

We thank you for your great efforts to handle this manuscript that have provided us with the opportunity of manuscript revision, that is, for your help to improve on our manuscript and the quality of our working hypotheses. In turn, we hope and are confident that our manuscript may now satisfy the needs for publication in C.P.

Sincerely,

Michael Sarnthein and Co-authors

.....
In particular we follow your recommendation to consider the following issues:

(1) As a highlight in its own right, to present in a dedicated Results section the "shift to the U/Th modeled Suigetsu chronology" (review #1)/the "new findings regarding the age scale of the target atmospheric (Suigetsu) 14C record" (review #2). This would basically correspond to part 1 of the paper (or a hypothetical series of two papers) as proposed by referee #1.

We now upgrade Section 2 of our manuscript to a “Results section” that further stresses our new findings regarding the age scale of the atmospheric (Suigetsu) 14C reference record.

We thank for a very constructive and helpful review.

Response to specific comments

The authors have gone to great lengths to try to organize the paper in a way that helps to wrangle the many topics presented, but I think this paper would benefit from being split into two (companion) papers.

We truly pondered to follow this interesting proposal. For two reasons, however, we see problems in its realization: (1) To be published in a journal named CP any dry report on a new marine dating method also needs to display some major implications in the field of paleoceanography (as now given in Sections 3.1–3.3) to be attractive for CP readers. (2) A subdivision of this manuscript and subsequent review process of two companion papers would be that time consuming that our manuscript might gradually lose timeliness.

,,, the paper could be simplified to enhance accessibility by deleting some of the unnecessary words (hence, thus, moreover etc.).

We are aware that native English readers may suffer from our wording being somewhat biased by a foreign mother tongue, where connective adverbs appear helpful to generate a 'red thread' of reasoning, though perhaps somewhat colloquial. We went through the manuscript and deleted such words where we felt they did not add to the flow.

I think it is very important that they have used the introduction to address some of the criticism that has been raised with the plateau tuning method. However, I think this is an area that could be expanded a bit more to address a few more points such as other explanations for marine ^{14}C plateaus, including local shifts in air-sea gas exchange or upwelling, and if so, how can we account for these.

This is an important remark. We now broaden our Results section by a two-page long new subsection 2.1 named "*Suite of planktic ^{14}C plateaus: Means to separate global atmospheric from local oceanographic forcings*". Based on this resumé we try to meet explicitly potential weak points of the ^{14}C plateau tuning technique (points that actually had already been discussed in our previous publications since Sarnthein et al., 2007).

,,, it would be helpful to address why using the Suigetsu record for plateau tuning is preferred to Intcal. It seems that correlation directly to Intcal may be more conservative.

As now added to our text (end of Subsection 1.2), we prefer the Suigetsu record, since it is based on original primary atmospheric data and results in small-scale spatio-temporal changes of reservoir age, whereas IntCal is mixing and smoothing a broad array of different data sources with comparatively coarse time resolution, including carbonate-based marine and speleothem records. Combining these diverse records results in various unsolved problems and assumptions that finally resulted in major differences between the IntCal 13 and 20 records.

(If the paper is split into two separate papers), , , , figures S2 and S3 should be included in the main text of the synthesis paper. I found these figures particularly helpful for visualizing the geographic spacing of Plateau tuned records and their findings.

Figs. S2 and S3 are now included in the main text.

More detail included for sections 3.2-3.3 would also be welcome along with a picture/diagram of the Zoophycus burrow.

Following the suggestion of Ref.#2 we now have deleted the 'Zoophycos story' of former Subsection 3.3, in particular, since details are published in detail by Küssner et al., 2018.

Specific notes: Figure 1: It isn't clear in the figure caption what the difference is between the top and bottom panels.

In the figure caption we now specify that the top panel shows the record from 19–29 cal. ka and the bottom panel that from 10–20 cal. ka.

Figure 7: Please include the references for the records used in this figure.

As cited in the caption of (new number) Fig. 8, all references are given in Table 3 a-c.

It would also be helpful if I could match the data points in the x-y plot to the data points on the map, perhaps using symbols or colors.

All data now are labeled with the sea region wherefrom a sediment record was obtained.

Also, I'm not sure inclusion of the surface currents in panel b or in figure S3 are helpful, they make it a bit more difficult to see where the cores are located and to read the reservoir age differences - especially because the currents are available in figure S2.

We regard the arrows of surface currents (now Fig. 8) as important for a straight-forward comparison of different reservoir ages to different sea regions linked to different surface water currents in east-west direction, important to assess the limits of spatial extrapolation of reservoir ages.

Lines 601-603: Include the unit that corresponds to the foraminifera habitat depths.
Thanks: (m)

Section 3.4, Lines 656-663: Might be good to mention the interspecies 14C differences from Lindsay et al., 2015.
Thanks (ref. is now included).

Sections 3.5.1 and 3.5.2: In a few spots it would be helpful if the results from plateau tuning studies were more clearly emphasized. This would nicely highlight the important role that this technique has played in our understanding of LGM and HS1 MOC. This is done very nicely in section 3.5.3.

Thanks for an important suggestion. We now highlight some of the results of our new technique in the text, for instance, the formation of NADW during LGM, the HS-1 reversal of global MOC, and the reach of NPDW up to the South China Sea during HS-1.

Figure 9: This figure is a bit small and hard to see. The overlapping arrows can also be a bit confusing.

Indeed, opposed arrows for ocean currents are a bit confusing, since the east-west structures of the ocean are projected on a simple 2D meridional transect. Many arrows show opposed directions because of differential Coriolis forcing, especially so in the North Pacific and North Atlantic (as now specified in figure caption and text).

Inversely, we followed the suggestion and deleted the subchapter on Zoophycos burrows. Also, we carved out a clearer separation of the RESULTS from the DISCUSSION AND IMPLICATIONS section.

, , , the paper should re-focus on the advantages and disadvantages of the ^{14}C plateau tuning technique

-->and:

I however miss a more nuanced discussion of potential disadvantages of the technique and the underlying assumptions in places. For instance, when is the technique best applied? What are the underlying assumptions, and are there uncertainties associated with these assumptions? What resolution of the tuning record is required?

-->We follow this helpful suggestion and broaden our Discussion section by a one-page long recap of our previous publications in the new *Subsection 2.1* named "*Suite of planktic ^{14}C plateaus: Means to separate global atmospheric from local oceanographic forcings*". In this way we address potential weak points of the ^{14}C plateau tuning method. We explicitly reject the referee's term "disadvantages". Subsection 2.1 also recaps some technical needs (e.g., minimum sedimentation rates of 10 cm/ky of hemipelagic deposits, minimum ^{14}C dating resolution of ~100-150 yr, as published in Sarin et al., 2007).

This would mean to significantly shorten or remove the bioturbation section and/or repetitions of previous published work e.g. on the carbon cycle.

-->The bioturbation section has now been deleted. Other recaps are maintained, as necessary parts of this synthesis paper.

The paper appears too "crowded", as a number of aspects are discussed: , , , , so I can just recommend once more to streamline the paper and remove redundancy.

-->Our philosophy on the traits of a 'synthesis paper' has been outlined above.

, , , so it should be more clearly highlighted what are the new findings

-->Thanks for a good suggestion. These are 'new findings' since our last synthesis paper 2015:

- Switch to U/Th-based model ages for ^{14}C plateaus boundaries in 18/20 sediment cores,
- Inclusion of ^{14}C records from nine new sediment cores into our synthesis,
- Global data-model intercomparison for LGM and Heinrich-1 surface waters,
- Generation of global deep-water transects.

-->The listing is now incorporated in the text at the end of the Introduction and in Section 3.1.

--> Response to 'major points' and specific questions (page C3-C4-C5)

(1) Comparison with latest compilation of surface ocean reservoir age variations of Skinner et al. (2019) and Stern and Lisiecki (2013). The authors have synthesized surface ocean reservoir age records based on the ^{14}C plateau tuning technique that are interpreted for potential driving mechanisms and implications regarding changes in atmospheric CO_2 . However, it is not clear why other reservoir age estimates have been neglected for instance those based on paired tephra-foraminifera ^{14}C analyses (Skinner et al., 2015; Sikes and Guilderson, 2016) or those resulting from stratigraphic tie points (e.g., Waelbroeck et al., 2001). The fact that these estimates are low in resolution, should not diminish their veracity. I strongly recommend that plateau-tuned surface ocean reservoir age estimates are compared with results from other techniques, in particular Skinner et al. (2019).

-->Detailed comparisons to other methods for tie points to reconstruct past variations in surface ocean reservoir age were given in Subsection 1.2 of the Introduction, in particular in "paragraph 2", that we do not like to repeat in the discussion. Now, however, no problem to enrich the paragraph by additional remarks and references to authors listed by Ref.#2.

-->• To be fair, the paper of Skinner et al. (2019) appeared only two weeks after our manuscript submission. Of course, we appreciate to read that these authors -- like ourselves - - now fully recognize the concept of strongly variable spatiotemporal patterns of surface water reservoir age. We feel happy to include into our discussion the results of this single-core study, that also includes detailed (though in part somewhat debatable) alignment of paleoclimate records.

-->• We agree, each low-resolution age tie point *per se* has full veracity. Being spaced over 5-10 ky, however, these tie points cannot depict the actual dramatic short-term variability of res. ages now revealed for glacial-to-deglacial records by means of ¹⁴C plateau tuning, hence won't provide the accurate timing of paleoclimatic events needed for proper age correlation.

-->• Stern and Lisiecki (2013) indeed had been cited in "§2", but unfortunately deleted in a "streamlining action" prior to our manuscript submission. Based on pers. comm. with L. Lisiecki (Cambridge, 9-2018), however, we (M.S.) learned that the uncertainty range of their age assignments for the LGM amounts to ± 1.5 – ± 2.0 kyr, a range problematic for any proper correlation of multi-centennial-scale events in paleoceanography.

-->• Valuable age tie points and reservoir ages were derived from ¹⁴C ages of planktic foraminifera paired with ¹⁴C dated tephra layers as cited in "§2" of Subsection 1.2. Most of these tie points, however, are far too wide-spaced in peak glacial-to-early deglacial sediment records to meet the need to specify millennial-scale LGM-to-deglacial changes in ocean circulation, which may involve wrong age correlations. A rare deglacial suite of four tephra-based reservoir ages off Chile (Siani et al., 2013) was clearly reproduced, its variability, however, was much refined by ¹⁴C plateau-based reservoir ages (Küssner et al. (subm.)). Accordingly, we now broaden our discussion of tephra-based ages in "§2". --
Tephra-based results of Waelbroeck et al., 2001 and 2011 had been properly cited in our text.

2) Drivers of ¹⁴C plateaus: The causes of ¹⁴C plateaus are seemingly not well understand. The plateau tuning technique assumes that oceanic and atmospheric ¹⁴C records occur simultaneously, with identical duration and without any temporal offsets, and can unequivocally be identified in the often low(er)-resolution ocean records (see lines 216-217, or line 223). Do all of these conditions always apply?

-->and:

The authors outline that "air-sea gas exchange transfers the atmospheric ¹⁴C fluctuations into the surface ocean" (line 178-179), but it remains unclear how ocean degassing (of ¹⁴C-depleted CO₂), sea ice and/or wind changes might have affected this one-to-one assumption.

-->We now added the new *Subsection 2.1* on the "*Suite of planktic ¹⁴C plateaus: Means to separate global atmospheric etc.*" to avoid this misunderstanding: Indeed, only plateaus during which local oceanography did not change significantly will correlate and without much delay or change in duration in view of the rapid atmosphere-surface ocean exchange. Thus, the possibility of local ocean effects necessitates the use of a complete suite of ¹⁴C plateaus (and their estimates of reservoir age) to achieve a best-possible tuning of each sediment core. In

this case one or two disturbed plateaus (out of up to 19) won't hinder valuable results for the others and, at the same time, provide evidence of local short-term oceanographic changes. Finally, our records show that reservoir ages generally vary with climate changes on time scales of 1000 and more years in contrast to generally much shorter atmospheric plateaus.

In my view, this poses serious challenges to the ^{14}C plateau tuning technique

-->These changes are at least as challenging for IntCal where a close correspondence between ^{14}C levels in the surface ocean and in the atmosphere is assumed to justify the use of ocean carbonate records for the reconstruction of atmospheric ^{14}C . A comparison of IntCal13, IntCal20, and MarineCal20 for the time period older than 14 cal. ka shows how much work still needs to be done and how plateau tuning can contribute valuable data. In contrast to Marine Cal20 and IntCal where the timescale of the ocean record is largely based on climate wiggle matching beyond 14 cal ka our plateau tuning is based on atmospheric wiggle matching.

, , , , These potential caveats are not fully discussed.

-->To meet this objection we now added the new *Subsection 2.1*.

recommend to address potential disadvantages , , , ,

-->and:

the community has not really embraced this technique yet.

-->The tuning technique does not have "disadvantages", rather potential weak points that need consideration. At least the technique is better than most other ways to produce R data with high spatial and centennial-to-millennial-scale resolution.

It might also be beneficial to tone down some of the overselling language.

-->We agree, it never is good to oversell. E.g., we may replace "far" by "a bit" superior.

, , , the method works "wherever [sediment is] retrieved in the global ocean"

-->Indeed, we need to specify and say: "wherever cores with high hemipelagic sedimentation rates are sampled"

Furthermore, the authors seem to make clear that the assumption "[. . .] these plateau/jump structures are real and widely reproducible in marine sediment records" (lines 245-246) remains a speculation.

-->The objection that our assumption remains a speculation is simply not true. Our assumption is, as stated, general and common with those of IntCal. Each new sediment record that, after high-resolution dating, provides a suite of jumps and plateaus that can be correlated with the atmospheric master curve and our planktic records, confirms the practical applicability of the assumption. These findings are no "speculation" but apply to ^{14}C records of by now 20 (plus one more recent, yet unpublished) sediment cores from the global ocean.

-->Yet, we agree, "one always needs to be cautious". Therefore, we insert a "most likely" because signs of local disturbing influences must always be looked for.

Line 395-398 and line 477-483: The authors compare the timing of atmospheric ^{14}C plateaus with major changes in the atmospheric CO_2 record in order to emphasize

the impact of ocean outgassing on the atmospheric CO₂ record. Their arguments based on this comparison is inherently weak, as a number of ¹⁴C plateaus are not associated with a major shift in atmospheric CO₂. This should be acknowledged and discussed in more detail.

-->In (former) L. 501-507 we had already acknowledged the weakness of our understanding of several causal links that might have controlled the origin of atmospheric plateaus and jumps. We broached pulsed ocean outgassing as one amongst various other forcings and now terminated (present) Subsection 2.3 with the following sentence (now L. 531):

<<However, there is still little information on the origin of several other peak glacial ¹⁴C plateaus 17.5–29 cal. ka. The actual linkages of these plateaus to events in ocean MOC still remain to be uncovered.>>

What causes a temporal agreement between the two, why would the same process not operate at other times of ¹⁴C plateaus? What does this tell about the mechanisms driving atmospheric ¹⁴C plateaus, and in particular the assumed synchronicity between atmospheric and oceanic ¹⁴C changes?

-->Reformulated *Subsection 2.3* tries to make clear that due to the many factors involved it is often not possible to pinpoint a single dominant forcing of an atmospheric ¹⁴C plateau. In some plateaus we can recognize the role of ¹⁴C production (via ¹⁰Be), while three others coincide with changes in CO₂ level shown by ice cores that indicate ocean outgassing and oceanic changes. The difference in length between the plateaus and the outgassing spikes suggests that the spikes were part of longer lasting oceanic processes. Such processes may also be the origin of other plateaus without a recognizable CO₂ signal. We here demonstrate that in some cases the origin of atmospheric ¹⁴C changes can be identified. Increased use of plateau tuning may provide data that will allow identification of further determining factors.

-->Also, the fairly fast air-sea transfer of atmospheric ¹⁴C signals that leads to a quasi-synchronicity was displayed at (former) L. 102-110.

3) Data in preparation by Küssner et al. and Ausin et al. or pers. communication 2018 (Line 263): The authors have compiled all existing ¹⁴C datasets obtained via the plateau tuning technique (mostly by the group involving the first author), among which are also two new datasets (Küssner et al. and Ausin et al.). I find it hard to follow the findings obtained from these datasets, as crucial metadata is lacking for these cores.

-->Küssner and Ausin are coauthors of this manuscript. In the meantime, the manuscript of Küssner et al. that we regard as important brick of this synthesis, has now been submitted to P&P. Also, the datasets of Küssner et al. are stored at PANGAEA.de, saved by a password until acceptance of this manuscript for publication.

-->For the ¹⁴C record of Ausin et al., we may refer to their records and results as "unpubl. data". Unfortunately, the manuscript of Ausin et al., perhaps particularly interesting to Ref.#2, will be ready for submission only later this spring.

4) Revision of the Suigetsu age scale: I consider this an important contribution of the paper to the community but I do not find Fig. 5 very informative. What role do siderite layers play (they are not mentioned in the main text)? And how does the figure show age uncertainties, as indicated in lines 352-254. Further elaboration is needed here.

--> Our text is supplemented in Section 2.2 and the caption of Fig. 5.

Also in lines 385-388, what are the age uncertainties of the Mono Lake and Laschamp paleomagnetic excursions? They should be considered when assessing and comparing different age scales.

-->We now refer to data of Lascu et al. (2016).

Why was plateau 2b chosen as test case? How successful is the comparison for any other of 10+ 14C plateaus?

-->Unerring question! In contrast to optical varve counts reaching back to >40 cal. ka, the base of ¹⁴C Plateau 2b marks the oldest tie point captured by XRF-based varve counts. Marshall et al. (2012) showed that the difference between optical and XRF-based varve numbers is modest back to ~15 varve ka. Before, it has risen dramatically back to 17 ka.

I am surprised to see in Table 3 that some plateaus are combined to one long plateau, e.g. 6-7-8. What is the basis for that?

-->All right, we need to mention: Table 3 is grouping the ¹⁴C plateaus of some climate units that can be reproduced by the time slots employed for the model-based res. ages of Muglia et al. Within these slots, the plateau-based res. ages are largely constant.

5) Zoophycos burrows (lines 562-576): This whole section is somewhat dubious and not very clearly written. I wonder how useful it is for the review of the 14C plateau tuning technique. The authors seem to suggest that 14C plateaus in host sediments can flag 14C outliers as such, but it is not clear how initial 14C measurements a priori exclude bioturbated material for dating. This should be explained in detail. It is entirely unclear how Zoophycos burrows "help to corroborated changes in MOC and climate". In general, I think that the paper goes off another tangent here. The authors could consider removing this section in my view.

-->The section on Zoophycos burrows has now been removed. Küssner et al., 2018, already gave all details on the principles how to separate foram tests of Z. burrows from those of the ambient host sediment.

6) Model comparison with Muglia et al. (2018): The authors compare their datasets with the model output of Muglia et al. (2018). Given that other modelling studies exist that studied past ocean reservoir ages variations (e.g., Franke et al., 2008; Butzin et al., 2017), it is unclear why this particular study has been chosen. What characterizes the model run of Muglia et al. (2018), and in particular the modeled AMOC?

-->The choice of model data of Muglia et al. was linked to (1) the simple availability of pertinent recent model data and explanations, kindly provided by Juan Muglia as coauthor. (2) Butzin informed me, when testing his data as alternative dataset and preparing this manuscript in spring 2019, that his dataset (then not particularly successful by comparison with our dataset) was outdated and that his group was preparing a major improvement of their model concept. (3) With regard to res. ages modeled by Franke et al. (2008), we see major age differences found both for high-latitude and upwelling regions. -- In summary, we now introduce three different modelling studies at display and their availability for our test (new L.588-607).

How were the simulations forced and what were the LGM boundary conditions? A comparison between the data and model results would be better facilitated by global plots of surface ocean reservoir ages.

-->To avoid extending the manuscript up to 'textbook' length, we now just add a brief remark on the background of the model simulations.

Is the distribution realistic? It is impossible for the reader to follow statements such as "with estimates of 13 Sv appearing somewhat more consistent with our results." (line 714-715) without any further elaboration or figures.

-->We now give a short explanation for our choice of MOC strength for the LGM: Validation test by Muglia et al. (2018) through a model-data comparison of radiocarbon data compiled by Skinner et al. (2017).

Is the time interval used for comparison the same between 14C data and model data? How was the LGM 14C data obtained? Were several plateaus averaged?

-->Time intervals and average of several plateaus are given in Table 3, as listed in Fig. 8 caption. Both model-based and observed reservoir ages focus on the Late LGM, 21-18.7 cal. ka (14C plateaus no. 4-5).

Response to 'minor comments'

The following long and/or complicated sentences are hard to follow and should be revised: lines 135-144, line 228-232, lines 302-307, line 357-361, line 461-466, and lines 646-649.

-->We now tried to simplify the sentences demurred by the reviewer.

Line 110-113: should cite paper(s) on coral reservoir ages here.

-->Without expanding our manuscript up to 'textbook' length we now add a few refs in addition to Adkins & Boyle, 1997.

Line 116: "that finally turned out to be the most valuable tracer of oceanography" This is in the eye of the beholder, and should be rephrased to "became a valuable tracer for xxx/tool in oceanography"

-->As authors we may regard it legitimate to present these findings in our eye as beholders.

Line 118: "benthic carbonate particles" should be "benthic foraminifera", also "reflect" might be a better word for "sum" here. -- o.k.

Line 121: Remove "the 14C level of" -- o.k.

Line 135: "provided" instead of "given" -- o.k.

Line 143-144: unclear what iv refers to.

-->Item 'iv' is now reworded to a separate sentence that spells out the great need for a generally accepted high-precision atmospheric reference record , , ,

Line 173: jumps --> o.k.

Line 286: remove "developed a special computer program"
--> o.k.(paragraph was deleted)

Line 442: remove "ones of" --> o.k.

Line 450: consider "propagated error of calendar age uncertainty of a plateau boundary and the uncertainty in its determination"

-->We agree but do not follow the idea to include the fishy statement "*and the uncertainty in its determination*".

Line 484: Use (Skinner et al., 2010; Burke and Robinson, 2012) as Southern Ocean reference. --> o.k.

1 **MANUSCRIPT WITH AUTHORS' CHANGES ARE MARKED UP in RED**

2
3 Plateaus and jumps in the atmospheric radiocarbon record – Potential origin and value
4 as global age markers for glacial-to-deglacial paleoceanography, a synthesis
5

6
7 Michael Sarnthein¹⁾, Kevin Küssner²⁾, Pieter M. Grootes³⁾, Blanca Ausin⁴⁾⁸⁾, Timothy
8 Eglinton⁴⁾, Juan Muglia⁵⁾, Raimund Muscheler⁶⁾, Gordon Scholout⁷⁾
9

10
11 1) Institute of Geosciences, University of Kiel, Olshausenstr. 40, 24098 Kiel, Germany,
12 michael.sarnthein@ifg.uni-kiel.de, (corresponding author)

13 2) Alfred-Wegener-Institut Helmholtz-Zentrum für Polar- und Meeresforschung,
14 Department for Marine Geology, 27570 Bremerhaven, Germany, kevin.kuessner@awi.de

15 3) Institute of Ecosystem Research, University of Kiel, Olshausenstr. 40, 24098 Kiel,
16 Germany, pgrootes@ecology.uni-kiel.de

17 4) Geological Institute, ETH Zürich, Sonneggstr. 5, 8092 Zuerich, Switzerland,

18 5) **Centro para el Estudio de los Sistemas Marinos, CONICET, 2915 Boulevard Brown,**
19 **U9120ACD, Puerto Madryn, Argentina,** jmuglia@cenpat-conicet.gob.ar

20 6) Quaternary Sciences, Department of Geology Lund University, Sölvegatan 12, 22362
21 Lund, Sweden, raimund.muscheler@geol.lu.se

22 7) Climate Dynamics and Landscape Evolution, GFZ German Centre for Geosciences,
23 Telegrafenberg, 14473 Potsdam, Germany, SchloloutG@gmail.com

24 **8) Geology Department-University of Salamanca, 37008 Salamanca, Spain,**
25 **<ausin@usal.es>**

26
27
28
29
30

31 ABSTRACT

32 Changes in the geometry of ocean Meridional Overturning Circulation (MOC) are crucial in
33 controlling changes of climate and the carbon inventory of the atmosphere. However, the
34 **accurate** timing and global correlation of short-term glacial-to-deglacial changes of MOC in
35 different ocean basins still present a major challenge. A possible solution is offered by the fine
36 structure of jumps and plateaus in the record of radiocarbon (^{14}C) concentration of the
37 atmosphere and surface ocean that reflects changes in atmospheric ^{14}C production as well as in
38 the ^{14}C exchange between air and sea and within the ocean. Boundaries of atmospheric ^{14}C
39 plateaus in the ^{14}C record of Lake Suigetsu, now tied to Hulu U/Th model-ages instead of optical
40 varve counts, provide a stratigraphic 'rung ladder' of ~30 age tie points from 29 to 10 cal. ka for
41 correlation with and dating of planktic oceanic ^{14}C records. The age differences between
42 contemporary planktic and atmospheric ^{14}C plateaus give an estimate of the global distribution
43 of ^{14}C reservoir ages for surface waters of the Last Glacial Maximum (LGM) and deglacial
44 Heinrich Stadial 1 (HS-1), as shown by **about 20** planktic ^{14}C records. Clearly elevated and
45 variable reservoir ages mark both **upwelling regions and** high-latitude sites covered by sea ice
46 and/or meltwater. ^{14}C ventilation ages of LGM deep waters reveal opposed geometries of
47 Atlantic and Pacific MOC. Similar to today, Atlantic deep-water formation went along with an
48 estuarine inflow of old abyssal waters from the Southern Ocean up to the northern North Pacific
49 and an outflow of upper deep waters. Vice versa, ^{14}C ventilation ages suggest a reversed MOC
50 during early HS-1 and a ~1500 year-long flushing of the deep North Pacific up to the South
51 China Sea, when estuarine circulation geometry marked the North Atlantic, gradually starting
52 near 19 ka. Elevated ^{14}C ventilation ages of LGM deep waters reflect a major drawdown of
53 carbon from the atmosphere. Inversely, the subsequent, massive age drop and **related** change
54 in MOC induced **3 to 4** major events of carbon release to the atmosphere as recorded in
55 Antarctic ice cores. These new features of MOC and the carbon cycle **provide detailed evidence**
56 **in terms of space and time needed to test and refine ocean** models that, in part because of
57 insufficient spatial model resolution and reference data for testing the model results, still poorly
58 reproduce them.

59 1. INTRODUCTION

60 1.1 A variety of terms linked to the notion '14C age'

61 The ¹⁴C concentration in the troposphere is mainly determined by ¹⁴C production,
62 atmospheric mixing, moreover, air-sea gas exchange, and ocean circulation that vary
63 over time (e.g., Alves et al., 2018; Alveson et al., 2018). The ¹⁴C content of living
64 terrestrial plants is in equilibrium with the atmosphere via processes of photosynthesis
65 and respiration, and accordingly, the ¹⁴C of terrestrial plant remains in a sediment
66 section directly reflects the amount of radioactive decay, thus the time passed since the
67 plant's death, and the ¹⁴C composition of the atmosphere during the time of plant
68 growth.

69

70 Contrariwise, ¹⁴C values of marine and inland waters are cut off from cosmogenic ¹⁴C
71 production in the atmosphere, hence depend on the carbon transfer at the air-water
72 interface and the result of local transport and mixing of carbon in the water. For surface
73 waters, the air-sea transfer is relatively fast and effective involving a time span of ten
74 years and less (e.g., Nydal et al., 1998). Yet, vertical and horizontal water mixing results
75 in surface ocean ¹⁴C concentrations on average 5 % lower than those in the contempo-
76 raneous atmosphere, a difference expressed as 'Marine Reservoir Age' (or 'reservoir
77 effect' *sensu* Alves et al., 2018). These 'ages' reflect the local oceanography and are
78 highly variable through time. They may range from near zero up to values of more than
79 700 yr, in some regions up to 2500 yr, induced, for example, by old waters upwelled
80 from below (e.g., Stuiver and Braziunas, 1993; Grootes and Sarnthein, 2006; Sarnthein
81 et al., 2015). Apart from U/Th dated corals (many papers on their reservoir age since
82 Adkins and Boyle, 1997) the ¹⁴C age of planktic foraminifers is the most common tracer
83 of surface water ages in marine sediments, a rough estimate of the time passed since

84 sediment deposition. Initially, marine geologists were most interested in this 'simple' age
85 value. Soon, however, they were confronted with age inconsistencies that implied a
86 series of unknowns, in particular the ^{14}C 'reservoir age' that finally became a most
87 valuable tracer for oceanography.

88

89 In turn, ^{14}C records of benthic foraminifers in deep-sea sediments reflect the time of
90 radioactive decay since their deposition with the apparent 'ventilation age' of the deep
91 waters in which they lived. Ventilation age is primarily the time span from the moment
92 when carbon dissolved in the (later) deep waters lost contact with the atmosphere and
93 the somewhat reduced ^{14}C level of surface waters until the precipitation of benthic
94 carbonate. Details on the derivation of ventilation ages are provided in Cook and
95 Keigwin (2015) and Balmer and Sarnthein (2018). In addition, however, ventilation ages
96 depict hardly quantifiable lateral admixtures of older and/or younger water masses,
97 moreover, ^{14}C -enriched organic carbon supplied by the biological pump, thus are called
98 'apparent'. Today, the apparent transit times of carbon dissolved in the deep ocean
99 range from a few hundred up to ~ 1800 ^{14}C yr found in upper deep waters of the
100 northeastern North Pacific (Matsumoto, 2007).

101

102 Over the last decades, it turned out that both the reservoir ages of surface waters and
103 the ventilation ages of deep waters present robust and high-resolution tracers essential
104 for drawing quantitative conclusions on past ocean circulation geometries, marine
105 climate change, and the processes that drive both past ocean dynamics and carbon
106 budgets, given the ages rely on a number of robust age tie points. Obtaining such tie
107 points presents a problem, since any attempt to date a deep-sea sediment record by
108 means of ^{14}C encounters a number of intricacies of how to disentangle the effects of

109 global atmospheric ^{14}C variations due to past changes in cosmogenic ^{14}C production
110 and carbon cycle from (i) local depositional effects such as sediment hiatuses and
111 winnowing, differential bioturbational mixing depth, and sediment transport by deep
112 burrows, (ii) the effects of local atmosphere-ocean exchange and ocean mixing resulting
113 in reservoir and ventilation ages that change through time and space (e.g., Alves et al.
114 2018; Grootes and Sarnthein, 2006), and (iii) from the final target, quantitatively 'pure'
115 ^{14}C ages due to radioactive decay. These problems are exacerbated by the need for a
116 generally accepted high-precision atmospheric reference record for the period 14–50
117 cal. ka, beyond tree ring calibration,

118

119 By now, ^{14}C -based chronologies of deep-sea sediment records, used to constrain and
120 correlate the age of glacial-to-deglacial changes in ocean dynamics and climate on a
121 global scale, are often of unsatisfactory quality when they are based on (i) age tie points
122 spaced far too wide (e.g., using DO-events 1, 2, and 3 only and/or sporadic tephra
123 layers for the time span 30–14 cal ka), (ii) disregarding atmospheric ^{14}C plateaus, (iii)
124 the risky assumption of \pm constant planktic ^{14}C reservoir ages and other speculative
125 stratigraphic correlations/compilations, and (iv) ignoring small-scale major differences in
126 low-latitude reservoir age. Likewise, clear conclusions are precluded by an uncertainty
127 range of 3-4 kyr sometimes accepted for tie points during the glacial-to-deglacial period
128 (Stern and Lisiecki, 2013; Lisiecki and Stern, 2016), where significant global climate
129 oscillations occurred on decadal-to-centennial time scales as widely shown on the basis
130 of speleothem and ice core-based records (Steffensen et al., 2008; Svensson et al.,
131 2008; Wang et al., 2001).

132

133 Thus marine paleoclimate and paleoceanographic studies today focus on the continuing
134 quest for a high-resolution and global, hence necessarily atmospheric ^{14}C reference
135 record that is marked by abundant, narrow-standing tie points on the calibrated (cal.)
136 age scale. Such pertinent tie points are provided by a suite of reproducible ‘plateaus’
137 and ‘jumps’ that mark the atmospheric ^{14}C record (Figs. 1 and S1; Sarnthein et al., 2007
138 and 2015; Bronk Ramsey et al., 2012 and 2019; Schlolaut et al., 2018; Umling and
139 Thunnell, 2017), hence form the basis of this synthesis.

140

141 *1.2 Review of tie points used to fix calibrated and reservoir ages in marine ^{14}C records*

142

143 The tree ring-based calibration of ^{14}C ages provides a master record of decadal
144 changes in atmospheric ^{14}C concentrations back to ~14 cal. ka (Reimer et al., 2013 and
145 2020) with floating sections beyond (from ~12.5–14.5 cal. ka and around 29–31.5 and
146 43 cal. ka; Turney et al., 2010, 2017, Reimer et al., 2020). The evolution of Holocene
147 and late deglacial ^{14}C ages with time is not linear but reveals variations with numerous
148 distinct jumps (= rapid change) and (short) plateau-shaped (slow or no change or even
149 inversion) structures indicative of fluctuations in atmospheric ^{14}C concentration. Prior to
150 8500 cal. yr BP, various plateaus extend over 400–600 cal. yr and beyond (Fig. 2).

151 Given the quality of the tree ring calibration data, these fluctuations can be considered
152 real, suitable for global correlation (Sarnthein et al., 2007, 2015; Sarnthein and Werner,
153 2018). Air-sea gas exchange transfers the atmospheric ^{14}C fluctuations into the surface
154 ocean where they can provide high-resolution tie points to calibrate the marine ^{14}C
155 record and marine reservoir ages back to ~14 ka (via the so-called ^{14}C wiggle match
156 approach). In the near future, however, it is unlikely that a continuous tree ring-based
157 record will become available to trace such atmospheric ^{14}C variations further back, over

158 the period 14–29 cal. ka crucial for the understanding of last-glacial-to-interglacial
159 changes in climate. Hence various other, less perfect ^{14}C archives have been employed
160 for this period to tie past changes in atmospheric ^{14}C concentration/age to an ‘absolute’
161 or ‘calibrated’ (e.g., incremental **and/or based on speleothem carbonate**) age scale. **This**
162 **record can then be used** to constrain the widely unknown evolution of ^{14}C reservoir ages
163 of surface waters for various regions of the ocean.

164

165 Suites of ^{14}C ages of paired marine and terrestrial plant-borne samples, e.g. paired
166 planktic foraminifers and wood chunks, provide most effective but rarely realizable
167 absolute-age markers and reservoir ages of local ocean surface waters (Zhao and
168 Keigwin, 2018; Rafter et al., 2018; Schroeder et al., 2016; Broecker et al., 2004).
169 Likewise successful appears the alignment of ^{14}C -dated variations in downcore sea-
170 surface temperatures (SST) with changes in hydroclimate as recorded in age-calibrated
171 sedimentary leaf-wax hydrogen isotope (δD) records from ancient lakes (Muschitiello et
172 al., 2019), assumed to be **coeval**. Further tie points are derived from volcanic ash layers
173 (Waelbroeck et al., 2001; **Siani et al, 2013**; Davies et al., 2014; **Sikes and Guilderson,**
174 **2016**), paired U/Th- and ^{14}C -based coral ages (Adkins and Boyle, 1997; **Robinson et al.,**
175 **2005; Burke and Robinson, 2012; Chen et al., 2015**), and the (fairly fragmentary)
176 alignment of major tipping points in ^{14}C dated records of marine SST and planktic $\delta^{18}\text{O}$
177 to the incremental age scale of climate events dated in **polar** ice core records
178 (Waelbroeck et al., 2011). Such well-defined tie points, however, are wide-spaced in
179 peak glacial-to-early deglacial ice core records, **too wide for properly resolving a clear**
180 **picture of the spatiotemporal pattern of marine paleoclimate events**. Finally, various
181 data compilations tentatively rely on the use of multiple age correlations amongst
182 likewise poorly dated marine sediment records, an effort necessarily problematic.

183 Skinner et al. (2019) recently combined new and existing reservoir age estimates from
184 North Atlantic and Southern Ocean to show coherent but distinct regional reservoir age
185 trends in subpolar ocean regions, trends that indeed envelop the range of actual major
186 small-scale and short-term oscillations in reservoir age revealed by our technique of ^{14}C
187 plateau tuning for the subpolar South Pacific (Küssner et al., 2020 subm.).

188

189 In the absence of robust age tie points an increasing number of authors resort to ^{14}C
190 reservoir age simulations for various sea regions by ocean General Circulation Models
191 (GCM) (e.g. Butzin et al., 2017; Muglia et al., 2018) to quantify the potential difference
192 between marine and atmospheric ^{14}C dates during glacial-to-interglacial times.

193 Considering the complexity of the ocean MOC and the global carbon cycle it is not
194 surprising that the results of a comparison of a selection of robust empiric vs. simulated
195 ^{14}C reservoir ages are not that encouraging yet (as discussed further below).

196

197 Accepting a generally close link between ^{14}C concentrations in the troposphere and in
198 the surface ocean, the fine structure of planktic ^{14}C records with centennial-scale-
199 resolution provides far superior (though costly) evidence, similar to that of tree rings, to
200 furnish a series of age tie points with semi-millennial-scale time resolution for a global
201 correlation of glacial-to-deglacial marine sediment sections. These suites of tie
202 structures can link the marine sediment records to a reference suite of narrow-standing
203 jumps and boundaries of the apparent plateaus robustly identified in the atmospheric
204 ^{14}C record of Lake Suigetsu, the only long, continuous record based on terrestrial plant
205 remains (Bronk Ramsey et al., 2012, 2019) provided that common ^{14}C variations are
206 robustly identified in both atmospheric and marine records. Prior to the reach of the tree
207 ring-based age scale ~ 14 cal. ka, the absolute age of these atmospheric ^{14}C structures

208 can be either calibrated by incremental (microscopy- or XRF-based) varve counts
209 (Schlolut et al., 2018; Marshall et al., 2012) or by a series of paired U/Th- and ^{14}C -
210 based model ages correlated from the Hulu Cave speleothem record (Bronk Ramsey,
211 2012 and 2019; Southon et al., 2012; Cheng et al., 2018). The difference between these
212 calibrations (Fig. 3) is discussed below. The difference, however, is of little importance
213 neither for the tuning of planktic to corresponding atmospheric ^{14}C plateaus nor for the
214 derivation of planktic reservoir ages that present the highly variable offset of the ^{14}C age
215 of a planktic plateau from that of the correlated atmospheric plateau. The offset is
216 deduced by subtracting the average ^{14}C age of an atmospheric ^{14}C plateau from that of
217 the correlated planktic ^{14}C plateau, independent of any absolute age value assigned. s
218

219 A basic philosophical controversy exists whether the apparent jump and plateau
220 structures in the Suigetsu and planktic ^{14}C records reflect real ^{14}C fluctuations or
221 statistical noise. In the 'null hypothesis' the ^{14}C values shaping plateaus of the
222 calibration curve are regarded as result of mere statistical scatter. Thus, the record of
223 atmospheric ^{14}C ages against time would form a simple continuous rise resulting from
224 radioactive decay and the advance of time, such as suggested by a fairly straight
225 progression of the highly resolved deglacial Hulu Cave ^{14}C record plotted vs. U/Th ages
226 (Southon et al., 2012; Cheng et al., 2018).

227

228 This null hypothesis is contradicted by the 'master record' of tree ring data (Fig. 2;
229 Reimer et al., 2013 /2020). Unequivocally it shows fluctuations in atmospheric ^{14}C
230 concentration on the order of 2–3 % over the last 10 kyr (Stuiver and Braziunas, 1993)
231 and even larger back to ~14 ka (Reimer et al., 2013, 2020). Though not resolved in
232 speleothem data these plateau/jump structures most likely are real and widely

233 reproducible in marine sediment records. Under glacial and deglacial low-CO₂
234 conditions beyond 14 ka, when climate and ocean dynamics were less constant than
235 during the Holocene, atmospheric ¹⁴C fluctuations were, most likely, even stronger than
236 those reported by Stuiver and Braziunas and ¹⁴C plateaus and jumps accordingly larger.
237 Also, plateau-jump structures are becoming increasingly evident in the evolving
238 atmospheric calibration record (Reimer et al., 2020).

239

240 Thus, the age-defined plateaus and jumps in the Suigetsu atmospheric ¹⁴C calibration
241 curve may most likely be regarded as a suite of 'real' structures, extending the tree ring
242 record for Holocene and B/A-to-Early Holocene times (Fig. 2) into early deglacial and
243 LGM times. In part the plateau/jump structures may be linked to changes in cosmogenic
244 ¹⁴C production, as possibly shown in the ¹⁰Be record (Fig. 4; based on data of Adolphi
245 et al., 2018), and – presumably more dominant – to short-term changes in ocean mixing
246 and the carbon exchange between ocean and atmosphere. The exchange is crucial,
247 since the carbon reservoir of the ocean contains up to 60 (preindustrial) atmospheric
248 carbon units (Berger and Keir, 1984). The apparent contradiction with the smooth Hulu
249 Cave ¹⁴C record (Southon et al., 2012; Cheng et al., 2018) may possibly be explained
250 by the Hulu Cave speleothem precipitation system acting as a low-pass filter for
251 fluctuating atmospheric ¹⁴C concentrations (statistical tests of Bronk Ramsey et al.,
252 pers. comm. 2018) and, to a very limited degree, by the obvious scatter in the Suigetsu
253 data. That scatter, however, appears insufficient to feign plateaus in view of the
254 evidence based on tree ring-based plateaus (Fig. 2). The filter for Hulu data possibly led
255 to a loss especially of short-lived structures in the preserved atmospheric ¹⁴C record,
256 though some remainders were preserved in the ¹⁴C records of Hulu Cave (Fig. 1). So

257 we rather trust in the amplitude of Suigetsu ^{14}C structures, but trust in the timing of
258 Hulu Cave data as discussed below.
259
260 Like a ‘rung ladder’ the age-calibrated suite of ^{14}C plateau boundaries and jumps is
261 suited for tracing the calibrated age of numerous plateau boundaries in glacial-to-
262 deglacial marine ^{14}C records likewise densely sampled, **even when some rungs have**
263 **been destroyed by local influences on gas exchange or ocean mixing. Also,** one may
264 record the **average** offset of planktic ^{14}C ages from paired atmospheric ^{14}C ages, **i.e.** the
265 planktic reservoir age, for each single ^{14}C plateau (Sarnthein et al., 2007, 2015). **We**
266 **prefer the Suigetsu record to IntCal, since it is based on original primary atmospheric**
267 **data and results in small-scale spatio-temporal changes of reservoir age, whereas**
268 **IntCal is mixing and smoothing a broad array of different data sources with comparativ-**
269 **ely coarse age resolution, including carbonate-based speleothem and marine records.**
270 For the first time, this suite of tie points may facilitate a precise temporal correlation of
271 all sorts of changes in surface and deep-water composition on a global scale, crucial for
272 a better understanding of past changes in ocean and climate dynamics.

273

274 *1.3 Items discussed in this synthesis*

275 **The Results Section is summarizing**

276 **(1) Some means to separate atmospheric and oceanic forcings, that overlap in**
277 **controlling the structure of a planktic ^{14}C plateau.**

278

279 **(2) Choice of a U/Th-based reference time scale** (Bronk Ramsey et al. 2012; Cheng et
280 al., 2018) **instead of the earlier varve-counted version** (Schlollaut et al., 2018) **to date the**

281 short-term structures in the global atmospheric ^{14}C record of Lake Suigetsu (Sarnthein
282 et al., 2015).

283

284 (3) An extension of the suite of age tie points from 23 back to 29 cal. ka, values crucial
285 for an accurate global correlation of ocean events over the period 10–29 cal. ka.

286 Supplement Text no. 1 is discussing uncertainties in age-calibrated ^{14}C plateau
287 boundaries and jumps of our redefined Suigetsu record (Bronk-Ramsey et al., 2012,
288 2019; Sarnthein et al., 2015) and their correlatives in ocean sediment cores.

289

290 (4) Attempts to explore the potential linkages of atmospheric ^{14}C plateaus and jumps to
291 cosmogenic ^{14}C production and/or ocean dynamics.

292

293 The Discussion and Implications section includes the following topics:

294 (1) A global summary of our records of marine ^{14}C reservoir ages (Sarnthein et al. 2015)
295 now amended by nine plateau-tuned records from the Southern Hemisphere (Balmer et
296 al., 2016 and 2018; Küssner et al., 2018, and *subm.*) and northeast Atlantic (Ausin et
297 al., *unpubl.*). In total, 18 (LGM) / 19 (HS-1) plus 3 wood chunk-based records (Broecker
298 et al., 2004; Zhao et al., 2018) now depict the spatio-temporal variability of past ^{14}C
299 reservoir ages of surface waters in different ocean regions.

300

301 (2) Comparison of our plateau-based reservoir ages with independent LGM estimates of
302 surface water ^{14}C reservoir ages simulated by the GCM of Muglia et al. (2018).

303 Differences between the results may help to constrain potential caveats in the boundary
304 conditions and fine structure of model simulations. This section includes a discussion of

305 some habitat- and season-specific ^{14}C reservoir ages characteristic of different planktic

306 foraminifera species, that monitor past changes in the local geometry of surface ocean
307 dynamics (Sarnthein and Werner, 2018).

308

309 (3) A global overview of ^{14}C reservoir and ventilation ages of surface and deep waters
310 that form a robust tracer of circulation geometries and the dissolved inorganic carbon
311 (DIC) in different basins of the ocean (Sarnthein et al., 2013) and provide crucial
312 insights into the origin of past changes in the global carbon cycle from glacial to
313 interglacial times, an important correlative to model simulations.

314

315 In this way we highlight the important role the technique of ^{14}C plateau tuning and its
316 revised cal. time scale are playing for global data-model intercomparison and a new
317 understanding of Ocean MOC during the LGM and its reversal during HS-1.

318

319 2. RESULTS – AGE TIE POINTS BASED ON ^{14}C PLATEAU BOUNDARIES

320

321 2.1 *Suite of planktic ^{14}C plateaus: Means to separate global atmospheric from local 322 oceanographic forcings*

323 The basic assumption of the ^{14}C plateau tuning technique is that the fine structure of
324 fluctuations of the global atmospheric ^{14}C concentration record can also be found in the
325 surface ocean. In a plot of ^{14}C age versus calendar age such fluctuations lead to a
326 pattern of plateaus/jumps that correspond to decreases/increases in ^{14}C concentration.
327 Here we refer to the derivation and interpretation of planktic ^{14}C plateaus, assuming a
328 global atmospheric origin with local oceanographic forcings. The series of planktic ^{14}C
329 plateaus and jumps are derived in cores with average sedimentation rates of >10 cm/ky
330 and dating resolution of <100 - 150 yr. The plateau-specific structures in a sediment age-

331 depth record form a well-defined suite for which absolute age and reservoir age are
332 derived by means of a strict alignment to the reference suite of global atmospheric ^{14}C
333 plateaus as a whole. Initially age tie points of marine $\delta^{18}\text{O}$ records showing (orbital)
334 isotope stages #1-3 serve as stratigraphic guideline for the alignment. Planktic reservoir
335 ages and their short-term changes are derived from the difference in average ^{14}C age
336 between atmosphere and surface waters in subsequent plateaus. To stick as close as
337 possible to the modern range of reservoir ages (Stuiver and Braziunas, 1993), tuned
338 reservoir ages are kept at a minimum unless stringent evidence requires otherwise.

339

340 A close correspondence between ^{14}C concentrations in atmosphere and surface ocean
341 is expected based on rapid gas exchange. In several cases, however, the specific
342 structure and relative length of a planktic ^{14}C plateau may deviate from those of the
343 pertinent plateau observed within the suite of atmospheric plateaus, thus indicate local
344 intra-plateau changes of reservoir age. Though less frequent, these changes may
345 indeed amputate and/or deform a plateau, then as result of variations in local ocean
346 atmosphere exchange and oceanic mixing. Two saspects help to sort out short-term
347 climate-driven intra- and inter-plateau changes in ^{14}C reservoir age: (i) The evaluation of
348 the structure and reservoir age of an individual plateau is strictly including the age
349 estimates deduced for the complete suite of plateaus. (ii) Our experience shows that
350 deglacial climate regimes in control of changes in surface ocean dynamics generally
351 occurred on (multi-) millennial time scales (e.g., YD, B/A, HS-1), whereas atmospheric
352 ^{14}C plateaus hardly lasted longer than a few hundred up to 1100 yr (Fig. 1 and S1).
353 Abrupt changes in gas exchange or ocean mixing usually affect one or only a few
354 plateaus of the suite. -- Absolute age estimates within a plateau are derived by linear
355 interpolation between the age of the base and top of an undisturbed plateau assuming

356 constant sedimentation rates. The potential impact of short-term sedimentation pulses
357 on ^{14}C plateau formation has largely been discarded by Balmer and Sarnthein (2016).

358

359 *2.2 Suigetsu atmospheric ^{14}C record: Shift to a chronology based on U/Th model ages*

360 Originally, we **have** based the chronology of ^{14}C plateau boundaries in the Suigetsu
361 record (Sarnthein et al., 2015) on a scheme of varve counts by means of light
362 microscopy of thin sections (Bronk Ramsey et al., 2012; Schlolaut et al., 2018). Over
363 the crucial sediment sections of the Last Glacial Maximum (LGM) and deglacial Heinrich
364 Stadial 1 (HS-1), however, the degree of varve quality / perceptibility in the Suigetsu
365 profile is highly variable (Fig. 5). In parallel, varve-based age estimates have been
366 derived from counting various elemental peaks in μXRF data, interpreted as seasonal
367 signals (Marshall et al., 2012). **The** results obtained from these two independent
368 counting methods and their interpolations widely support each other. The **optical** counts
369 ultimately formed the backbone of a high-resolution chronology obtained by tying the
370 Suigetsu ^{14}C record to the U/Th based time scale of the Hulu cave ^{14}C record (Bronk
371 Ramsey et al., 2012). **Recently, Schlolaut et al. (2018) amended the scheme of varve**
372 **counts. Accordingly,** Suigetsu varve preservation (*i.e.*, **the number of siderite layers per**
373 **20 cm thick sediment section**) is fairly high **prior to ~32 ky BP and** over late glacial
374 Termination I **but** fairly poor over large parts of the LGM and HS-1, from ~15 - 32 cal ka
375 (17.3-28.5 m c.d. in Fig. 5). **Here only** less than 20-40 % of the annual layers expected
376 from interpolation between clearly varved sections are distinguished by microscopy.
377 **Varve counts that** use μXRF data (Marshall et al., 2012) can distinguish subtle changes
378 in seasonal element variations, **that** are not distinguishable in thin section microscopy,
379 hence result in higher varve numbers **especially** during early deglacial-to-peak glacial
380 times. Yet, some subtle variations are difficult to distinguish from noise, **which adds**

381 uncertainty to the μ XRF-based counts. Thus, the results from either counting method
382 are subject to uncertainties that rise with increased varve age (Fig. 5).
383

384 Bronk Ramsey et al. (2012) established a time scale based on ^{14}C wiggle matching to
385 U/Th dated ^{14}C records of the Hulu Cave and Bahama speleothems. In part, this calibr-
386 ated (cal.) age scale was based on Suigetsu varve counts, in part on the prerequisite of
387 the best-possible fit of a pattern of low-frequency changes in ^{14}C concentration obtained
388 from Suigetsu and Hulu Cave. The two ^{14}C records were fitted within the uncertainty
389 envelope of the Hulu 'Old / Dead Carbon Fraction' (OCF/DCF) of ^{14}C concentration. The
390 uncertainty of this model is debatable while the character of the Hulu DCF and thus, its
391 uncertainty back in time is still incompletely understood. We surmise that the U/Th-
392 based age model of Suigetsu may suffer from the wiggle matching of atmospheric ^{14}C
393 ages of Lake Suigetsu with ^{14}C ages of the Hulu Cave (Southon et al., 2012) in case of
394 major short-term changes in atmospheric ^{14}C concentration due to a memory effect of
395 soil organic carbon in carbonate-free regions of the cave overburden. The speleothem-
396 carbonate-based Hulu ages may have been influenced far more strongly by short-term
397 changes in the local DCF than assumed, as suggested by major variations in a paired
398 $\delta^{13}\text{C}$ record, that reach up to 5 ‰, mostly subsequent to short-term changes in past
399 monsoon climate (Kong et al., 2005). The uncertainty regarding the assumption of a
400 constant OCF/DCF (Southon et al. 2012; Cheng et al., 2018) may hamper the age
401 model correlation between Hulu and Suigetsu records and the Suigetsu chronology.
402

403 To test and optimize the age calibration we compared the results of the two timescales
404 independently deduced from varve counts with those of the U/Th-based model age
405 scale using as test case the base of ^{14}C Plateau 2b, the oldest tie point constrained by

406 μ XRF-based counts. In contrast to 16.4 cal. ka, supposed by optical varve counts,
407 μ XRF-based counts suggest an age of ~16.9 cal. ka (Marshall et al., 2012; Schlolaut et
408 al., 2018), which matches closely the U/Th-based estimate of 16.93 ka. This is a robust
409 argument for the use of the U/Th-based Suigetsu time scale as 'best possible' age scale
410 to calibrate the age of thirty ^{14}C plateau boundaries (Fig. 1). In its older part, the U/Th
411 model time scale is further corroborated by a decent match of short-term increases in
412 ^{14}C concentration with the low geomagnetic intensity of the Mono Lake and Laschamp
413 events at ~34 and 41.1 ± 0.35 ka (Lascau et al., 2016), independently dated by other
414 methods. The new U/Th-based model ages of ^{14}C plateau boundaries are significantly
415 higher than our earlier microscopy-based varve ages over HS-1 and LGM, a difference
416 increasing from ~200 yr near 15.3 cal. ka to ~530 near 17 ka and 2000 yr near ~29 ka
417 (Fig. 3).

418

419 Note, any readjustment of the calendar age of a ^{14}C plateau boundary does not entail
420 any change in ^{14}C reservoir ages afore deduced for surface waters by means of the
421 plateau technique (Sarnthein et al., 2007, 2015), since each reservoir age presents the
422 simple difference in average ^{14}C age for one and the same ^{14}C plateau likewise defined
423 in both the Suigetsu atmospheric and planktic ^{14}C records of marine surface waters,
424 independent of the precise position of this plateau on the calendar age scale.

425

426 In view of the recent revision of time scales (Schlolaut et al., 2018; Bronk Ramsey et al.,
427 2019) we now extended our plateau tuning and now also defined the boundaries and
428 age ranges of ^{14}C plateaus and jumps for the interval ~23–29 cal. ka, which results in a
429 total of ~30 atmospheric age tie points for the time span 10.5–29 cal. ka (Fig. 1;
430 summary in Table 1; following the rules of Sarnthein et al., 2007 and 2015). Prior to 25

431 cal. ka, the definition of ^{14}C plateaus somewhat suffered from an enhanced scatter of
432 raw ^{14}C values of Suigetsu. -- In addition to visual inspection, the ^{14}C jumps and
433 plateaus were also defined with higher statistical objectivity by means of the first-
434 derivative of all trends in the ^{14}C age-to-calendar age relationship (or –core depth
435 relationship, respectively) by using a running kernel window (Sarnthein et al., 2015).

436

437 *2.3 Linkages of short-term structures in the atmospheric ^{14}C record to changes in*
438 *cosmogenic ^{14}C production versus changes in ocean dynamics*

439

440 Potential sources of variability in the atmospheric ^{14}C record have first been discussed
441 by Stuiver and coworkers in the context of Holocene fluctuations deduced from tree ring
442 data (e.g., Stuiver and Braziunas 1993). -- Similar to changes in ^{14}C , variations in ^{10}Be
443 deposition in ice cores reflect past changes in ^{10}Be production as a result of changes in
444 solar activity and the strength of the Earth's magnetic field (Adolphi et al., 2018).
445 Correspondingly, the changes in ^{10}Be also reflect past changes in the cosmogenic
446 production of ^{14}C . If we accept to omit assumptions on the modulation of past ^{14}C
447 concentrations by changes in the global carbon cycle we can calculate the atmospheric
448 ^{14}C changes over last glacial-to-deglacial times with ^{10}Be and a carbon cycle model and
449 convert them into ^{14}C ages (Fig. 4). This neglects, however, the influence of climate and
450 carbon cycle changes over this period that necessarily modified the ^{10}Be -based ^{14}C
451 record if included correctly into the modeling. Between 10 and 13.5 cal. ka, the ^{10}Be -
452 modeled ^{14}C record displays a number of plateau structures that appear to match the
453 Suigetsu-based atmospheric ^{14}C plateaus. Between 15 and 29 cal. ka, however, ^{10}Be -
454 based ^{14}C plateaus are far more rare and/or less pronounced than those in the Suigetsu
455 record. Most modelled plateaus are far shorter than those displayed in the suite of

456 atmospheric ^{14}C plateaus of Lake Suigetsu (e.g., plateaus near to the top 2a, 2b, top 5a,
457 and 9), **except for a distinct equivalent of plateau no. 6a**. On the whole, the **modelled**
458 **and observed** structures show little coherence. **This may** indicate that any direct
459 relationship between variations in cosmogenic ^{14}C production and the Suigetsu plateau
460 record is **largely** obscured by the carbon cycle, uncorrected climate effects on the ^{10}Be
461 deposition, and/or noise in the ^{14}C data. **Also, a relatively high uncertainty of the**
462 **measured ^{10}Be concentrations in the ice, (in many cases ~7%; Raisbeck et al., 2017),**
463 **and a lower sample resolution in the order of 50 to 200 yr may contribute to the**
464 **smoothed character of the ^{10}Be record in Fig. 4.**

465

466 **On the other hand, the 'new' U/Th-based cal. ages of plateau boundaries may suggest**
467 **some** reasonable stratigraphic correlations **between peak glacial and deglacial change in**
468 **atmospheric CO_2 and ^{14}C plateaus with** millennial-scale events in paleoceanography (Fig.
469 6, Table 2): **The** suite of deglacial ^{14}C plateaus **no. 2a, 1, and Top YD** indeed displays a
470 temporal match with **three brief but** major deglacial **jumps** in ocean degassing of CO_2
471 **documented in the WDC ice core** (Marcott et al., 2014). **The two records have been**
472 independently dated by means of annual-layer counts **in ice cores and U/Th ages of**
473 stalagmites. **The match suggests that these atmospheric ^{14}C plateaus may largely result**
474 from changes in air-sea gas exchange, and in turn, from changes in ocean **dynamics**.

475

476 **In particular,** these events may **have been** linked to a variety of fast changes such as **in**
477 sea ice cover in the Southern Ocean and/or in the salinity and buoyancy of **high-latitude**
478 surface waters (**Skinner et al., 2010; Burke and Robinson, 2012**). These factors control
479 upwelling and meridional overturning of deep waters, **in particular found** in the Southern
480 Ocean (Chen et al., 2015) and/or North Pacific (Rae et al. 2014, Gebhardt et al., 2008).

481 Such events of changes in MOC geometry and intensity may be responsible for ocean
482 degassing and the ^{14}C plateaus.
483
484 In an extreme case, ventilation ages in the Southern Ocean near New Zealand (SO213-
485 76 in Fig. S2; Küssner et al., 2020 subm.) have short-term dropped around 18 cal. ka
486 from 4000 to 1000 yr (Fig. 4c). Over this time, the ^{14}C level of the atmosphere was
487 constant at 1.4 FMC (Fraction of Modern Carbon). Hence a ventilation age of 4000 yr is
488 equal to ~60 % of the contemporaneous level of past atmosphere 1.4 FMC, at that time
489 leading to $1.4 \times 0.6 = 0.84$ FMC. In turn, the ventilation age of 1000 yr was equal to 88
490 % of past atmosphere FMC. This implies an increase of local deep ocean ^{14}C to $1.4 \times$
491 $0.88 = 1.232$ FMC at this site. The concentration difference of ~0.4 FMC means a major
492 ^{14}C shift in DIC at that very MOC key region of the deep Southern Ocean (Rae and
493 Broecker, 2018) over 200 yr. This enhanced mixing of the Southern Ocean and a
494 similar, slightly later mixing event in the North Pacific (MD02-2489; Fig. S2d) may have
495 triggered – with phase lag – two trends in parallel, (1) a rise in atmospheric CO_2 , in part
496 abrupt (*sensu* Chen et al., 2015; Menviel et al., 2018), and (2) a gradual enrichment in
497 ^{14}C depleted atmospheric carbon, reflected as ^{14}C plateau.
498
499 Plateau 6a matches a ^{14}C plateau deduced from atmospheric ^{10}Be concentrations, thus
500 suggests changes in ^{14}C production. Other changes in atmospheric ^{14}C (plateaus 4 and
501 8) match short-term North Atlantic warmings during peak glacial and earliest deglacial
502 times, similar to that at the end of HS-1 and during plateau 'YD', hence may reflect
503 minor changes in ocean circulation and ocean-atmosphere exchange without major
504 degassing of old ^{14}C depleted deep waters in the North Atlantic (Table 2, Fig. S2a).
505 There is still little information, however, on the origin of several other peak glacial ^{14}C

506 plateaus 17.5–29 cal. ka. The **actual linkages** of these plateaus to events in ocean MOC
507 still remain to be uncovered.

508

509 3. DISCUSSION **and IMPLICATIONS**

510 *3.1 ¹⁴C plateau boundaries – A suite of narrow-spaced age tie points to **rate** short-term*
511 *changes in marine sediment budgets, chemical inventories, and climate 29–10 cal. ka*

512

513 In continuation of previous efforts (Sarnthein et al., 2007 and 2015) the tuning of high-
514 resolution **planktic** ¹⁴C records of ocean sediment cores to the new age-calibrated
515 atmospheric ¹⁴C plateau boundaries now makes it possible to establish a ‘rung ladder’
516 of ~30 age tie points covering the time span 29 – 10.5 cal. ka. **These global** tie points
517 **have** a time resolution of several hundred to thousand years, **and can be** used to
518 constrain the chronology and potential leads and lags of **events** that occurred during
519 peak glacial and deglacial times (Fig. 1). The locations of the 18 (20) cores are shown in
520 Fig. 7. The time histories of the benthic and planktic reservoir ages are summarized in
521 Figs. 8 and S2 and the information these provide is discussed below.

522

523 **Six prominent** examples showing the power and value of additional information obtained
524 by means of the ¹⁴C plateau-tuning method **are:**

525 (i) Signals of the onset of northern hemisphere deglaciation can now be distinguished
526 in detail from the subsequent beginning of deglaciation in the southern hemisphere **and**
527 **reveal that changes began ~1400 yr earlier in the north** (Fig. S2) (Kawamura et al.,
528 2007; Küssner et al., 2020 **subm.**; **in harmony with Schmittner and Lund, 2015**).

529 (ii) **In southeast Pacific surface waters** the end of the Antarctic Cold Reversal (ACR;
530 **WDC Project Members, 2013**) was found precisely coeval with the onset of the Younger

531 Dryas cold spell (Küssner et al., 2020 *subm.*), a finding important to further constrain the
532 details of ‘bipolar see-saw’ (Stocker and Johnsen, 2003).

533 (iii) Signals of deep-water formation in the subpolar North Pacific can now be
534 separated from signals originating in the North Atlantic (Rae et al. 2014; Sarnthein et al.,
535 2013). In this way we now can specify and tie major short-lasting reversals in Atlantic
536 and Pacific MOC on a global scale.

537 (iv) Signals of deglacial meltwater advection can now be distinguished from short-
538 term interstadial warmings in the northern subtropical Atlantic, which helps to locate
539 meltwater outbreaks far beyond the well-known Heinrich belt of ice-rafted debris
540 (Balmer and Sarnthein, 2018).

541 (v) As outlined above, the timing of marine ^{14}C plateaus can now be compared in
542 detail with that of deglacial events of *climate and* the atmospheric CO_2 rise independ-
543 ently dated by means of ice core-based stratigraphy (Table 2; Fig. 6). These linkages
544 *offer a tool to explore details* of deglacial changes in deep-ocean MOC once the suite of
545 ^{14}C plateaus has been properly tuned at any particular ocean site.

546 (vi) *The* refined scale of age tie points *also* reveals unexpected details for changes in
547 the sea ice cover of high latitudes as reflected by anomalously high ^{14}C reservoir ages
548 (e.g. north of Iceland and near to the Azores Islands) and for the evolution of Asian
549 summer monsoon in the northern and southern hemisphere as reflected by periods of
550 reduced sea surface salinity (e.g., Sarnthein et al., 2015; Balmer et al., 2018).

551 Finally, the plateau-based high-resolution chronology has led to *the* detection of
552 numerous millennial-scale hiatuses (e.g., Sarnthein et al., 2015; Balmer et al., 2016;
553 Küssner et al., 2020 *subm.*) *overlooked* by conventional, e.g., *AnalySerie*-based
554 methods (Paillard et al. 1996) of stratigraphic correlation (Fig. *S2*). In turn, the hiatuses
555 give intriguing new insights into past changes of bottom current dynamics linked to

556 different millennial-scale geometries of overturning circulation and climate change such
557 as in the South China Sea (Sarnthein et al., 2013 and 2015), in the South Atlantic
558 (Balmer et al. 2016) and southern South Pacific (Ronge et al., 2019).

559

560 Clearly, the new atmospheric ^{14}C 'rung ladder' of closely-spaced chronostratigraphic tie
561 points has evolved to a valuable tool to uncover functional chains in paleoceanography,
562 that actually have controlled events of climate change over glacial-to-deglacial times.

563

564 *3.2 Observed vs. model-based ^{14}C reservoir ages acting as tracer of past changes in*
565 *surface ocean dynamics and as incentive for model refinements (Fig. 8)*

566

567 The atmospheric ^{14}C plateaus of Suigetsu provide a suite of up to 18 reference plateaus
568 over the time span 10 – 29 cal. ka (Fig. 1). Tuning ^{14}C plateau boundaries in ^{14}C -dated
569 marine sediment sections to the Suigetsu ^{14}C record allows us to establish a suite of
570 highly resolved and robust age tie points on short and long time scales, wherever cores
571 with high hemipelagic sedimentation rates are sampled in the global ocean (Fig. 7). In
572 addition, and likewise intriguing, the difference between the average ^{14}C age of an
573 atmospheric ^{14}C plateau and that of a coeval ^{14}C plateau yields a suite of changing ^{14}C
574 reservoir ages over time, a prime tracer of past oceanography of local surface waters
575 and data set crucial to deduce past apparent deep-water ventilation ages (e.g., Muglia
576 et al., 2018; Cook and Keigwin, 2015; Balmer and Sarnthein, 2018).

577

578 To better constrain the water depth of past reservoir ages we dated monospecific
579 planktic foraminifera (Sarnthein et al., 2007); in low-to-mid latitudes on *G. bulloides*, *G.*
580 *ruber*, or *G. sacculifer* with habitat depths of 0–80/120 m (Jonkers and Kucera, 2017)

581 and in high latitudes, mostly on *N. pachyderma* (s) living at 0–200 m depth (Simstich et
582 al., 2003). Averaging of ^{14}C ages within a ^{14}C plateau helps to bypass the analytical
583 noise in ^{14}C records such as short-term apparent ^{14}C age reversals and to deduce the
584 regional evolution of planktic ^{14}C reservoir ages with semi-millennial-scale resolution.
585 Nine plateaus are located in the LGM, 18–27 cal. ka (Fig. 1). Here, plankton-based
586 reservoir ages show analytical uncertainties of >200 to >300 yr each. By comparison,
587 short-term temporal variations in reservoir age reach 200–400 yr, occasionally up to 600
588 yr, in particular, close to the end of the LGM (Table 3).

589

590 To better decode the informative value of our ^{14}C reservoir ages for late LGM we
591 compared average ages of ^{14}C Plateaus 4-5 with estimates generated by a global
592 ocean model (Muglia et al., 2018; 0–50 m w.d.; Fig. 8c-d; Table 3), an approach similar
593 to that of Toggweiler et al. (2019) applied to modern reservoir ages of the global ocean.
594 In an earlier paper (Balmer et al., 2016) we compared our empiric reservoir ages for the
595 LGM with GCM-based estimates of Franke et al. (2008) and Butzin et al. (2012). Franke
596 et al. (2008) underestimated our mid-latitude values by up to ~2000 ^{14}C yr, while LGM
597 reservoir age estimates of Butzin et al. (2012) were more consistent with ours. Their
598 GCM considered more realistic boundary conditions such as the LGM freshwater
599 balance in the Southern Ocean and, in particular, LGM SST and wind fields plus the gas
600 transfer velocity for the exchange of ^{14}C of CO_2 (Sweeney et al., 2007). Initially we also
601 planned a continuation of these intercomparison tests with our present data set, but
602 were advised by Butzin (pers. com. 2019, Butzin et al., 2020) to wait for results from a
603 revised GCM capable to resolve more properly the details of continental margins and
604 adjacent seas, that frequently form the origin of our sediment-based data sets. We thus
605 focus on a comparison of our empiric values with model estimates of Muglia et al. only.

606 Their model includes ocean surface reservoir age and ocean radiocarbon fields that
607 have been validated through a comparison to LGM radiocarbon data compilation made
608 by Skinner et al. 2017. It conforms two plausible, recent model estimates of surface
609 reservoir ages that can be compared to our results (Table 3).

610

611 Low LGM values (300–750 yr) supposedly document an intensive exchange of surface
612 waters with atmospheric CO₂, most common in model- and foraminifera-based
613 estimates of the low- and mid-latitude Atlantic. Low empiric values also mark LGM
614 waters in mid to high latitudes off Norway and off middle Chile, that is, close to sites of
615 potential deep and/or intermediate water formation. Off Norway and in the northeastern
616 Atlantic, model-based reservoir ages of Muglia et al. (2018) largely match the empiric
617 range. However, the uncertainty envelopes for data shown in Fig. 8c (± 560 yr; $r = 0.59$)
618 generally exceed by far the spatial differences calculated for the empiric data.

619 Conversely, model-based reservoir ages reproduce only poorly the low plankton-based
620 estimates off Central Chile and values in the Western Pacific and Southern Ocean.

621

622 In part, the differences may be linked to problems like insufficient spatial resolution
623 along continental margins, ignoring east-west differences within ocean basins, and/or
624 the estimates of a correct location and extent of seasonal sea ice cover used as LGM
625 boundary condition such as east off Greenland, in the subpolar northwest Pacific, and
626 off Southern Chile, where sea ice hindered the exchange of atmospheric carbon (per
627 analogy to that of temperature exchange, as recorded by Sessford et al, 2019). Also,
628 yearly mean model estimates are compared to ¹⁴C signals of planktic foraminifera that
629 mostly formed during summer only, when large parts of the Nordic Seas were found ice-

630 free (Sarnthein et al., 2003). Hence, models may need to better constrain local and
631 seasonal sealing effects of LGM sea ice cover.

632

633 In general, however, the foraminifera-based reservoir age estimates for our sites that
634 represent various hydrographic key regions in the high-latitude ocean appear much
635 higher than model-derived values. **These** deviations reach up to 1400 yr, in particular in
636 the Southern Ocean. In part, **they** may result from the fact that present models may not
637 yet be suited to capture small-scale **ocean structures such as the interference of ocean**
638 **currents with local bathymetry and local upwelling cells**. Here, model-based reservoir
639 ages appear far too low in LGM regions influenced by regional upwelling such as the
640 South China Sea then governed by an estuarine overturning system (Wang et al., 2005;
641 Fig. 9), by coastal upwelling off N.W. Australia (Xu et al., 2010; Sarnthein et al., 2011),
642 or by a melt water lid such as off eastern New Zealand (Bostock et al., 2013; Küssner et
643 al., 2020 subm.). Local oceanic features are likely to be missed in **a coarse-resolution**
644 **model such as Muglia et al. (2018)**. **Our** more narrow-spaced empiric data **could** help to
645 **test** and **refine** the skill of models to capture past ^{14}C reservoir ages.

646

647 Various differences amongst plankton- and model-based reservoir ages may **also** result
648 from differential seasonal habitats of the different planktic species analyzed that, in turn,
649 may trace different surface and subsurface water currents. Pertinent details are largely
650 unknown for the modern scenario because of the ‘bomb effect’, likewise no pertinent
651 data exist yet for the LGM. However, distinct interspecies differences were found in **Baja**
652 **California that record differential, upwelling-controlled habitat conditions (Lindsay et al,**
653 **2015)**. In the northern Norwegian Sea **interspecies differences amount up to 600 yr** for
654 the time span of the Preboreal ^{14}C plateau, 9.6–10.2 cal. ka (Sarnthein and Werner,

655 2018). Here ^{14}C records of Arctic *Turborotalita quinqueloba*, dominantly grown close to
656 the sea surface during peak summer, differ from the paired record of *Neogloboquadrina*
657 *pachyderma*, formed in subsurface waters, and that of subpolar species *N. incompta*,
658 mainly advected from the south by Norwegian Current waters well mixed with the
659 atmosphere during peak winter. This makes closer specification of model results as
660 product of different seasonal extremes a further target.

661

662 **3.3 Plankton-based ^{14}C reservoir ages – A prime database to estimate past changes in**
663 **the ^{14}C ventilation age of deep waters, ocean MOC, and DIC of the ocean of the past**

664

665 ‘Raw’ apparent benthic ventilation ages (in ^{14}C yr; ‘raw’ *sensu* Balmer et al., 2018)
666 express the difference between the (coeval) atmospheric and benthic ^{14}C levels
667 measured at any site and time of foraminifer deposition. These ages are the sum of (1)
668 the planktic reservoir age of the ^{14}C plateau that covers a group of paired benthic and
669 planktic ^{14}C ages and (2) the (positive or negative) ^{14}C age difference between any
670 benthic ^{14}C age and the average ^{14}C age of the paired planktic ^{14}C plateau. The benthic
671 ventilation ages necessarily rely on the high quality of ^{14}C plateau-based chronology,
672 since the atmospheric ^{14}C level has been subject to substantial short-term changes over
673 glacial-to-deglacial times. Necessarily, the ventilation ages include a mixing of different
674 water masses that might originate from different ocean regions and may contribute
675 differential ^{14}C ventilation ages, an unknown justifying the modifier ‘apparent’.

676

677 In a further step, the $\Delta\Delta^{14}\text{C}$ equivalent of our ‘raw’ benthic ventilation age may be
678 adjusted to changes in atmospheric ^{14}C that occurred over the (short) time span
679 between deep-water formation and benthic sediment deposition (e.g., Balmer and

680 Sarnthein, 2018; Cook and Keigwin, 2015). In most cases, however, this second step is
681 omitted since its application usually does not imply any major modification of the
682 ventilation age estimates (Fig. S2a; Skinner et al., 2017; Sarnthein et al., 2013).

683

684 On the basis of ^{14}C plateau tuning we now can rely on 18 accurately dated records of
685 apparent benthic ^{14}C ventilation ages (Fig. S2a-d) to reconstruct the global geometry of
686 LGM and HS-1 deep and intermediate water circulation as summarized in ocean
687 transects and maps (Figs. 9–11) and discussed below. The individual matching of our
688 20 planktic ^{14}C plateau sequences with that of the Suigetsu atmospheric ^{14}C record is
689 displayed in Sarnthein et al. (2015), Balmer et al., (2016), Küssner et al. (2020, *subm.*),
690 and Ausin et al. (2019, *unpubl.*). In addition, robust estimates of past reservoir ages are
691 obtained for 4 planktic and benthic ^{14}C records from paired atmospheric ^{14}C ages of
692 wood chunks (Rafter et al., 2018; Zhao and Keigwin, 2018; Broecker et al., 2004).

693

694 **3.3.1** — *Major features of ocean meridional overturning circulation during LGM (Fig. 10)*

695

696 Off Norway and near the Azores Islands very low benthic ^{14}C ventilation ages of <100–
697 750 yr suggest ongoing deep-water formation in the LGM northern North Atlantic
698 reaching down to more than 3000–3500 m water depth, with a flow strength possibly
699 similar to today (and a coeval deep countercurrent of old waters from the Southern
700 Ocean flowing along the East Atlantic continental margin off Portugal). This pattern
701 clearly corroborates the assembled benthic $\delta^{13}\text{C}$ record showing plenty of elevated $\delta^{13}\text{C}$
702 values for the northwestern, eastern and central North Atlantic (Sarnthein et al., 1994;
703 Millo et al., 2006; Keigwin and Swift, 2017). Irrespective of unspecified potential zonal
704 variations in deep-water ventilation age at mid latitudes and different from a number of

705 published models (e.g., Ferrari et al., 2014; Butzin et al., 2017) this ‘anti-estuarine’
706 pattern has been confirmed by MIROC model simulations (Gebbie, 2014; Sherriff-
707 Tadano et al., 2017, Yamamoto et al., 2019) and, independently, by ϵ_{Nd} records (Howe
708 et al., 2016; Lippold et al., 2016). The latter suggest an overturning of AMOC possibly
709 even stronger than today, in particular due to a ‘thermal threshold’ (Abé-Ouchi, pers.
710 comm.) overlooked in other model simulations.

711

712 In contrast to the northern North Atlantic, deep waters in the southern North Atlantic and
713 Circumpolar (CP) deep waters in the subpolar South Atlantic show an LGM ^{14}C
714 ventilation age of ~3640 yr, finally rising up to 3800 yr (Figs. 10, 11, S2b). These waters
715 were upwelled and admixed from below to surface waters near to the sub-Antarctic
716 Front during terminal LGM (Fig. S2b; Skinner et al., 2010; Balmer and Sarnthein, 2016;
717 model of Butzin et al., 2012).

718

719 In the southwestern South Pacific abyssal, in part possibly Antarctic-sourced waters
720 (Rae and Broecker, 2018) likewise show high apparent ^{14}C ventilation ages that rise
721 from 3900 to 4800 yr over the LGM, in particular close to its end (Figs. 10 top and S2c)
722 (^{14}C dates of Ronge et al., 2016, modified by planktic ^{14}C reservoir ages of Küssner et
723 al., 2020 subm.). A vertical transect of benthic $\delta^{13}C$ (McCave et al., 2008) suggests that
724 the abyssal waters were overlain by CP waters, separated by pronounced stratification
725 near ~3500–4000 m water depth. In part, the CP waters stemmed from North Atlantic
726 Deep Water. Probably, their apparent ventilation age came close to 3900–4500 yr,
727 similar to the values found in the southern South Atlantic. East of New Zealand the CP
728 waters entered the deep western Pacific and spread up to the subpolar North Pacific,

729 where LGM ^{14}C ventilation ages reached ~3700 yr, possibly occasionally 5000 yr (Fig.
730 S2d).

731

732 Similar to today, the MOC of the LGM Pacific was shaped by estuarine geometry,
733 probably more weakened than today (Du et al., 2018) and more distinct in the far
734 northwest than in the far northeast. This geometry resulted in an upwelling of old deep
735 waters in the subarctic Northwest Pacific, here leading to a ^{14}C reservoir age of ~1700
736 yr for surface waters at terminal LGM. On top of the Lower Pacific Deep Waters we may
737 surmise Upper Pacific Deep Waters that moved toward south (Figs. 10 top and 11).

738

739 The Pacific deep waters were overlain by Antarctic / Pacific Intermediate Waters (IW)
740 with LGM ^{14}C ventilation ages as low as 1400–1600 yr, except for a shelf ice-covered
741 site at the southern tip of Chile with IW ages of 2460–3760 yr, possibly a result of local
742 upwelling of CP waters. In general, however, the low values of Pacific IW are similar to
743 those estimated for South Atlantic IW and likewise reflect a vivid exchange with
744 atmospheric CO_2 in their source regions in the Southern Ocean (Skinner et al., 2015).

745

746 When entering and crossing the entrance sill to the marginal South China Sea the
747 ‘young’ IW were mixed with ‘old’ CP waters entrained from below, here leading to ^{14}C
748 ventilation ages of 2600–3450 yr (Figs. 9 and S2d). The LGM South China Sea was
749 shaped by an estuarine-style overturning system marked by major upwelling near to its
750 distal end in the far southwest (Wang L. et al., 1999). This upwelling led to planktic ^{14}C
751 reservoir ages as high as 1200–1800 yr, values rarely found elsewhere in surface
752 waters of low latitudes.

753

754 Our wide-spaced distribution pattern of 18 **open-ocean** ^{14}C ventilation ages (plus 4
755 values based on paired wood chunks) in Figs. 10 and 11 agrees only in part with the
756 circulation patterns suggested by the much larger datasets of ^{14}C ventilation ages
757 compiled by Skinner et al. (2017) and Zhao et al. (2018). Several features in Figs. 10
758 and 11 directly deviate, e.g., the ages we derive for the North Atlantic and mid-depth
759 Pacific. These deviations may be linked to both the different derivation of our ^{14}C
760 ventilation age estimates and the details of our calendar-year chronology now based on
761 the narrow-standing suite of ^{14}C plateau-boundary ages. The quality of our ^{14}C reservoir
762 ages of surface waters also controls the 'apparent' ventilation age of deep-waters, as it
763 results from direct **addition of the short-term average ^{14}C age of a planktic ^{14}C plateau to**
764 **a paired, that is coeval benthic ^{14}C age (formed during the time of benthic foraminiferal**
765 **growth, somewhat after the actual time of deep-water formation).**

766

767 **3.3.2** — *Major features of meridional overturning circulation during early HS-1 (Fig. 10)*

768

769 Near the onset of deglacial Heinrich Stadial 1 (HS-1; ~18–14.7 cal. ka) major shifts in
770 ^{14}C ventilation age suggest some short-lasting but fundamental changes in the
771 circulation geometry of the deep ocean, a central theme of marine paleoclimate
772 research (lower panel of Figs. 10, 11 and **S2a** and b). Deep waters in the eastern
773 Nordic Seas, west of the Azores Islands, and off northern Brazil show a rapid rise to
774 high ^{14}C ventilation ages of ~2000–2500 yr and up to 4000 yr off Brazil, values that give
775 first proof for a brief switch from 'anti-estuarine' to 'estuarine' circulation that governed
776 the central North Atlantic and Norwegian Sea during early HS-1. This geometry
777 continued – except for a brief but marked and widespread event of recurring NADW
778 formation near 15.2 ka – until the very end of HS-1 near 14.5 ka (Fig. **S2a**; Muschitiello

779 et al., 2019). The MOC switch from LGM to HS-1 is in line with changes depicted in
780 paired benthic $\delta^{13}\text{C}$ data (Sarnthein et al., 1994), but not confirmed by the coeval ϵ_{Nd}
781 record that suggests a constant source of 'mid-depth waters', with the $\delta^{13}\text{C}$ drop being
782 simply linked to a higher age (Howe et al., 2018).

783

784 Conversely, benthic ^{14}C ventilation ages in the northeastern North Pacific (Site MD02-
785 2489) show a coeval and distinct but brief minimum of 1050-1450 yr near 3640 m w.d.
786 during early HS-1 (~18.1–16.8 ka; Figs. 10, 11, and S2d). This minimum was produced
787 by extremely small benthic-planktic age differences of 350–650 yr and provides robust
788 evidence for a millennial-scale event of deep-water formation, that has flushed the
789 northeastern North Pacific down to more than 3640 m w.d. (Gebhardt et al., 2008;
790 Sarnthein et al., 2013; Rae et al., 2014). Similar circulation geometries were reported for
791 the Pliocene (Burls et al., 2017). 'Young' Upper North Pacific Deep Waters (North
792 Pacific Intermediate Waters *sensu* Gong et al., 2019) then penetrated as 'western
793 boundary current' far south, up to the northern continental margin of the South China
794 Sea (Figs. 9b, 11, and S2d). The short-lasting North Pacific regime of anti-estuarine
795 overturning was similar to that we find in the modern and LGM Atlantic and, most
796 interesting, simultaneous with the Atlantic's estuarine episode.

797

798 Recent data on benthic-planktic ^{14}C age differences (Du et al., 2018) precisely recover
799 our results in a core at ~680 m w.d. off southern Alaska. However, they do not depict
800 the 'young' deep waters at their Site U1418 at ~3680 m w.d., as corroborated by a
801 paired autigenic ϵ_{Nd} maximum suggesting a high local bottom water age nearby. We
802 assume that the amazing difference in local deep-water ventilation ages is due to small-
803 scale differences in the effect of Coriolis forcing at high latitudes between a site located

804 directly at the **base of the** Alaskan continental margin (U1418; Fig. 10b) and that on the
805 distal Murray Sea Mount in the 'open' Pacific (MD02-2489; Figs. 7 and 11), which
806 **probably has been** been washed by a plume of newly formed North Pacific deep waters
807 probably stemming from the Bering and/or Ochotsk Seas. In contrast, the incursion of
808 almost 3000 yr old deep waters from the Southern Ocean has continued along the
809 continental margin all over HS-1. In summary we may conclude that the geometry of
810 ocean MOC was briefly reversed in the 'open' North Pacific over almost 1500 years
811 during HS-1, far deeper than suggested by previous authors (e.g., Okazaki et al., 2012;
812 Gong, S., et al. 2019), but similar to changes in geometry first proposed by Broecker et
813 al. (1985) then, however, for an LGM ocean.

814

815 **3.3.3** — *Deep-Ocean DIC inventory*

816

817 Apart from the changing geometries in ocean MOC **during LGM and HS-1**, the global
818 set of ^{14}C plateau-based, hence refined estimates of apparent ^{14}C ventilation ages (Fig.
819 10) has ultimately **also** revealed new insights into glacial-to-deglacial changes in **deep-**
820 ocean DIC inventories (Sarnthein et al., 2013; **Skinner et al., 2019**). On the basis of
821 GLODAP data (Key et al., 2004) any drop in ^{14}C concentration (i.e., any rise in average
822 ^{14}C ventilation age) of modern deep waters is tied linearly to a rise of carbon (DIC)
823 dissolved in deep ocean waters below ~ 2000 m, making for 1.22 micromole C / -1 ‰
824 ^{14}C . By and large, GCM and box model simulations of Chikamoto and Abé-Ouchi (2012)
825 and Wallmann et al. (2016) suggest that this ratio may also apply to LGM deep-water
826 circulation, when apparent ^{14}C ventilation ages in the Southern Ocean increased
827 significantly (from 2400 up to ~ 5000 yr) and accordingly, thermohaline circulation was
828 more sluggish and transit times of deep waters extended. Accordingly, a 'back-of-the-

829 envelope' calculation of LGM ventilation age averages in the global deep ocean
830 suggests an additional carbon absorption of 730–980 Gt (Sarnthein et al., 2013). This
831 estimate can easily accommodate the glacial transfer of ~200 Gt C from the atmosphere
832 and biosphere, moreover, may also explain 200–450 Gt C then most probably removed
833 from glacial Atlantic and Pacific intermediate waters. These estimates offer an
834 independent evaluation of ice core-based data, other proxies, and model-based data on
835 past changes in the global carbon cycle (e.g., Menviel et al., 2018).

836

837 4. SOME CONCLUSIONS AND PERSPECTIVES

838 – Despite some analytical scatter, ^{14}C ages for the top and base of Lake Suigetsu-
839 based atmospheric ^{14}C plateaus and coeval planktic ^{14}C plateaus do not present
840 statistical 'outliers' but real age estimates that are reproduced by tree ring-based ^{14}C
841 ages over the interval 10–13 cal. ka and further back.

842 – Hulu U/Th model-based ages of ^{14}C plateau boundaries of the Suigetsu atmospheric
843 ^{14}C record appear superior to those derived from microscopy-based varve counts only,
844 since U/Th model-based ages match far more closely the age deduced from XRF-based
845 varve counts for the test case of lower plateau boundary 2b in the early deglacial, and
846 the age assigned to the Laschamp event prior to the LGM.

847 – During deglacial times, several ^{14}C plateaus paralleled a rise in air-sea gas exchange,
848 and, in turn, distinct changes in ocean MOC. By contrast, changes in cosmogenic ^{14}C
849 production rarely provide a complete explanation for the plateaus identified in the
850 Suigetsu ^{14}C data under discussion.

851 – In total, ^{14}C plateau boundaries in the range 29–10 cal. ka provide a suite of ~30 age
852 tie points to establish – like chronological ladder rungs – a robust global age control for
853 deep-sea sediment sections and global stratigraphic correlations of last glacial to

854 deglacial climate events, 29–10 cal. ka. U/Th model ages confine the cal. age
855 uncertainty of Suigetsu plateau boundaries assigned halfway between two ^{14}C ages
856 nearby inside and outside a plateau's scatter band to less than ± 50 to ± 70 yr.
857 – The difference in ^{14}C age between coeval atmospheric and planktic ^{14}C plateaus
858 presents a robust tracer of planktic ^{14}C reservoir ages and **shows** their temporal and
859 spatial variability, for the LGM and HS-1 now established for 18/20 sediment sites.
860 – Paired reservoir ages obtained from different planktic species document the local
861 distribution patterns of different surface water masses and prevailing foraminiferal
862 habitats at different seasons.
863 – **New**, more **robust** deep-water ^{14}C ventilation ages can be derived on the basis of our
864 robust planktic ^{14}C reservoir ages. These ventilation ages reveal geometries of LGM
865 overturning circulation **similar** to those of today. In contrast, ^{14}C ventilation ages of early
866 HS-1 suggest an almost 1500 yr long event of widely reversed circulation patterns
867 marked by deep-water formation and brief flushing of the northern North Pacific and
868 estuarine circulation geometry in the northern North Atlantic.
869 – Increased glacial ^{14}C ventilation ages and carbon (DIC) inventories of ocean deep
870 waters suggest an LGM drawdown of about 850 Gt C into the deep ocean. **Starting with**
871 **HS-1 a drop of ventilation age suggests** carbon released to the atmosphere (Sarnthein
872 et al., 2013).
873 – Comparison of planktic and model-based reservoir age estimates reveals some major
874 discrepancies, in particular at sites in middle to high latitudes, and **highlights the need**
875 **for** further model refinements to make the models better reflect the real complex
876 patterns of ocean circulation, including seasonality.

877

878 ACKNOWLEDGMENTS

879 We owe sincere thanks for plenty of stimulations to the 23rd International Radiocarbon
880 Conference in Trondheim, in particular to M-J. Nadeau, and to the IPODS–OC3
881 workshop in Cambridge U.K, 2018, convened by A. Schmittner and L. Skinner.
882 Moreover, we thank for most valuable basic discussions with R. Staff, Glasgow, J.
883 Southon, Irvine CA, and M. Butzin, AWI Bremerhaven, who kindly helped us to discuss
884 the comparison of his model results, and S. Beil, Kiel, for computer assistance. Over the
885 last three years, G. Mollenhauer measured with care hundreds of supplementary ¹⁴C
886 ages in her MICADAS laboratory at AWI Bremerhaven. This study obtained long lasting
887 special support from R. Tiedemann and his colleagues at the AWI Bremerhaven.

888

889 **Author contribution**

890 All authors contributed data and valuable suggestions to write up this synthesis. MS and
891 PG designed the outline of this manuscript. KK, BA, TE and MS provided new marine
892 ¹⁴C records in addition to records previously published. GS displayed the details of
893 Suigetsu varve counts. RM provided a ¹⁰Be-based ¹⁴C record and plots of raw ¹⁴C data
894 sets of Suigetsu und Hulu Cave. Discussions amongst PG, RM, GS and MS served to
895 select U/Th-based model ages as best-possible time scale. **JM streamlined the sections**
896 **on data-model intercomparison.**

897

898 **Data availability**

899 Primary radiocarbon data of most sites are available at PANGAEA de, except for the
900 ¹⁴C data of 5 marine cores still under publication by Küssner et al. (2020 subm.) and
901 Ausin et al. (unpubl.; also see caption of Fig. S2).

902

903 **REFERENCES (99)**

904 Adkins, J. F. and Boyle, E. A.: Changing atmospheric $\Delta^{14}\text{C}$ and the record of
905 paleoventilation ages. *Paleoceanography*, 12(3), 337–344, 1997.

906 Adolphi, F., Bronk Ramsey, C., Erhard, T., Lawrence Edwards, R., Cheng, H.,
907 Turney, C.S.M., Cooper, A., Svensson, A., Rasmussen, S.O., Fischer, H., and

908 Muscheler, R.: Connecting the Greenland ice-core and U/Th timescales via cosmogenic
909 radionuclides: testing the synchronicity of Dansgaard–Oeschger events. *Clim. Past*, 14,
910 1755–1781. <https://doi.org/10.5194/cp-14-1755-2018>, 2018.

911 Alves, E.Q., Macario, K., Ascough, P., and Bronk Ramsey, C.: The worldwide
912 marine radiocarbon reservoir effect: definitions, mechanisms, and prospects. *Review of*
913 *Geophysics*, 56, <https://doi.org/10.1002/2017RG000588>, 2018.

914 Alveson, E.Q.: Radiocarbon in the Ocean, *EOS*, 99,
915 <https://doi.org/10.1029/2018EO095429>, 2018.

916 Ausin, B., Haghpor, N., Wacker, L., Voelker, A. H. L., Hodell, D., Magill, C., et al.:
917 Radiocarbon age offsets between two surface dwelling planktonic foraminifera species
918 during abrupt climate events in the SW Iberian margin. *Paleoceanography and*
919 *Paleoclimatology*, 34. <https://doi.org/10.1029/2018PA003490>, 2019.

920 Balmer, S., Sarnthein, M., Mudelsee, M., and Grootes, P. M.: Refined modeling and
921 ^{14}C plateau tuning reveal consistent patterns of glacial and deglacial ^{14}C reservoir ages
922 of surface waters in low-latitude Atlantic. *Paleoceanography*, 31.
923 <https://doi.org/10.1002/2016PA002953>, 2016.

924 **Balmer, S. and Sarnthein, M.: Planktic ^{14}C plateaus, a result of short-term**
925 **sedimentation pulses? – *Radiocarbon*, 58, DOI:10.1017/RDC.2016.100, 11 pp., 2016.**

926 Balmer, S. and Sarnthein, M.: Glacial-to deglacial changes in North Atlantic melt-
927 water advection and deep-water formation – Centennial-to-millennial-scale ^{14}C records
928 from the Azores Plateau. *Geochim. Cosmochim. Acta*, 236, 399-415,
929 <https://doi.org/10.1016/j.gca.2018.03.001>, 2018.

930 Berger W.H. and Keir, R.S.: Glacial-Holocene changes in atmospheric CO_2 and the
931 deep-sea record. J.E. Hansen, T. Takahashi (Eds.), *Geophysical Monograph*, 29,
932 American Geophysical Union, Washington, DC, pp. 337–351, 1984.

933 Bostock, H.C., Barrows, T.T., Carter, L., Chase, Z., Cortese, G., et al.: A review of
934 the Australian – New Zealand sector of the Southern Ocean over the last 30 ka (Aus-
935 INTIMATE project). *Quaternary Science Reviews* 74, 35-57, 2013.

936 Broecker W.S, Peteet, D.M., and Rind, D.: Does the ocean-atmosphere system have
937 more than one stable mode of operation? *Nature*, **315**, 21-26, doi:10.1038/315021a0,
938 1985

939 Broecker W.S., Barker, S., Clark, E., Hajdas, I., Bonani, G., and Stott, L.: Ventilation
940 of the Glacial deep Pacific Ocean, *Science*, 306, 1169–1172, 2004.

941 Bronk Ramsey, C., Staff, R. A., Bryant, C. L., Brock, F., Kitagawa, H., van der Plicht,

942 J., Scholaut, G., Marshall, M. H., Brauer, A., Lamb, H. F., Payne, R. L., Tarasov, P. E.,
943 Haraguchi, T., Gotanda, K., Yonenobu, H., Yokoyama, Y., Tada, R., and Nakagawa, T.:
944 A complete terrestrial radiocarbon record for 11.2 to 52.8 kyr B.P., *Science*, 338, 370–
945 374, 2012.

946 Bronk Ramsey, C. et al., *Radiocarbon*, (in press) 2020.

947 **Burke, A. and Robinson, L.F.: The Southern Ocean's role in carbon exchange during**
948 **the last deglaciation. *Science*, 335, 557-561, 2012.**

949 Burls, N.J., Fedorov, A.V., Sigman, D.M., Jaccard, S.L., Tiedemann, R., and Haug,
950 G.H.: Active Pacific meridional overturning circulation (PMOC) during the warm
951 Pliocene. *Sci. Adv.* 2017;3: e1700156, 2017.

952 Butzin, M., Prange, M., Lohmann, G.: Radiocarbon simulations for the glacial ocean:
953 The effects of wind stress, Southern Ocean sea ice and Heinrich events. *Earth Planet.*
954 *Sci. Lett.*, 235, 45-61, 2005.

955 Butzin, M., Prange, M., and Lohmann, G.: Readjustment of glacial radiocarbon
956 chronologies by self-consistent three-dimensional ocean circulation modeling. *Earth*
957 *Planet Sci. Lett.*, 317, 177-184, 2012.

958 Butzin, M., Köhler, P., and Lohmann, G.: Marine radiocarbon reservoir age
959 simulations for the past 50,000 years. *Geophys. Res. Lett.*, 44, 8473–8480,
960 doi:10.1002/2017GL074688, 2017.

961 **Butzin, M., Heaton, T.J., Köhler, P., and Lohmann, G.: A short note on marine**
962 **reservoir age simulations used in INTCAL20. *Radiocarbon*, oo, 1-7, DOI:10.1017/RDC.2020.9,**
963 **2020.**

964 Chen, T., Robinson, L.F., Burke, A., Southon, J., Spooner, P., Morris, P.J., and Ng,
965 H.C.: Synchronous centennial abrupt events in the ocean and atmosphere during the
966 last deglaciation, *Science*, 349, 1537-1541, 2015.

967 Cheng, H., Edwards, R.L., Southon, J., Matsumoto, K., Feinberg, J.M., Sinha, A.,
968 Zhou, W., Li, H., Li, X., Xu, Y., Chen, S., Tan, M., Wang, Q., Wang, Y., and Ning, Y.:
969 Atmospheric $^{14}\text{C}/^{12}\text{C}$ changes during the last glacial period from Hulu Cave, *Science*,
970 362, 1293-1297, 2018.

971 Chikamoto, M.O., Abé-Ouchi, A., Oka, A., Ohgaito, R., and Timmermann, A.:
972 Quantifying the ocean's role in glacial CO_2 reductions, *Climate of the Past*, 8, 545–563,
973 doi:10.5194/cp-8-545-2012, 2012.

974 Cook M.S. and Keigwin L.D.: Radiocarbon profiles of the NW Pacific from the LGM
975 and deglaciation: Evaluating ventilation metrics and the effect of uncertain surface

976 reservoir ages, *Paleoceanography*, 30, 174–195, 2015.

977 Davies, S.M., Davies, P.M., Abbott, Meara, R.H., et al.: A North Atlantic tephro-
978 stratigraphical framework for 130-60 ka b2k: New tephra discoveries, marine based
979 correlations, and future challenges, *Quaternary Science Rev.*, 106, 101-121, 2014.

980 Du, J., Haley, B.A., Mix, A.C., Walczak, M.H., and Praetorius, S.K.: Flushing of the
981 deep Pacific Ocean and the deglacial rise of atmospheric CO₂ concentrations, *Nature*
982 *geoscience*, 11, 749-755, 2018.

983 Ferrari, R., Jansen, M.F., Adkins, J.F., Burke, A., Stewart, A.L., and Thompson, A.F.:
984 Antarctic sea ice control on ocean circulation in present and glacial climates, *Proc.*
985 *National Academy Science*, 111 (24), 8753–8758, 2014.

986 Gebbie, G.: How much did Glacial North Atlantic Water shoal? *Paleoceanography*,
987 29, 190-209, doi:10.1002/2013PA002557, 2014.

988 Gebhardt, H., Sarnthein, M., Kiefer, T., Erlenkeuser, H., Schmieder, F., and Röhl, U.:
989 Paleonutrient and productivity records from the subarctic North Pacific for Pleistocene
990 glacial terminations I to V. *Paleoceanography* 23, PA4212, 1-21,
991 doi:10.1029/2007PA001513, 2008.

992 Gong, S., Lembke-Jene, L., Lohmann, G., Knorr, G., Tiedemann, R., Zou, J.J and
993 Shi, X.F.: Enhanced North Pacific deep-ocean stratification by stronger intermediate
994 water formation during Heinrich Stadial 1. *Nature Communications*, 10: 656.
995 <https://doi.org/10.1038/s41467-019-08606-2>, 2019.

996 Grootes P.M. and Stuiver, M.: Oxygen 18/16 variability in Greenland snow and ice
997 with 1000 to 100000 year time resolution, *J. Geophys. Res.: Oceans* (1978–2012)
998 102(C12), 26455–26470, 1997.

999 Grootes, P.M. and Sarnthein, M.: Marine ¹⁴C reservoir ages oscillate, *PAGES News*,
1000 14/3, 18-19, 2006.

1001 Howe, J.N.W., Piotrowski, A.M., Noble, T.L., Mulitza, S., Chiessi, C.M., and Bayon,
1002 G.: North Atlantic deep-water production during the last glacial maximum, *Nat.*
1003 *Commun.*, 7, 11765, 2016. s

1004 Howe, J.N.W., Huang, K-F., Oppo, D.W., Chiessi, C.M., Mulitza, S., Blusztajn, J.,
1005 and Piotrowski, A.M.: Similar mid-depth Atlantic water mass provenance during the Last
1006 Glacial Maximum and Heinrich Stadial 1, *Earth Planetary Science Letters*, 490, 51-61,
1007 2018.

1008 Jonkers, L. and Kucera, M.: Quantifying the effect of seasonal and vertical habitat
1009 tracking on planktonic foraminifera proxies, *Climate of the Past*, 13, 573-586, 2017.

1010 Kawamura, K., Parrenin, F., Lisiecki, L., Uemura, R., Vimeux, F., Severinghaus, J.P.,
1011 Hutterli, M.A., Nakazawa, T., Aoki, S., Jouzel, J., Raymo, M.E., Matsumoto, K., Nakata,
1012 H., Motoyama, H., Fujita, S., Goto-Azuma, K., Fujii, Y., and Watanabe, O.: Northern
1013 Hemisphere forcing of climatic cycles in Antarctica over the past 360,000 years, *Nature*,
1014 448, 912-916, doi:10.1038/nature06015, 2007.

1015 Keigwin, L.D. and Swift, S.A.: Carbon isotope evidence for a northern source of
1016 deep water in the glacial western North Atlantic, *PNAS*, 114 (11), 2831-2835, 2017.

1017 Key R. M., Kozyr, A., Sabine, C.L., Lee, K., Wanninkhof, R., Bullister, J.L., Feely,
1018 R.A., Millero, F.J., Mordy, C., and Peng, T.-H. (2004) A global ocean carbon climat-
1019 ology: Results from Global Data Analysis Project (GLODAP), *Global Biogeochem. Cy.*,
1020 18, GB4031, doi:10.1029/2004GB002247, 2004.

1021 Kong, X., Wang, Y., Wu, J., Cheng, H., Edwards, R.L., and Wang, X.: Complicated
1022 responses of stalagmite $\delta^{13}\text{C}$ to climate change during the last glaciation from Hulu
1023 Cave, Nanjing, China, *Science in China Ser. D Earth Sciences*, 48, (12), 2174-2181,
1024 2005.

1025 Küssner, K., Sarnthein, M., Lamy, F., and Tiedemann, R.: High-resolution
1026 radiocarbon-based age records trace episodes of *Zoophycos* burrowing, *Marine*
1027 *Geology*, 403, 48-56, <http://doi:10.1016/j.margeo.2018.04.01>, 2018.

1028 Küssner, K., Sarnthein, M., Lamy, F., Michel, E., Mollenhauer, G., Siani G., and
1029 Tiedemann, R.: Glacial-to-deglacial reservoir ages of surface waters in the southern
1030 South Pacific, *Paleoc. and Paleoclim.* 30 ms-pp, 2020 *subm.*).

1031 Lascu, I., Feinberg, J.M., Dorale, J.A., Cheng, H., and Edwards, R.L.: Age of the
1032 Laschamp excursion determined by U-Th dating of a speleothem geomagnetic record
1033 from North America. *Geology*, 44, 139-142, doi:10.1130/G37490.1. 2016

1034 Lindsay, C.M., Lehman, S.J., Marchitto, T.M., and Ortiz, J.D.: The surface
1035 expression of radiocarbon anomalies near Baja California during deglaciation. *Earth*
1036 *Planetary Science Letters*, 422, 67-74, 2015.

1037 Lippold, J., Gutjahr, M., Blaser, P., Christner, E., de Cavalho-Fereira, M.L., Mulitza,
1038 S. et al.: Deep-water provenance and dynamics of the (de)glacial Atlantic meridional
1039 overturning circulation, *Earth Planetary Science Letters*, 445, 68-78, 2016.

1040 Lisiecki, L.E. and Stern, J.V.: Regional and global benthic $d^{18}\text{O}$ stacks for the last
1041 glacial cycle. *Paleoceanography*, 31, doi:10.1002/2016PA003002, 2016.

1042 Löwemark, L. and Grootes, P.M.: Large age differences between planktic
1043 foraminifers caused by abundance variations and *Zoophycos* bioturbation,

1044 Paleoceanography, 19, PA2001, doi:10.1029/2003PA000949, 2004.

1045 Marcott, S.A., Bauska, T.K., Buizert, C., Steig, E.J., Rosen, J.L., Cuffey, K.M., Fudge,
1046 T.J., Severinghaus, J.P., Ahn, J., Kalk, M.L., McConnell, J.R., Sowers, T., Taylor, K.C.,
1047 White, J.W.C., and Brook, E.J.: Centennial-scale changes in the global carbon cycle
1048 during the last deglaciation, *Nature*, 514, 616-619, doi:10.1038/nature13799, 2014.

1049 Marshall, M., Schlolaut, G., Brauer, A., Nakagawa, T., Staff, R.A., Bronk Ramsey,
1050 C., Lamb, H., Gotanda, K., Haraguchi, T., Yokoyama, Y., Yonenobu, H., Tada, R.,
1051 SG06 project members: A novel approach to varve counting using μ XRF and X-
1052 radiography in combination with thin-section microscopy, applied to the Late Glacial
1053 chronology from Lake Suigetsu, Japan, *Quaternary Geochronology* 13, 70-80, 2012.

1054 McCave, I.N., Carter, I., and Hall, I.R.: Glacial-interglacial changes in water mass
1055 structure and flow in the SW Pacific Ocean, *Quaternary Science Rev.*, 27, 1886–1908,
1056 2008.

1057 Matsumoto, K.: Radiocarbon-based circulation age of the world oceans, *J. Geophys.*
1058 *Res.: Oceans* 112(C9), C09004. <https://doi.org/10.1029/2007JC004095>, 2007.

1059 Menviel, L., Spence, P., Yu, J., Chamberlain, M.A., Matear, R.J., Meissner K.J., and
1060 England, M.H.: Southern Hemisphere westerlies as a driver of the early deglacial
1061 atmospheric CO₂ rise, *Nature communications*, 9:2503, DOI:10.1038/s41467-018-
1062 04876-4, 2018.

1063 Millo, C., Sarnthein, M., and Erlenkeuser, M.: Variability of the Denmark Strait
1064 Overflow during the Last Glacial Maximum, *Boreas*, 35, 50-60, 2006.

1065 Muglia, J., Skinner, L., and Schmittner, A.: Weak overturning circulation and high
1066 Southern Ocean nutrient utilization maximized glacial ocean carbon, *Earth and*
1067 *Planetary Science Letters* 496, 47-56, 2018.

1068 Muschitiello, F., D'Andrea, W.J., Schmittner, A., Heaton, T.J., Balascio, N.L.,
1069 deRoberts, N., Caffee, M.W., Woodruff, T.E., Welten, K.C., Skinner, L.C., Simon, M.H.,
1070 and Dokken T.M.: Deep-water circulation changes lead North Atlantic climate during
1071 deglaciation, *Nature Communications* 10, 1272, doi.org/10.1038/s41467-019-09237-3,
1072 2019.

1073 Naughton, F., Costas, S., Gomes, S.D., Desprat, S., Rodrigues, T., Sanchez Goñi,
1074 M.F., Renssen, H., Trigo, R., Bronk-Ramsey, C., Oliveira, D., Salgueiro, E., Voelker,
1075 A.H.L., and Abrantes, F.: Coupled ocean and atmospheric changes during Greenland
1076 stadial 1 in southwestern Europe, *Quaternary Science Reviews*, 212, 108-120, 2019.

1077 Nydal R., Lovseth K., and Skogseth F. H.: Transfer of bomb ¹⁴C to the ocean surface,

1078 Radiocarbon 22(3), 626–635, 1980.

1079 Okazaki, Y., Sagawa, T., Asahi, H., Horikawa, K., and Onodera, J.: Ventilation
1080 changes in the western North Pacific since the last glacial period, *Climate of the Past*, 8,
1081 17-24, doi:10.5194/cp-8-17-2012, 2012.

1082 Paillard, D., Labeyrie, L., and Yiou, P.: Macintosh program performs time-series
1083 analysis, *Eos Trans, AGU*, **77**: 379, 1996.

1084 Rae, JW.B. and W. Broecker, W.: What fraction of the Pacific and Indian oceans'
1085 deep water is formed in the Southern Ocean? *Biogeosciences*, 15, 3779-3794, 2018.

1086 Rae, J., Sarnthein, M., Foster, G., Ridgwell, A., Grootes, P.M., and Elliott T.: Deep
1087 water formation in the North Pacific and deglacial CO₂ rise, *Paleoceanography*, 29,
1088 doi:10.1002/2013PA002570, 645–667, 2014.

1089 Rafter, P.A., Herguera, J.-C., and Southon, J.R.: Extreme lowering of deglacial
1090 seawater radiocarbon recorded by both epifaunal and infaunal benthic foraminifera in a
1091 wood-dated sediment core, *Climate of the Past* 14, 1977–1989, 2018.

1092 Reimer P.J., Bard, E., Bayliss, A., Beck, J. W., Blackwell, P.G., Bronk Ramsey, C.,
1093 Buck, C.E., Cheng, H., Edwards, R.L., and Friedrich, M.: IntCal13 and Marine13
1094 radiocarbon age calibration curves 0–50,000 years cal. BP, *Radiocarbon* 55, 1869–
1095 1887, 2013.

1096 Reimer, P.J., et al.: The IntCal 20 northern hemisphere radiocarbon calibration curve
1097 (0-55 kcal BP), *Radiocarbon*, 2020 (in press).

1098 Robinson, L.F., Adkins, J.F., Keigwin, L.D., et al.: Radiocarbon variability in the
1099 western North Atlantic during the last deglaciation, *Science*, 310, 1469-1473, 2005.

1100 Ronge, T. A., Tiedemann, R., Lamy, F., et al.: Radiocarbon constraints on the extent
1101 and evolution of the South Pacific glacial carbon pool, *Nature Comm.* 7:11487, 2016.

1102 Ronge, T.A., Sarnthein, M., Roberts, J., Lamy, F., and Tiedemann, R.: East Pacific
1103 Core PS75/059-2: Glacial-to-deglacial stratigraphy revisited, *Paleoceanography and*
1104 *Paleoclimatology*, 34 (4), 432-435, DOI:10.1029/2019PA003569, 2019.

1105 Sarnthein, M., Winn, K., Jung, S.J., Duplessy, J.C., Labeyrie, L., Erlenkeuser, H.,
1106 and Ganssen, G.: Changes in east Atlantic deepwater circulation over the last 30,000
1107 years: eight time slice reconstructions, *Paleoceanography*, 9(2), 209–267, 1994.

1108 Sarnthein, M., Pflaumann, U., and Weinelt, M.: Past extent of sea ice in the northern
1109 North Atlantic inferred from foraminiferal paleotemperature estimates,
1110 *Paleoceanography*, 18(2), 2003.

1111 Sarnthein, M., Grootes, P.M., Kennett, J.P., and Nadeau, M.: ¹⁴C Reservoir ages

1112 show deglacial changes in ocean currents and carbon cycle, *Geophys. Monograph –*
1113 *Am. Geophys. Union*, 173, 175–196, 2007.

1114 Sarnthein, M., Grootes, P.M., Holbourn, A., Kuhnt, W., and Kühn, H.: Tropical
1115 warming in the Timor Sea led deglacial Antarctic warming and almost coeval
1116 atmospheric CO₂ rise by >500 yr, *Earth Planetary Science Letters*, 302, 337-348, 2011.

1117 Sarnthein, M., Schneider, B., and Grootes, P.M.: Peak glacial 14C ventilation ages
1118 suggest major draw-down of carbon into the abyssal ocean, *Climate of the Past*, 9 (1),
1119 925–965, 2013.

1120 Sarnthein, M., Balmer, S., Grootes, P.M., and Mudelsee, M.: Planktic and benthic
1121 14C reservoir ages for three ocean basins, calibrated by a suite of 14C plateaus in the
1122 glacial-to-deglacial Suigetsu atmospheric 14C record, *Radiocarbon*, 57, 129–151, 2015.

1123 Sarnthein, M. and Werner, K.: Early Holocene planktic foraminifers record species-
1124 specific ¹⁴C reservoir ages in Arctic Gateway, *Marine Micropaleontology*, 135, 45-55.
1125 DOI:10.1016/j.marmicro.2017.07.002, 2018.

1126 Schlolaut, G.: A unique and easy-to-use-tool to deal with incompletely varved
1127 archives 782 – the Varve Interpolation Program 3.0.0, *Quaternary Geochronology*, 2019
1128 (in press).

1129 Schlolaut, G., Staff, R.A., Marshall, M.H., Brauer, A., Bronk Ramsey, C., Lamb, H.F.,
1130 and Nakagawa, T.: Microfacies analysis of the Lake Suigetsu (Japan) sediments from
1131 ~50 to ~10 ka BP and an extended and revised varve based chronology, *Quaternary*
1132 *Science Reviews*, 200, 351-366, 2018.

1133 Schmittner, A. and Lund, D.C.: Early deglacial Atlantic overturning decline and its
1134 role in atmospheric CO₂ rise inferred from carbon isotopes ($\delta^{13}\text{C}$), *Climate of the Past*,
1135 11, 135-152, 2015.

1136 Schroeder, J., Holbourn, A., Küssner, K., and Kuhnt, W.: Hydrological variability in
1137 the southern Makassar Strait during the last glacial termination, *Quaternary Science*
1138 *Reviews*, 154, 143-156, 2016.

1139 Sessford, E.G., Jensen, M.F., Tisserand, A.A., Muschitiello, F., Dokken, T.,
1140 Nisancioglu, K.H., and Jansen, E.: Consistent fluctuations on intermediate water
1141 temperature off the coast off Greenland and Norway during Dansgaard-Oeschger
1142 events, *Quaternary Science Reviews*, 223, 105887, 1-17, 2019.

1143 Sherriff-Tadano, S., Abe-Ouchi, A., Yoshimori, M., Oka, A., and Chan, W.-L.:
1144 (Influence of glacial ice sheets on the Atlantic meridional overturning circulation through
1145 surface wind change, *Climate Dynamics*, 50 (7-8), 2881–2903, 2017.

1146 Siani, G., Michel, E., De Pol-Holz, R., DeVries, T., Lamy, F., Carel, M., Isguder, G.,
1147 Dewilde, F., Lourantou, A.: Carbon isotope records reveal precise timing of enhanced
1148 Southern Ocean upwelling during the last deglaciation, *Nature Communications*, 4,
1149 2758, 2013.

1150 Sikes, E.L. and Guilderson, T.P.: Southwest Pacific Ocean surface reservoir ages
1151 since the last deglaciation: Circulation insights from multiple-core studies. *Paleocean-*
1152 *ography*, 31, 298–310, doi:10.1002/2015PA002855, 2016.

1153 Simstich, J., Sarnthein, M., and Erlenkeuser, H.: Paired $\delta^{18}\text{O}$ signals of
1154 *Neogloboquadrina pachyderma* (s) and *Turborotalita quinqueloba* show thermal
1155 stratification structure in Nordic Seas, *Mar. Micropaleontol.*, 912, 1–19, 2003.

1156 Skinner, L.C., Fallon, S., Waelbroeck, C., Michel, E., and Barker, S.: Ventilation of
1157 the deep Southern Ocean and deglacial CO₂ rise, *Science*, 328, 1147–1151, 2010.

1158 Skinner, L.C., Waelbroeck, C., Scrivner, A.E., and Fallon, S.J.: Radiocarbon
1159 evidence for alternating northern and southern sources of ventilation of the deep
1160 Atlantic carbon pool during the last deglaciation, *PNAS*, 111, 5480–5484, 2014.

1161 Skinner, L.C. *et al.*: Reduced ventilation and enhanced magnitude of the deep
1162 Pacific carbon pool during the last glacial period, *Earth Planetary Science Letters*, **411**,
1163 45-52, 2015.

1164 Skinner, L.C., Primeau, F., Freeman, E., de la Fuente, M., Goodwin, P.A.,
1165 Gottschalk, J., Huang, E., McCave, I.N., Noble, T.L., and Scrivner A.E.: Radiocarbon
1166 constraints on the glacial ocean circulation and its impact on atmospheric CO₂, *Nature*
1167 *communications*, 8:16010, DOI: 10.1038/ncomms16010, 2017.

1168 Skinner, L.C., Muschitiello, F., and Scrivner, A.E.: Marine reservoir age variability
1169 over the last deglaciation: Implications for marine carbon cycling and prospects for
1170 regional radiocarbon calibrations. *Paleoceanography and Paleoclimate*, 34,
1171 doi.org/10.1029/2019PA003667, 2019.

1172 Southon, J., Noronha, A.L., Cheng, H, Edwards, R.L., and Wang, Y.: A high-
1173 resolution record of atmospheric ¹⁴C based on Hulu Cave speleothem H82, *Quaternary*
1174 *Science Reviews*, 33:32-41, 2012.

1175 Steffensen, J.P., Andersen, K.K., Bigler, M., et al.: High-Resolution Greenland Ice
1176 Core Data Show Abrupt Climate Change Happens in Few Years, *Science*, 321, 680;
1177 DOI: 10.1126/science.1157707, 2008.

1178 Stern, J.V. and Lisiecki, L.E.: North Atlantic circulation and reservoir age changes
1179 over the past 41,000 years, *Geophysical Research Letters*, 40, 3693-3697,
1180 doi:10.1002/grl.5067, 2013.

1181 Stocker, T. and Johnsen, S.J.: A minimum thermodynamic model for the bipolar
1182 seesaw, *Paleoceanography*, 18 (4), 1087, doi:10.1029/2003PA000920, 2003.

1183 Stuiver, M. and Braziunas, T.V.: Modeling atmospheric ¹⁴C influences and ¹⁴C ages
1184 of marine samples to 10,000 B.C., *Radiocarbon*, 35, 137–189, 1993.

1185 Svensson, A., Andersen, K.K., Bigler, M., Clausen, H.B., Dahl-Jensen, D., Davies,
1186 S.M., Johnsen, S.J., Muscheler, R., Parrenin, F., Rasmussen, S.O., Röthlisberger, R.,
1187 Seierstad, I., Steffensen, J.P., and Vinther, B.M.: A 60 000 year Greenland stratigraphic
1188 ice core chronology, *Climate of the Past*, 4, 47–57, 2008.

1189 Toggweiler, J.R., Druffel, E.R.M., Key, R.M., and Galbraith, E.D.: Upwelling in the
1190 ocean basins north of the ACC. Part 2: How cool Subantarctic water reaches the
1191 surface in the tropics, *J. Geophysical Research*, DOI:[10.1029/2018JC014795](https://doi.org/10.1029/2018JC014795), 2019 (in
1192 press).

1193 Turney, C.S.M., Fifield, L.K., Hogg, A.G., et al.: Using New Zealand kauri (*Agathis*
1194 *australis*) to test the synchronicity of abrupt climate change during the Last Glacial
1195 Interval (60,000–11,700 years ago), *Quatern. Sci. Rev.*, 29, 3677–3682, 2010.

1196 Turney, C.S.M., Jones, R.T., Phipps, S.J., et al.: Rapid global ocean-atmosphere
1197 response to Southern Ocean freshening during the last glacial, *Nature communications*,
1198 8:520, doi:10.1038/s41467-017-00577-6, 2017.

1199 Umling, N.E. and Thunnell, R.C.: Synchronous deglacial thermocline and deep-
1200 water ventilation in the eastern equatorial Pacific, *Nature communications*, 8, 14203.
1201 DOI: 10.1038/ncomms14203, 2017.

1202 Waelbroeck, C., Duplessy, J.-C., Michel, E., Labeyrie, L., Paillard, D., and Duprat, J.:
1203 The timing of the last deglaciation in North Atlantic climate records, *Nature*, 412, 724–
1204 727, 2001.

1205 Waelbroeck, C., Skinner, L.C., Labeyrie, L., Duplessy, J.-C., Michel, E., Riveiros,
1206 N.V., Gherardi, J.-M., and Dewilde, F.: The timing of deglacial circulation changes in the
1207 Atlantic, *Paleoceanography*, 26, PA3213, <https://doi.org/10.1029/2010PA002007>, 2011.

1208 Wallmann, K., Schneider, B., and Sarnthein, M.: Effects of eustatic sea-level
1209 change, ocean dynamics, and nutrient utilization on atmospheric pCO₂ and seawater
1210 composition over the last 130,000 years – a model study, *Climate of the Past*, 12, 339-
1211 375, doi: 10.5194/cp-12-339-2016, 2016.

1212 Wang Y.C, Cheng, H., Edwards, R.L., An, Z.S., Wu, J.Y., Shen, C.-C., and Dorale,
1213 J.A.: A high-resolution absolute-dated Late Pleistocene monsoon record from Hulu
1214 Cave, China, *Science*, 294, 2345-2348. DOI: 10.1126/science.1064618, 2001.

1215 Wang, L.J., Sarnthein, M., Erlenkeuser, H., Grimalt, J., Grootes, P., Heilig, S.,
1216 Ivanova, E., Kienast, M., Pelejero, C., and Pflaumann, U.: East Asian monsoon climate
1217 during the late Pleistocene: High-resolution sediment records from the South China
1218 Sea, *Marine Geology*, 156, 245-284, 1999.

1219 Wang, P., Clemens, S., Beaufort, L., Braconnot, P., Ganssen, G., Jian, Z., Kershaw,
1220 P., and Sarnthein, M.: SCOR/IMAGES Working Group 113 SEAMONS: Evolution and
1221 variability of the Asian Monsoon System: State of the art and outstanding issues,
1222 *Quaternary Science Reviews*, 24 (5-6), 595-629, 2005.

1223 **WAIS Divide Project Members: Onset of deglacial warming in West Antarctica driven**
1224 **by local orbital forcing. *Nature*, 500, 440-444. doi:10.1038/nature12376, 2013.**

1225 Xu, J., Kuhnt, W., Holbourn, A., Regenber, M., and Andersen, N.: Indo-Pacific
1226 Warm Pool variability during the Holocene and Last Glacial Maximum, *Paleoceanogr.*,
1227 25, 16, 2010.

1228 Yamamoto, A., Abe-Ouchi, A., Ohgaito, R., Ito, A., and Oka, A.: Glacial CO₂
1229 decrease and deep-water deoxygenation by iron fertilization from glaciogenic dust,
1230 *Climate of the Past*, 15, 981-996.

1231 Yashayaev, I., Seidov, D., and Demirov, E.: A new collective view of oceanography
1232 of the Arctic and North Atlantic basins, *Progress in Oceanography*, 132, 21 pp.,
1233 DOI:<http://dx.doi.org/10.1016/j.pocean.2014.12.012>, 2015.

1234 Zhao, N. and Keigwin, L.D.: An atmospheric chronology for the glacial-deglacial
1235 Eastern Equatorial Pacific, *Nature communications*, 9:3077, DOI:10.1038/s41467-018-
1236 05574-x, 2018.

1237 Zhao, N., Marchal, O., Keigwin, L., Amrhein, D., and Gebbie, G.: A synthesis of
1238 deep-sea radiocarbon records and their (in) consistency with modern ocean ventilation,
1239 *Paleoceanography and Paleoclimatology*, 33, 128-151, 2018.

1240 TABLE CAPTIONS

1241

1242 **∇ Table 1 a and b.** Summary of varve- and U/Th model-based age estimates (Schlolut
 1243 et al., 2018; Bronk Ramsey et al., 2012) for ~30 plateau (pl.) boundaries in the
 1244 atmospheric ¹⁴C record identified in Lake Suigetsu Core SG06₂₀₁₂ by means of visual
 1245 inspection over the interval 10.5–27 cal. ka (Sarnthein et al., 2015, suppl. and modified).
 1246 At the right hand side, three columns give the average (Ø) and uncertainty range of ¹⁴C
 1247 ages for each ¹⁴C plateau.

1248

SUIGETSU SG06_2012 Plateau no.	Plateau Top Varve-based age (yr BP)	U/Th-based age (yr BP)	Depth (cm c.d.)	Plateau Base Varve-based age (yr BP)	U/Th-based age (yr BP)	Depth (cm c.d.)	Ø 14C Age of 14C Plateau (14C yr)	±Uncertainty (14C yr)	14C age BP min/max. (1.6 σ range)
'Preboreal'	10525	10560	1325	11100	11108	1383	9525	–170/+110	9356/9635
'Top YD'	11290	11281	1402	11760	11755	1453	10060	–100/+35	9963/10095
'YD'	11950	11895	1467	12490	12475	1525	10380	–170/ 124	10211 10504
1a	13580	13656	1626	13980	14042	1657	12006	100	11857 12050
1	14095	14160	1666	15095	15100	1740	12471	185	12315 12683
2a	15310	15420	1754	16140	16520	1802	13406	245	13174 13665
2b	16075	16520	1802	16400	16930	1820	13850	40	13808 13885
3	16835	17500	1847	17500	18220	1888	14671	105	14582 14792
4	17880	18650	1913	18830	19590	1971	15851	190	15661 16044
5a	18960	19720	1978	19305	20240	2003	16670	90	16570

1249

									16750
5b	19305	20240	2003	20000	20900	2032	17007	190	16830 17247
6a	20190	21000	2050	20920	21890	2105	17667	262	17435 17960
6b	20920	21890	2105	21275	22300	2132	18075	140	17960 18240
7	21375	22400	2140	21790	22870	2171	18843	117	18741 18975
8	21835	22940	2175	22730	24250	2257	19715	-290 325	19425 20041
9	22730	24250	2257	23395	25150	2312	20465	-227 263	20238 20728
10a	23935	25880	2358	25080	27000	2400	22328	-380 270	21946 22600
10b	25080	27000	2400	25800	27600	2426	22708	-475 440	22233 23147
11	26110	27770	2443	27265	28730	2525	24088	-360 505	23727 24595

1250

1251

1252

1253 **Table 2.** Temporal match of various ¹⁴C plateaus with deglacial periods of major
 1254 atmospheric CO₂ rise and ocean warmings (AA = Antarctic; GIS = Greenland
 1255 Interstadial).

pCO ₂ RISE (~12 ppm)	Plateau no.	Plateau boundaries
AGE based on annual layers AA ice core (Marcott et al. 2014)		AGE range (cal. ka) based on U/Th model ages (Bronk Ramsey et al., 2012)
11.7 – 11.5	# 'Top YD'	11.83 – 11.3
14.8 – 14.53	# 1	15.1 – 14.2
16.4 – 16.15	# 2a	16.52 – 15.5
17.4 – ~17.1	(data gap)	17.3 – 17.1

FURTHER POTENTIAL CORRELATIVES:

Progressive N. Atlantic warming during the YD at 12.39 – 12.03 ka *	# 'YD'	12.46 – 11.98
Onset of Antarctic ** warming at 18.3–17.6 ka (ice-based time scale)	#3	18.22 – 17.5
Onset of North Atlantic *** warming at 19.3–18.6 ka (U/Th-based time scale)	# 4	19.6 – 18.65
Top H2: GIS 2 N. Atlantic warming at 23.4 – 23.3 ka ****	#8	24.25 – 22.95

AGE CONTROL based on

* Naughton et al. (2019), ** Kawamura et al. (2007),

*** Balmer and Sarnthein (2018), **** Grootes and Stuiver (1997)

1256

1257 **Table 3** a-c. ¹⁴C reservoir / ventilation ages of surface (top 50-100 m) and bottom
 1258 waters vs. U/Th-based model age at 19/22 core sites in the ocean. (a) Spatial and
 1259 temporal changes over **early and late LGM** (24–21 and 21–18.7 cal. ka), (b) HS-1, and
 1260 the B/A. **Late LGM estimates (average res. age of Plateau 4-5)** are compared to model-
 1261 based estimates of Muglia et al. (2018). (c) Data sources. For core locations see Fig. 7.

1262

1263 (a)

Sediment Core U/Th-based model age Plateau (Pl.) no.	Latitude	Longitude	Water depth (m)	LGM pla. res. age				LGM model res. age	
				24–21 ka (early LGM)		21–18.7 ka (late LGM)		strong AMOC	weak
				Pl. 8 - 7 - 6	Error (yr)	Pl. 5 - 4	Error (yr)	(yr)	(yr)
ATLANTIC O.									
PS2644	67°52.02'N	21°45.92'W	777	2100	±390	1920–2200	±325 –±125	1136	1100
GIK 23074	66°66.67'N	4°90'E	1157	620–790	±145–±270	550–1175	±100–±200	1054	1059
MD08-3180	38°N	31°13.45'W	3064	–	–	320–605	±125–±405	827	887
SHAK06-5K (= MD99-2334)	37°34'N (37°48'N)	10°09'W 10°10'W	2646 3146	700–930	–	330–650	–	872	855
ODP 1002	10°42.37'N	65°10.18'W	893	700–210	±230–±310	25 – -205	±205–±215	751	738
GeoB 3910-1	4°15'S	36°21'W	2361	–	–	–	–	779	796
GeoB 1711-4	23°17'S	12°23'W	1976	1080	±290	730–840	±240–±190	711	721
KNR 159-5-36GC	27°31'S	46°48'W	1268	540	±140	870	±120	757	777
MD07-3076	44°4'S	4°12'W	3770	–	–	2300	±200	928	989
INDIAN O./TIMOR SEA									
MD01-2378	13°08.25'S	121°78.8'E	1783	–	–	2000–1700	±300–±320	885	890
PACIFIC O.									
MD02-2489	54°39.07'N	148°92.13'W	3640	–	–	1560–1110	±310–±335	972	965
MD01-2416	51°26.8'N	167°72.5'E	2317	–	–	1710	±440	1227	1202
ODP 893A	34°17.25'N	120°02.33'W	588	–	–	1065	±280	839	846
MD02-2503	34°16.6'N	120°01.6'W	580	–	–	–	–	839	846
GIK 17940	20°07.0'N	117°23.0'E	1727	1820–1260	±320–±230	hiatus	–	836	838
(= SO50-37)	18°55'N	115°55'E	2655	1820–1260	–	–	–	836	840
PS75/104-1	44°46'S	174°31'E	835	1650–1280	–	1500	–	881	895
(= SO213-84)	45°7.5'S	174°34.9'E	972	1650–1280	–	1500	–	881	895
MD07-3088	46°S	75°W	1536	380	–	200-350	–	917	–
SO213-76-2	46°13'S	178°1.7'W	4339	–	–	1600–1560	–	915	842
PS97/137-1	52°39.5'S	75°33.9'E	1027	2290–2110	–	2400–1800	–	1505	1419

1264

1265

1266 (b)

Sediment Core U/Th-based model Plateau (Pl.) no.	HS-1 pla. res. age		16.5–15.5 ka		B/A pla. res. age		LGM be. vent age		LGM b.w. model age			
	18 –16.5 ka		Pl. 3 - 2b (yr)	Error (yr)	Pl. 2a (yr)	Error (yr)	Pl. 1 - 1a	Error (yr)	(yr)	strong AMOC weak	(yr)	(yr)
ATLANTIC O.												
PS2644	1775–1660	±105–±160	1900	±355	–	–	–	–	345	2400	948	918
GIK 23074	1730–2000	±125–±160	670	±310	140–310	±250–±100	–	–	375	375	960	931
MD08-3180	1420–1610	±310–±160	1460	±390	630–360	±310	–	–	600	600	1031	1004
SHAK06-5K (= MD99-2334)	350–420	–	550	–	800–1200	–	–	–	–	–	–	–
ODP 1002	–100 – 20	±140	90	±345	355	±200	–	–	2200–2700	1900	–	–
GeoB 3910-1	630–560	±160–±180	175	±475	210–230	±220–±110	–	–	2150	2150	–	–
GeoB 1711-4	660–690	±195–±45	420	±320	880	±255	–	–	1500	1500	1387	1714
KNR 159-5-36GGC	460–340	±380–±300	170	±700	180–230	±370–±310	–	–	1470	1470	1354	1563
MD07-3076	1650	±180	–	–	920	±230	–	–	3640	3640	1653	2060
INDIAN O./TIMOR SEA												
MD01-2378	740	±125	–	–	200–185	±345–±135	–	–	2720	–	1679	1881
PACIFIC O.												
MD02-2489	800–550	±155–±120	550	±305	440	±285	–	–	–	2625	2332	2595
MD01-2416	1480–1140	±135–±195	–	–	720–570	±285–±140	–	–	–	3700/510	2400	2683
ODP 893A	1065–1490	±280–±125	1400	±370	520	±185	–	–	–	1430	1677	1705
MD02-2503	965–1365	±160–±165	1215	±325	395–535	±240–±130	–	–	–	–	–	–
GIK 17940	1210–1370	±200–±470	1045	±320	870–970	325–±100	–	–	3300–1800	–	1807	1897
(= SO50-37)	–	–	–	–	–	–	–	–	3225	3225	2373	2667
PS75/104-1 (= SO213-84)	1050	–	1100	–	800–250	–	–	–	–	–	–	–
MD07-3088	800–1090	–	1010	–	730–940	–	–	–	1500	2400	1101	1146
SO213-76-2	200	–	–	–	–	–	–	–	1600	1600	1808	1701
PS97/137-1	1500–670	–	435	–	–	–	–	–	4685	4685	1712	2001
									3300	2100	1631	1871

1267

1268 (c)

Sediment Core	DATA Source
ATLANTIC O.	
PS2644	Samthein et al. 2015 Be.data suppl.
GIK 23074	Samthein et al. 2015
MD08-3180	Balmer et al. 2018
SHAK06-5K (= MD99-2334)	Ausin et al., 2019 Skinner et al. 2014
ODP 1002	Samthein et al. 2015
GeoB 3910-1	Balmer et al. 2016
GeoB 1711-4	Balmer et al. 2016
KNR 159-5-36GGC	Balmer et al. 2016 data suppl.
MD07-3076	Balmer et al. 2016
INDIAN O./TIMOR SEA	
MD01-2378	Samthein et al. 2015
PACIFIC O.	
MD02-2489	Samthein et al. 2015
MD01-2416	Samthein et al. 2015 modified
ODP 893A	Samthein et al. 2015 data suppl.
MD02-2503	Samthein et al. 2015
GIK 17940 (= SO50-37)	Samthein et al. 2015
PS75/104-1 (= SO213-84)	Küssner et al., 2018 Ronge et al., 2016
MD07-3088	Küssner et al., 2019
SO213-76-2	Küssner et al., 2019
PS97/137-1	Küssner et al., 2019

1269

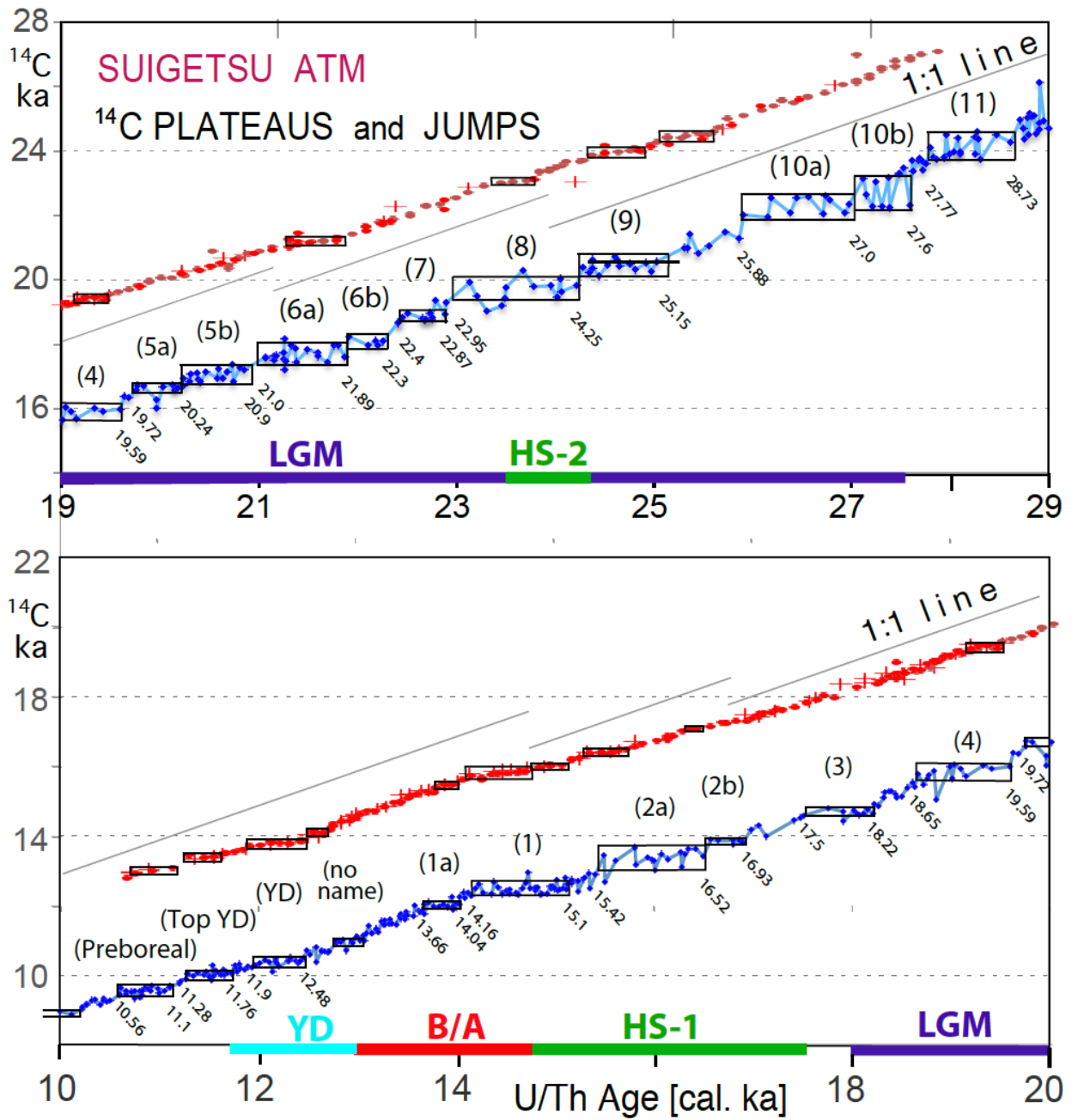
1270

1271

1272 FIGURE CAPTIONS

1273

1274 – Fig. 1. Atmospheric ^{14}C ages of Lake Suigetsu plant macrofossils 10–20 cal. ka
1275 (bottom panel) and 19–29 cal. ka (top panel) vs. U/Th-based model age (blue dots;
1276 Bronk Ramsey et al., 2012). The 1:1 line reflects gradient of one ^{14}C yr / cal. yr. Double
1277 and triple ^{14}C measurements are averaged. (In part large) error bars of single ^{14}C ages
1278 are given in Suppl. Fig. S1. Suite of labeled horizontal boxes that envelop scatter bands
1279 of largely constant ^{14}C ages shows ^{14}C plateaus longer than 250 yr (plateau boundary
1280 ages listed in Table 1). Red and brown dots (powder samples from trench and wall) and
1281 + signs (off-axis samples) depict raw ^{14}C ages of Hulu stalagmites H82 and MSD
1282 (Cheng et al., 2018; Southon et al., 2012; plot offset by +3000 ^{14}C yr). Suite of short ^{14}C
1283 plateaus (black boxes) tentatively assigned to Hulu-based record occupies age ranges
1284 slightly different from those deduced for Suigetsu-based plateaus. The difference
1285 possibly results from short-term changes in the Old / Dead Carbon Fraction (ocf / dcf)
1286 that in turn may reflect major short-term changes in LGM and deglacial monsoon
1287 climate (Wang et al., 2001; Kong et al., 2005).

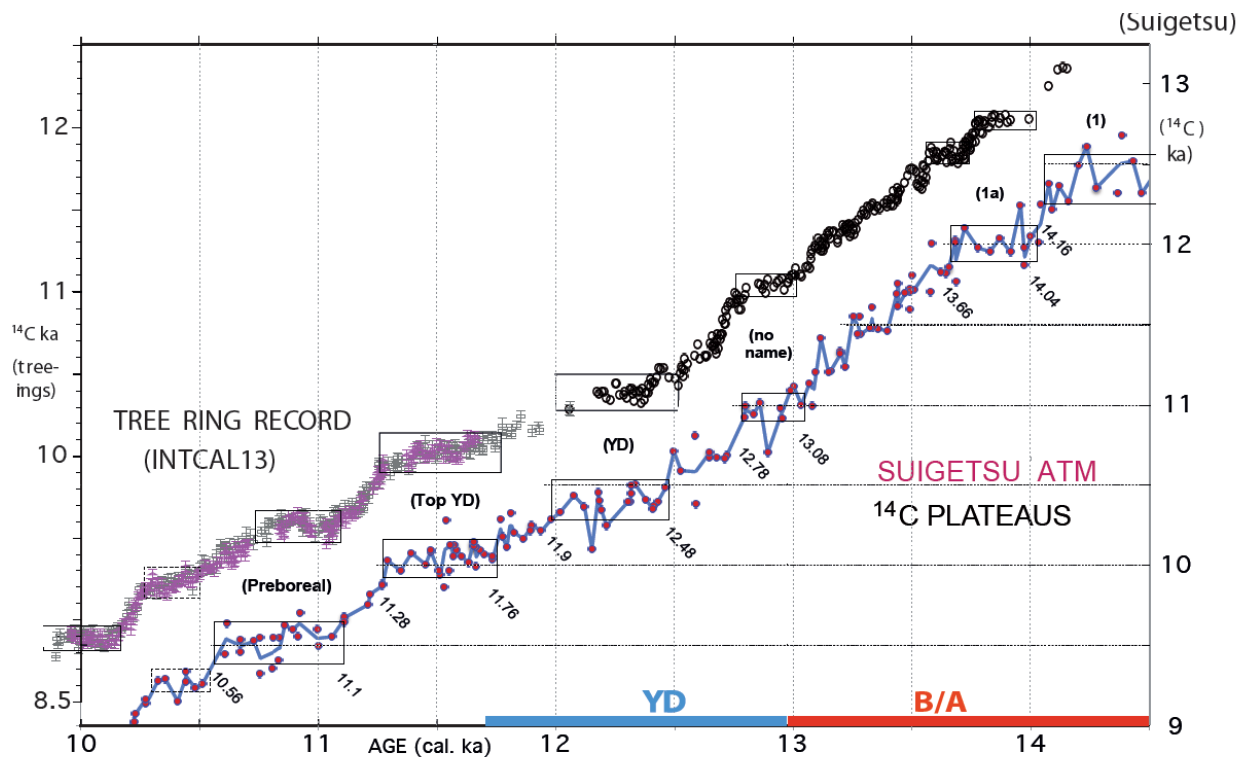


1288

1289

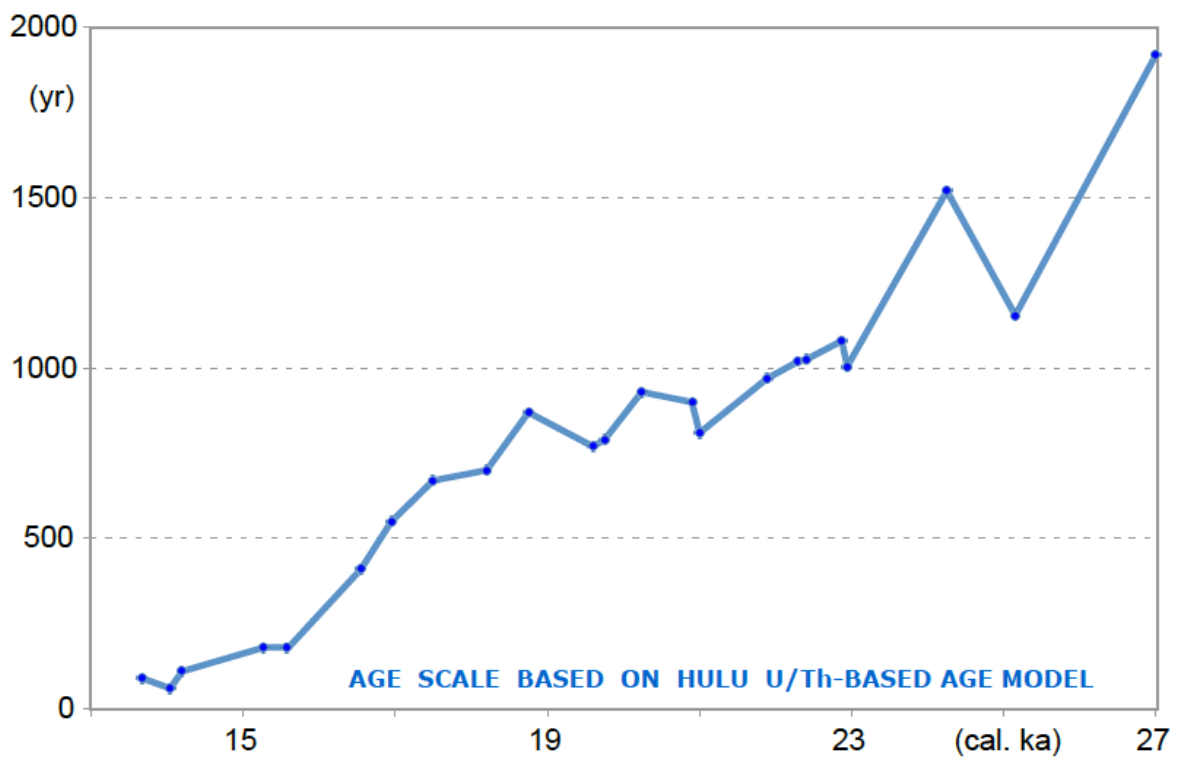
1290

1291 √ Fig. 2. High-resolution record of atmospheric ¹⁴C jumps and plateaus (= suite of
 1292 labeled horizontal boxes that envelop scatter bands of largely constant ¹⁴C ages
 1293 extending over >300 cal. yr) in a sediment section of Lake Suigetsu vs. tree ring-based
 1294 ¹⁴C jumps and plateaus 10–14.5 cal. ka (Reimer et al., 2013). Blue line averages paired
 1295 double and triple ¹⁴C ages of Suigetsu plant macrofossils. Age control points (cal. ka)
 1296 follow varve counts (Scholaut et al., 2018) and U/Th model-based ages of Bronk
 1297 Ramsey et al. (2012). YD = Younger Dryas, B/A = Bølling-Allerød.
 1298



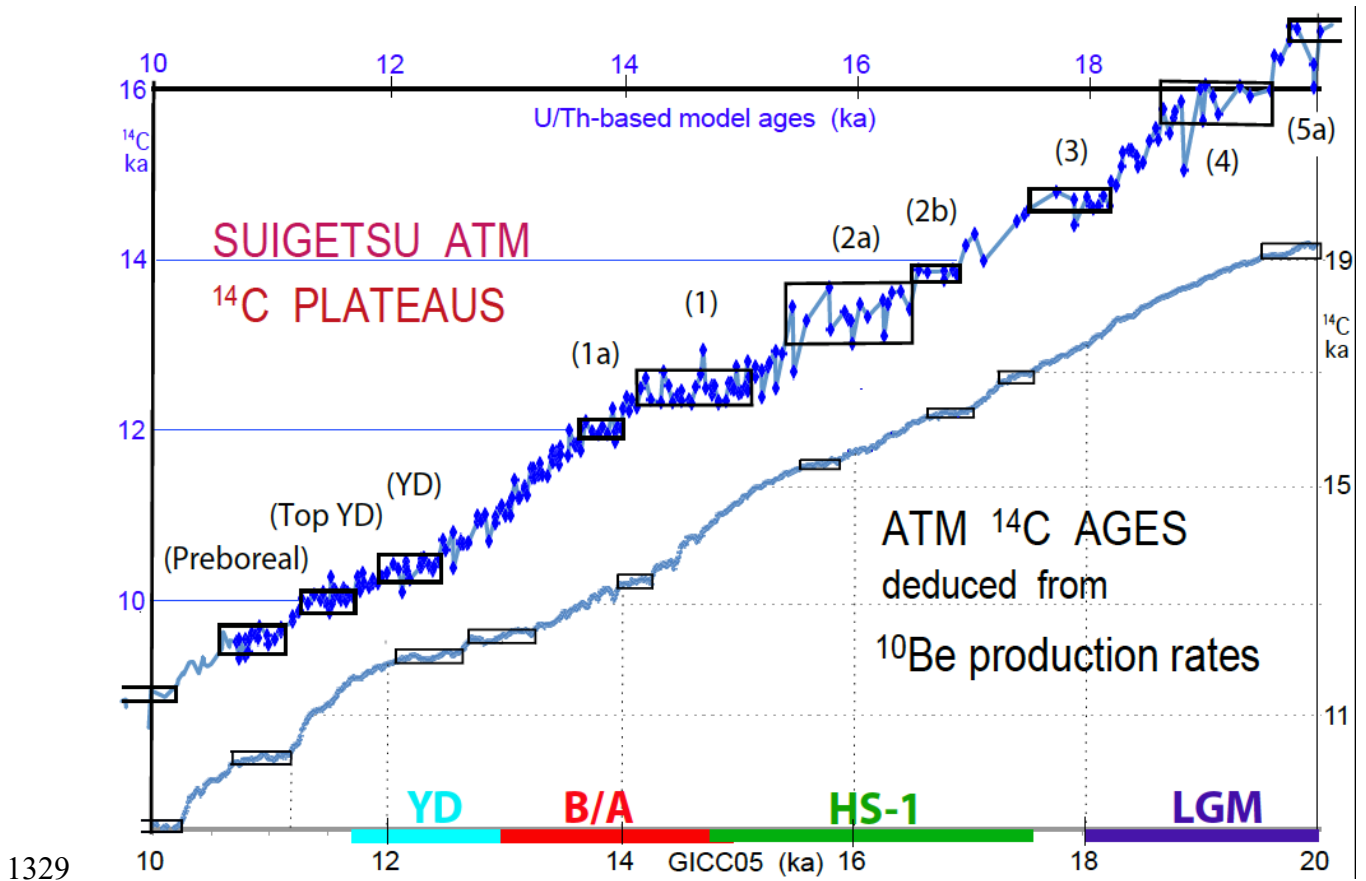
1299
 1300
 1301
 1302
 1303
 1304
 1305
 1306
 1307
 1308
 1309

1310 √ Fig. 3. Difference between Hulu Cave U/Th-based model ages (Southon et al., 2012;
1311 Bronk Ramsey et al., 2012; Cheng et al., 2018) and varve count-based cal. ages for
1312 atmospheric ¹⁴C plateau boundaries in Lake Suigetsu sediment record (Schlollaut et al.,
1313 2018) (Sarnthein et al., 2015, suppl. and revised), displayed on the U/Th-based time
1314 scale 13–27 cal. ka.
1315

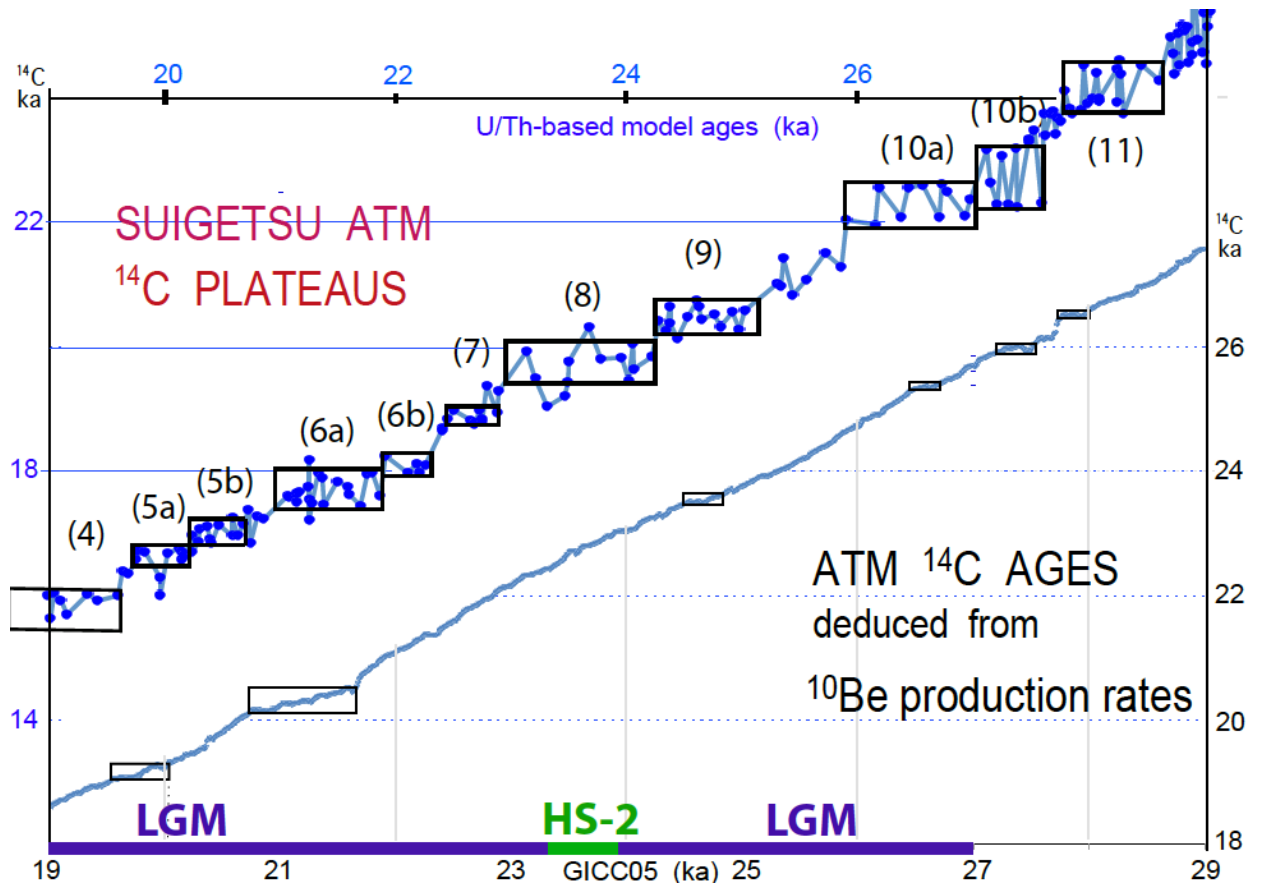


1316
1317
1318
1319
1320
1321
1322
1323
1324

1325 √ Fig. 4 a and b. Atmospheric ^{14}C ages and plateaus (horizontal boxes) deduced from
 1326 ^{10}Be production rates vs. GICC05 age scale (Adolphi et al., 2018) compared to the
 1327 Suigetsu record of atmospheric ^{14}C plateaus vs. Hulu U/Th-based model ages (Southon
 1328 et al., 2012; Cheng et al., 2018) for the intervals a) 10-20 and b) 19-29 cal ka BP.



1329



1330

1331

1332

1333

1334

1335

1336

1337

1338

1339

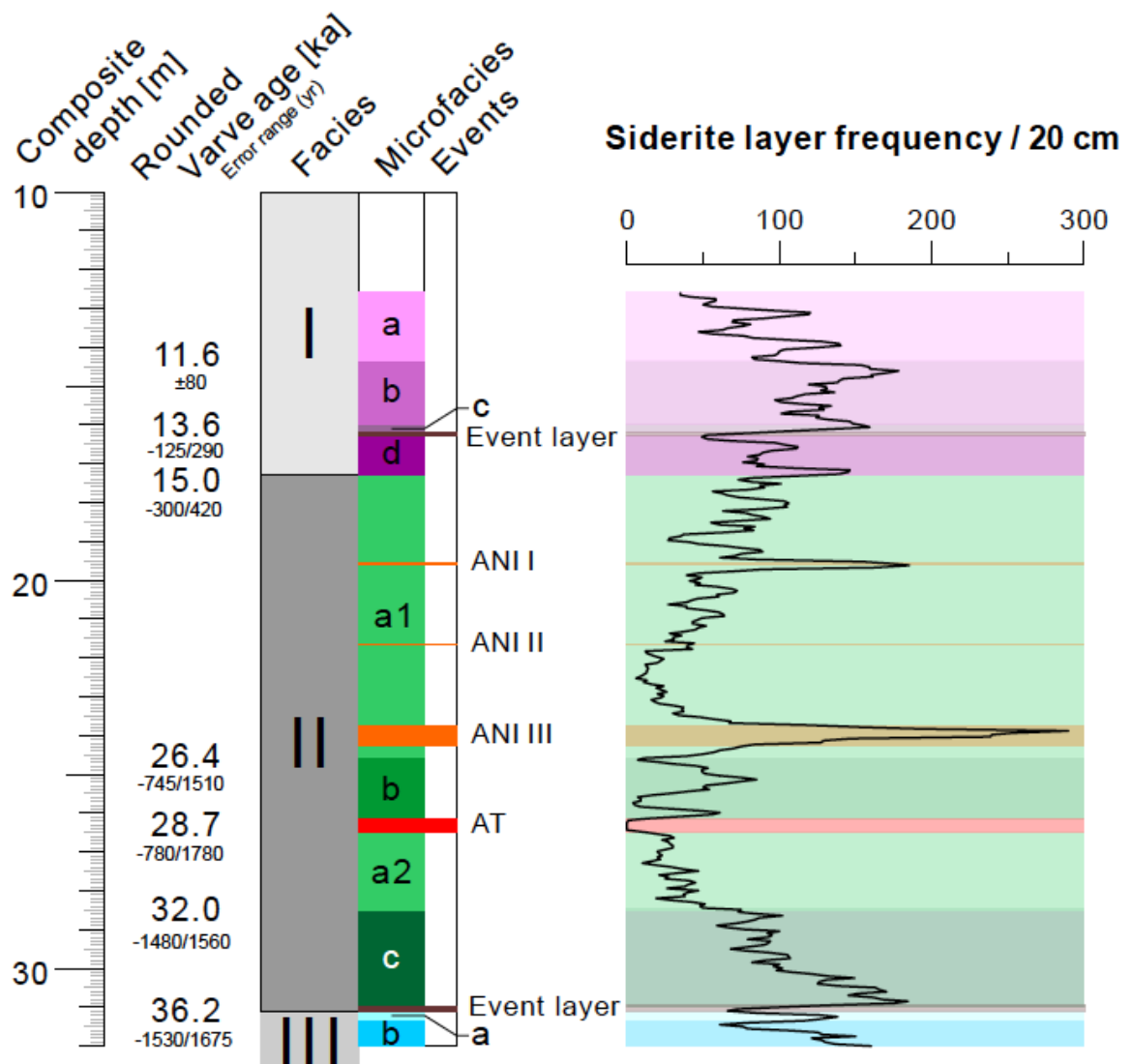
1340

1341

1342

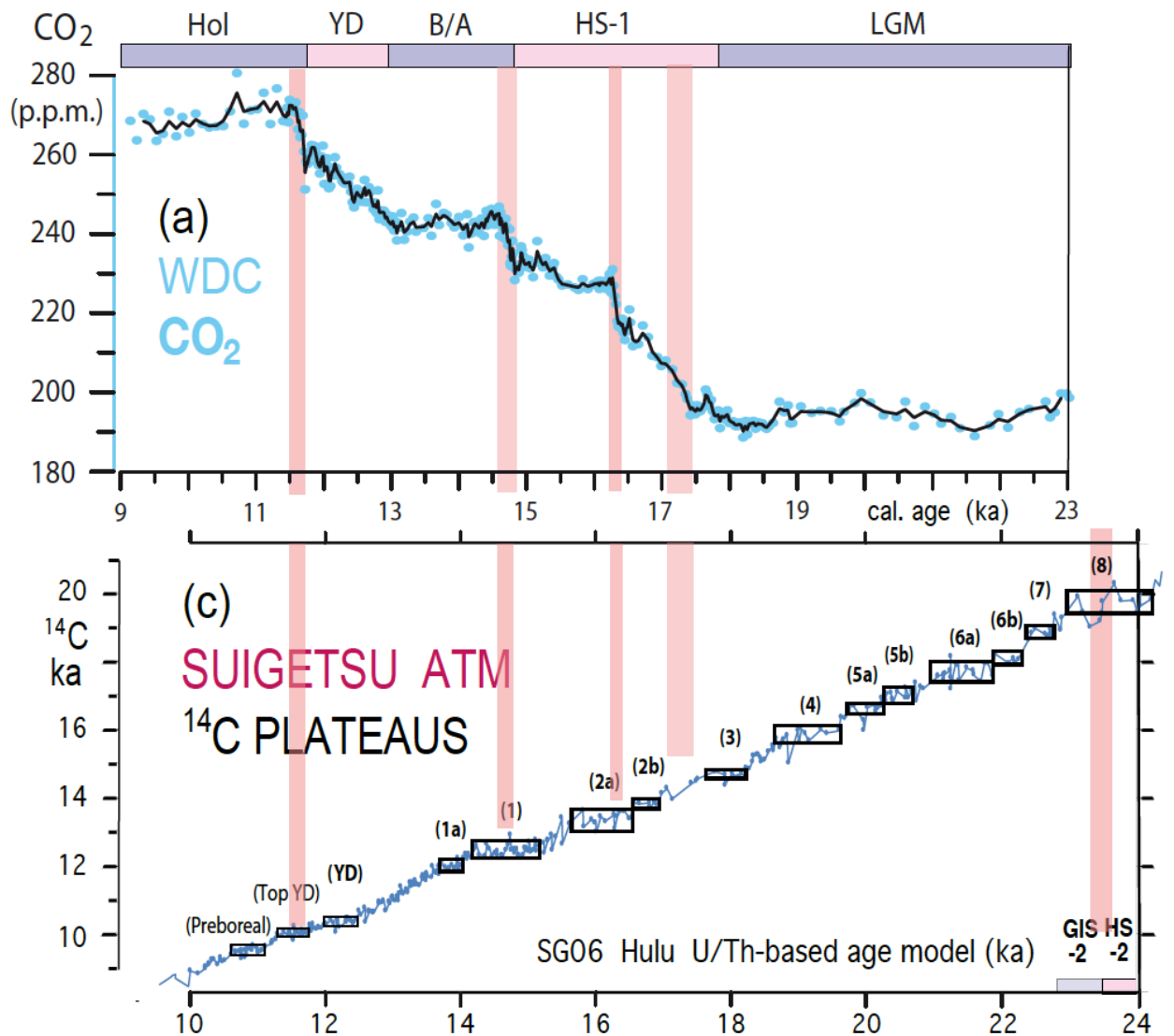
1343

1344 √ Fig. 5. Sediment facies and microfacies zones in Lake Suigetsu Core SG06, ~13–32
 1345 m depth (simplified and suppl. from Schlolaut et al., 2018). Microscopy-based frequency
 1346 of siderite layers with quality level 1–3 (= running average of layer counts per 20 cm
 1347 thick sediment section) serves as measure of seasonal lamination quality and shows
 1348 gradual transitions between varved and poorly varved sediment sections. Rounded
 1349 varve ages are microscopy based and constrain age of major facies and microfacies
 1350 boundaries. ANI I to ANI III mark core sections with ultrafine lamination due to
 1351 sedimentation rate minima, AT marks tephra layer named AT, ‘Event layers’ label major
 1352 thin mud slides probably earth quake-induced.s



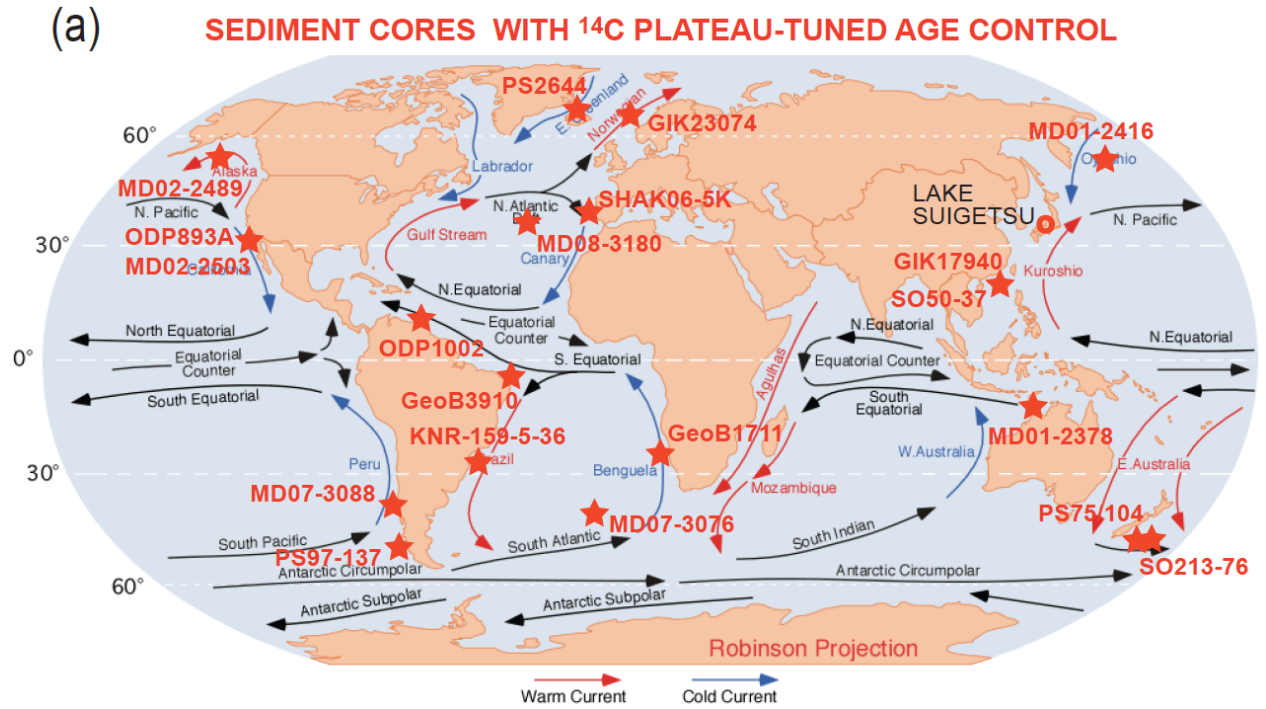
1353

1354 √ Fig. 6 (a). Four sudden steps (pink bars) in the deglacial atmospheric CO₂ rise at
 1355 West Antarctic Ice Sheet Divide ice core (WDC) reflect events of fast ocean degassing,
 1356 that may have contributed to the origin of deglacial ¹⁴C plateaus. Age control based on
 1357 ice cores (Marcott et al., 2014). (b) The steps are compared to suite of atmospheric ¹⁴C
 1358 plateaus dated by Hulu U/Th-based model ages (Bronk Ramsey et al., 2012). Hol =
 1359 Holocene; YD = Younger Dryas; B/A = Bølling-Allerød; HS = Heinrich stadials 1 and 2;
 1360 LGM = Last Glacial Maximum, GIS-2 = Greenland interstadial 2.
 1361

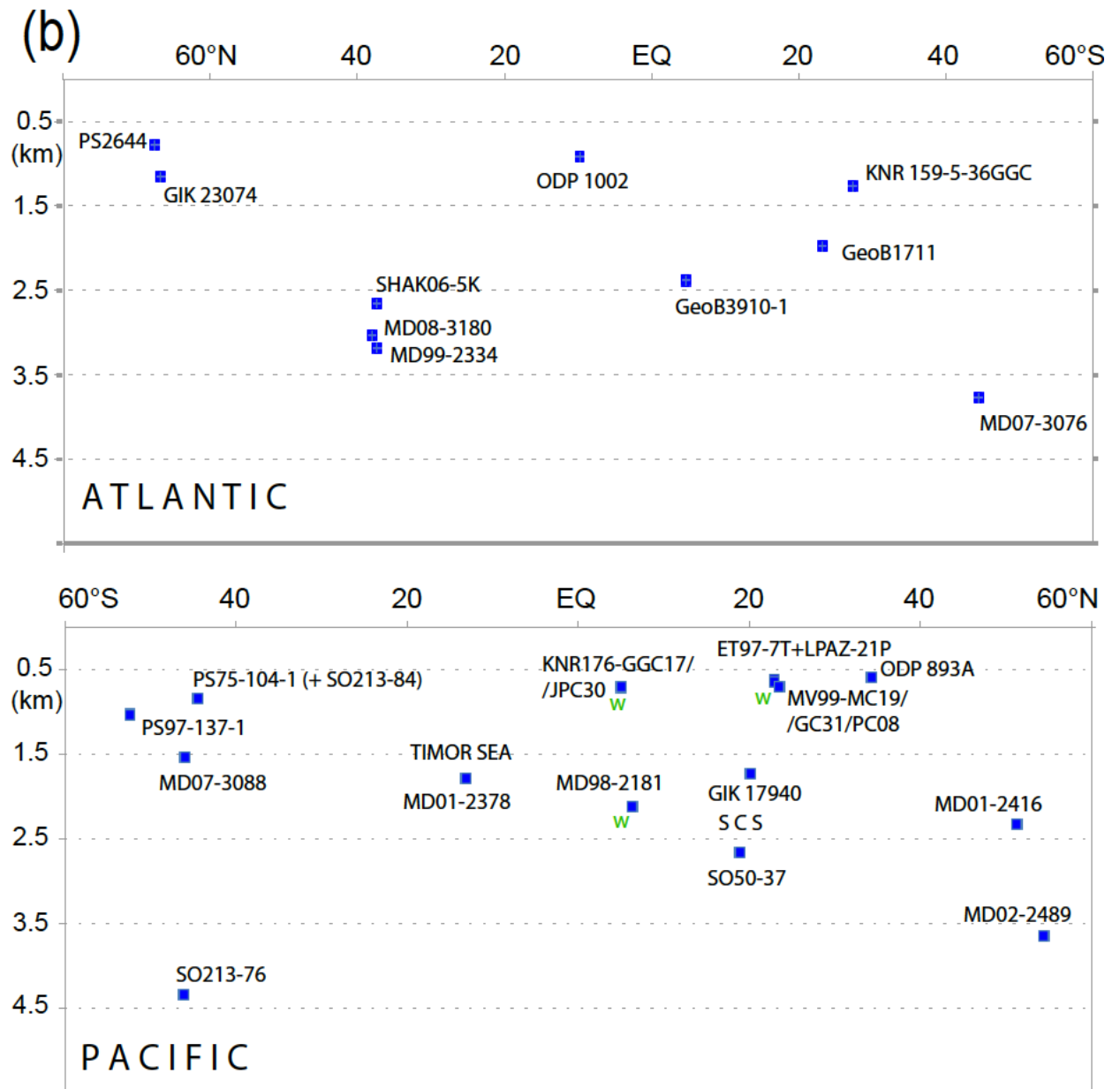


1362
 1363

1364 √ Fig. 7. Location (a) and water depth (km) (b) of sediment cores with age control based
 1365 on ^{14}C plateau tuning. ^{14}C reservoir ages of cores labeled with 'w' are derived from
 1366 samples with paired wood chunks and planktic foraminifers.



1367

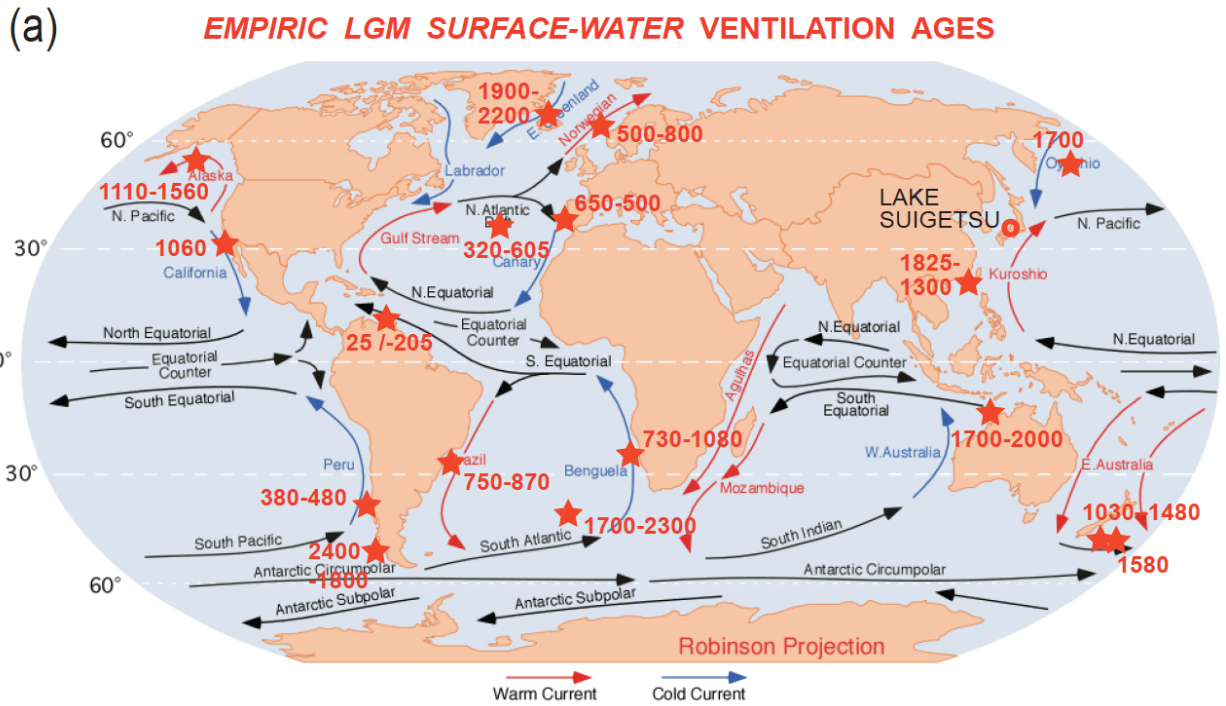


1368

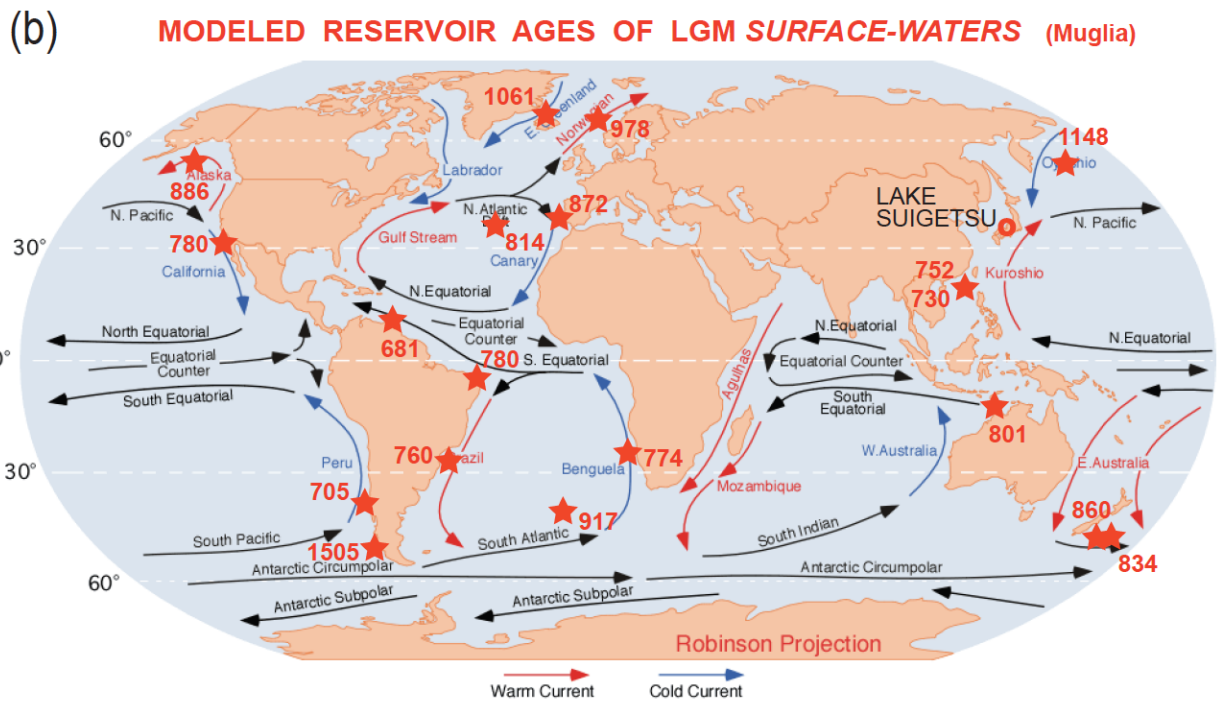
1369

1370 √ Fig. 8. Global distribution of ^{14}C reservoir ages of Late LGM surface waters estimated
 1371 (a) by means of ^{14}C plateau tuning of planktic ^{14}C records. (b) Model-based estimates
 1372 (GCM of Muglia et al., 2018, assuming an AMOC strength of 13 Sv) for sites with
 1373 plankton-based age values. X-Y graph (c) and map (d) show (rounded) differences
 1374 between observed and modeled values and their intra-LGM trends. Minor differences
 1375 are displayed in magenta, larger differences of >400 yr in red. Planktic habitat depths
 1376 and model estimates are largely confined to 0–100 m water depth. Arrows of surface

1377 currents delineate different sea regions important to assess potential limits of spatial
 1378 extrapolation of reservoir ages. Distribution of core numbers and references for ^{14}C
 1379 records are given in Table 3a-c and Fig. 7a.

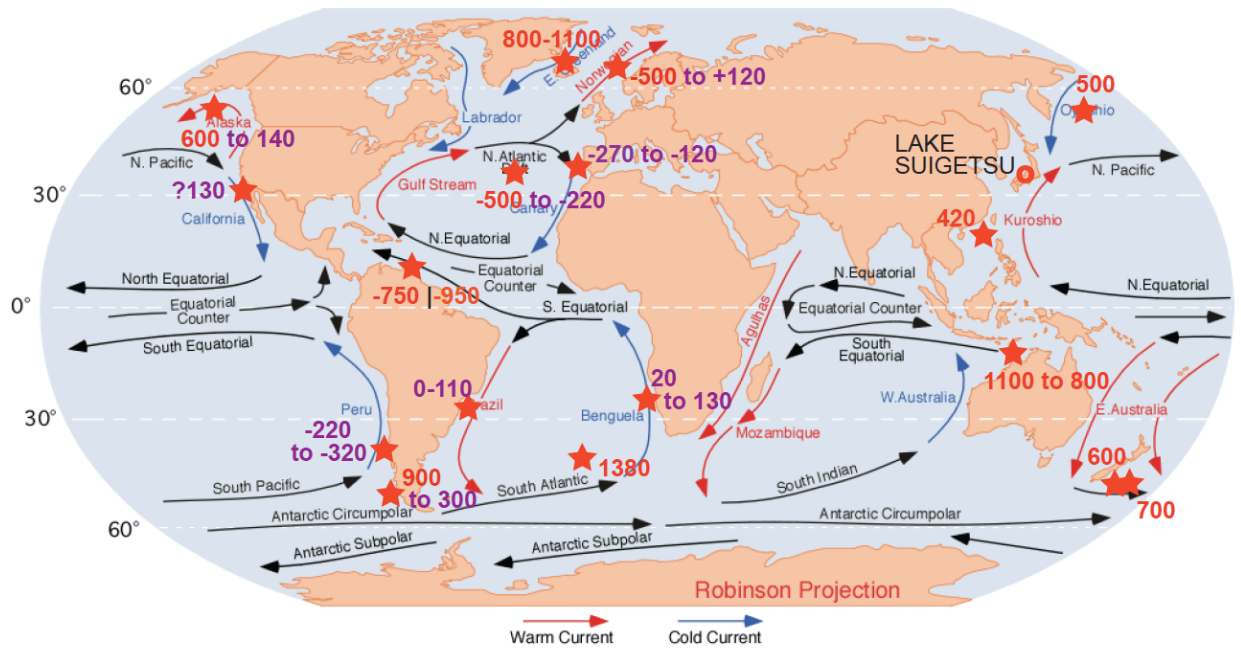


1380



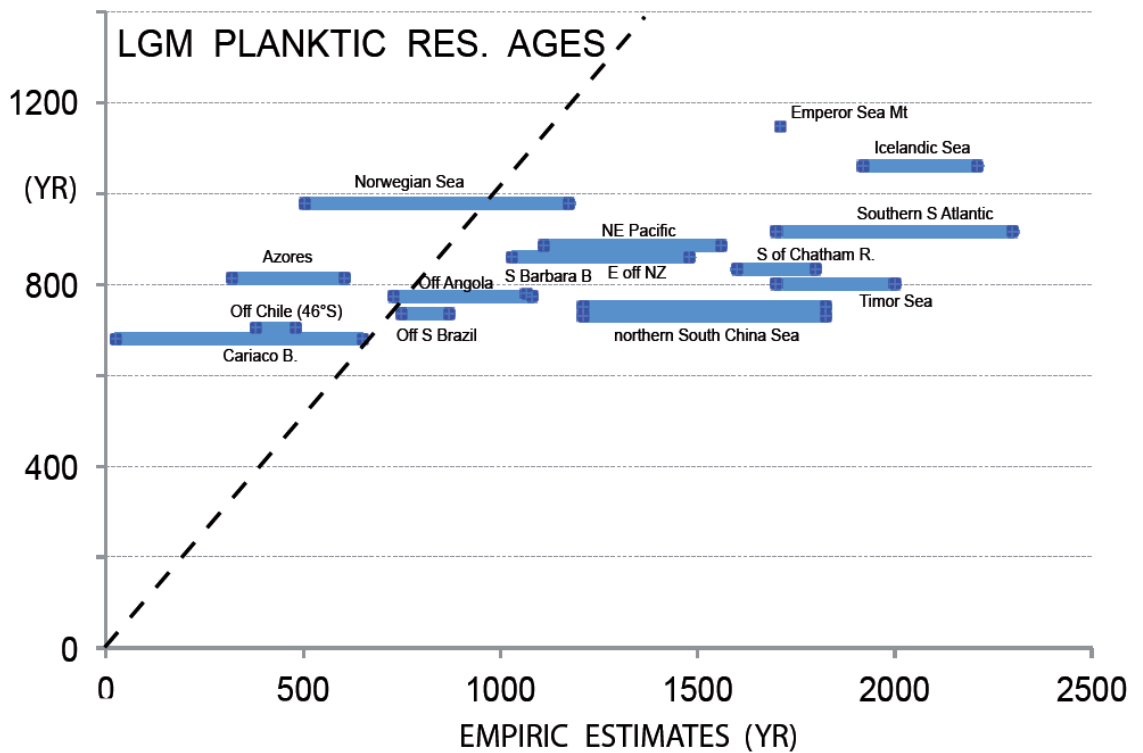
1381

(c) **EMPIRIC minus Muglia MODEL RESERVOIR AGES (yr) of LGM S.W.**



1382

(d) **MODEL ESTIMATES**



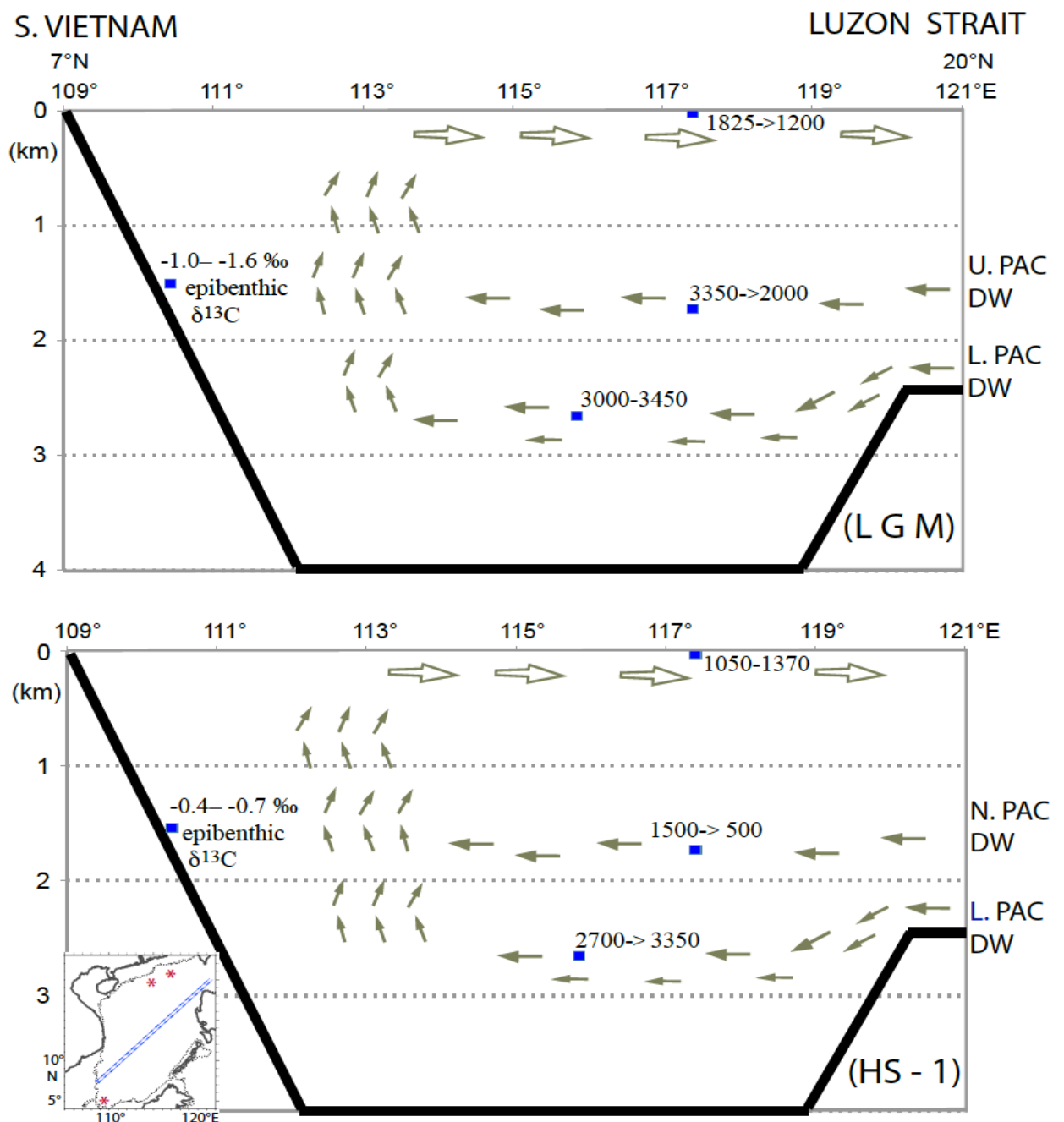
1383

1384

1385 √ Fig. 9. SW–NE transect of ¹⁴C reservoir age and changes in ventilation age across

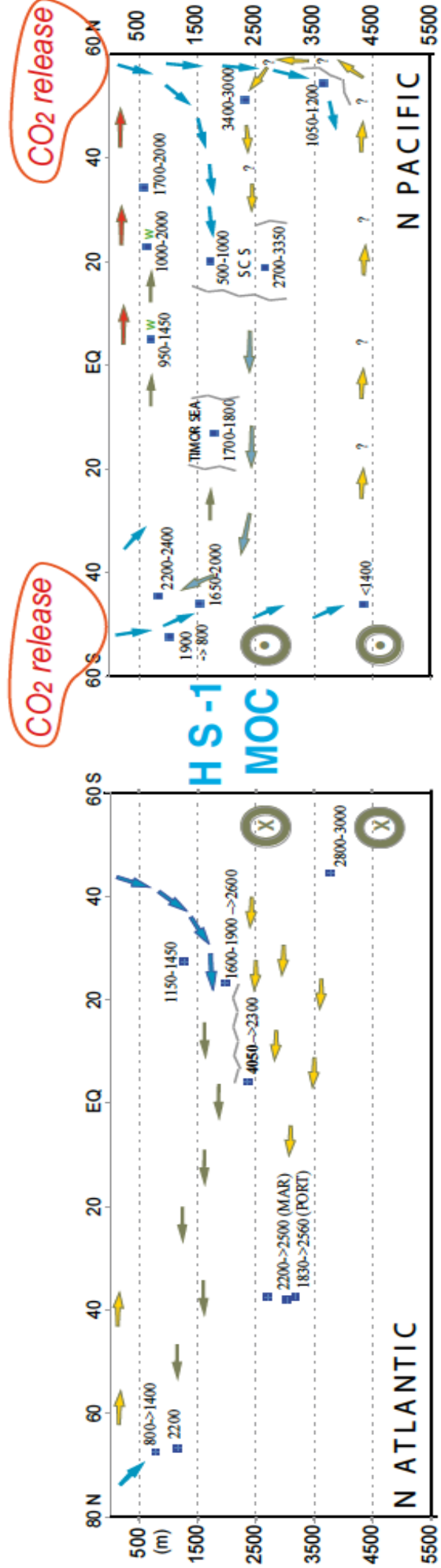
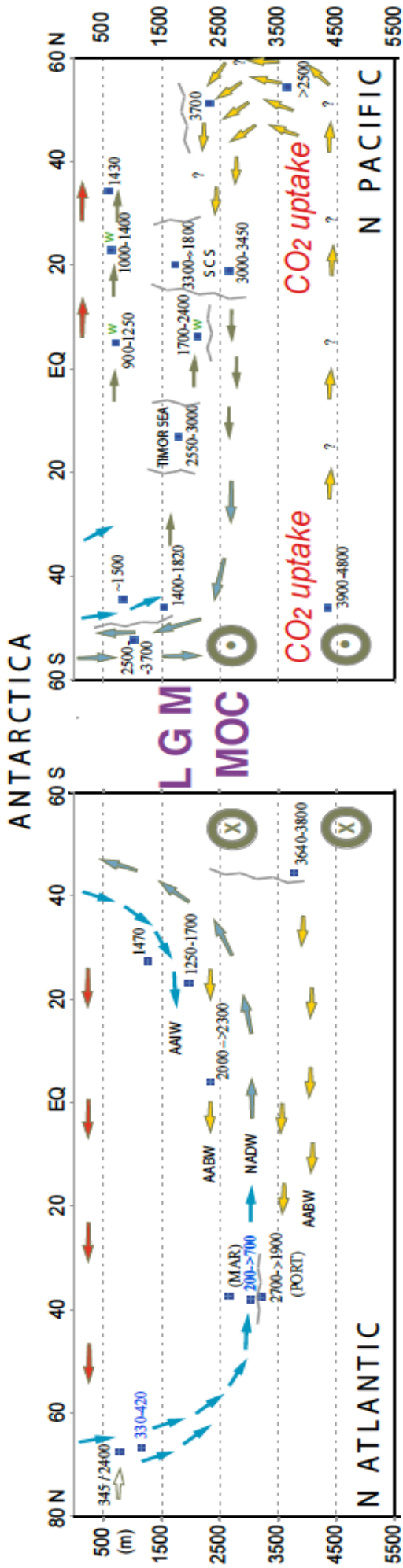
1386 sites GIK17940 and SO50-37 in the South China Sea during late LGM (¹⁴C Plateaus 5

1387 and 4; upper panel) and HS-1 (lower panel). Insert map shows location of transect and
 1388 core locations. Core locations are given in Fig. 7. An extreme epibenthic $\delta^{13}\text{C}$ minimum
 1389 in far southwest (Core GIK17964; Sarnthein et al., 1999) reflects an LGM incursion of
 1390 Lower/Upper Pacific Deep Waters (L./ U. PAC DW) with extremely high ^{14}C ventilation
 1391 age and DIC enrichment in contrast to a low ventilation age of North Pacific Deep Water
 1392 (N. PAC DW). Arrows show direction of potential deep and intermediate-water currents.



1393

1394 √ Fig. 10. 2D transects of the geometries of global ocean MOC. Arrows (blue = high,
1395 yellow = poor ventilation) suggest average deep and intermediate-water currents that
1396 follow the gradient from low to high benthic ventilation ages based on paired planktic
1397 ¹⁴C reservoir ages derived by means of ¹⁴C plateau tuning technique (Sarnthein et al.,
1398 2013, Balmer et al., 2018, Küssner et al., 2020 subm.). Reservoir ages at some Pacific
1399 sites are based on paired ¹⁴C ages of planktic foraminifera and wood chunks (marked
1400 by green 'w'; Sarnthein et al., 2015; Zhao and Keigwin, 2018, Rafter et al., 2018). Red
1401 arrows suggest poleward warm surface water currents. Zigzag lines mark location of
1402 major frontal systems separating counter rotating ocean currents (e.g., W of Portugal
1403 and N of MD07-307; after Skinner et al., 2014). (a) Late LGM circulation geometry,
1404 largely similar as today. Note the major east-west gradient of ventilation ages in the
1405 central North Atlantic, between Portugal (PORT) and Mid-Atlantic Ridge W of Azores
1406 (MAR)). (b) HS-1 benthic ventilation ages reveal a short-lasting MOC reversal leading to
1407 Atlantic-style overturning in the subpolar North Pacific and coeval Pacific-style stratific-
1408 ation in the northern North Atlantic, with seesaw-style reversals of global MOC at the
1409 onset and end of early HS-1 (first proposed by Broecker et al., 1985, however, for LGM
1410 times). Increased ventilation ages reflect enhanced uptake of dissolved carbon in the
1411 LGM deep ocean (Sarnthein et al., 2013), major drops suggest major degassing of CO₂
1412 from both the deep Southern Ocean and North Pacific during early HS-1. – SCS =
1413 South China Sea. AABW = Antarctic Bottom Water; AAIW = Antarctic Intermediate
1414 Water. NADW = North Atlantic Deep Water. Small arrows within age numbers reflect
1415 temporal trends. Many arrows are speculative using circumstantial evidence of benthic
1416 δ¹³C records and local Coriolis forcing at high-latitude sites per analogy to modern
1417 scenarios. Location of sediment cores are given in Fig. 7, short-term variations in
1418 planktic and benthic ¹⁴C reservoir/ventilation age in Suppl. Fig. S2 and Table 3.



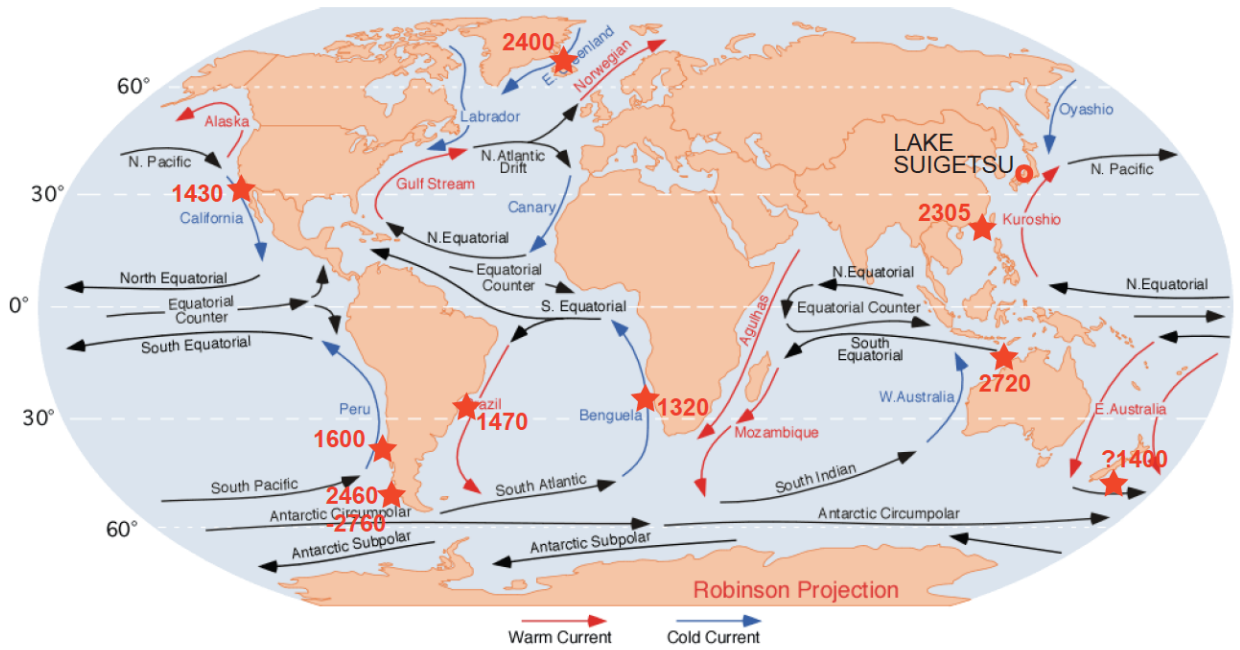
1420

1421 √ Fig. 11. Global distribution of ¹⁴C reservoir ages obtained (a) for late LGM

1422 intermediate waters (100–1800 m w.d.) and (b) for LGM deep waters (>1800 m w.d.,

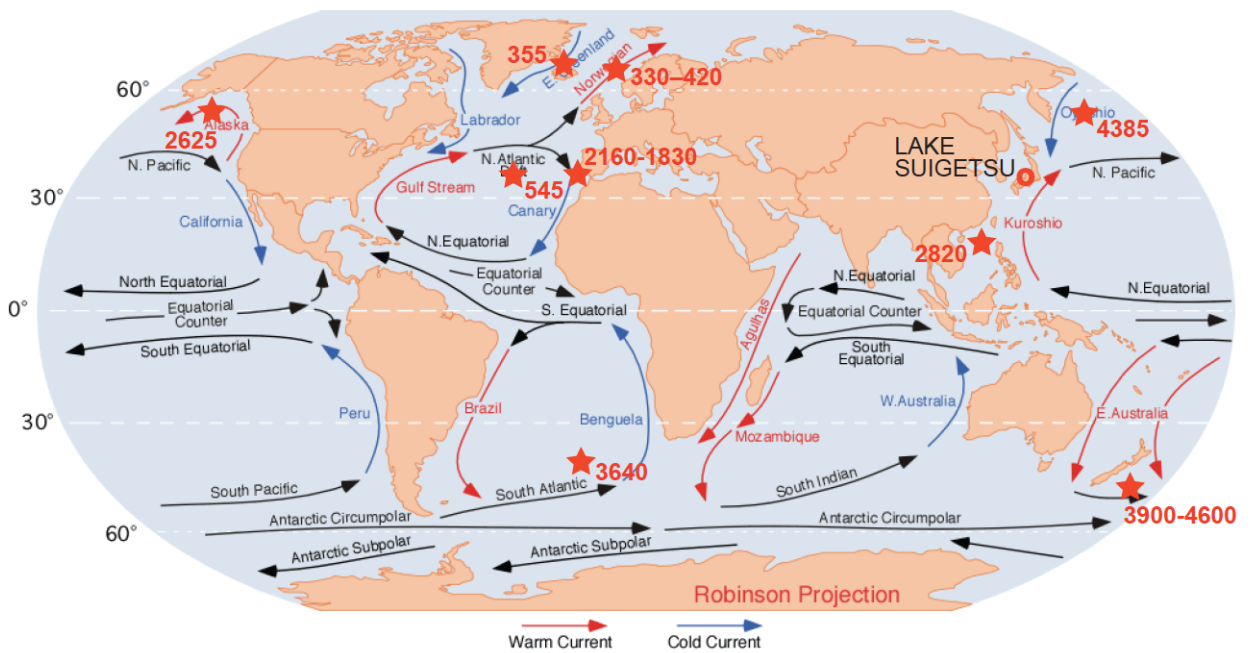
1423 including Site GIK 23074 at 1157 m in the Norwegian Sea).

(a) **EMPIRIC LGM INTERMEDIATE-WATER VENTILATION AGES**



1424

(b) **EMPIRIC LGM DEEP-WATER VENTILATION AGES**



1425

1426

1427 -----

1428 -----

1429 **Supplementary Materials**

1430

1431 *SUPPLEMENTARY TEXT #1. Uncertainties of age control*

1432

1433 Rough estimates of uncertainty and aspects of analytical quality were published by
1434 Sarnthein et al. (2007, 2015). We now focus on uncertainties tied to the calendar age
1435 definition for each ^{14}C plateau boundary both in the Suigetsu atmospheric and the
1436 various marine sediment records (Table 1). To recap, an age/sediment section is
1437 formally defined as containing a ' ^{14}C plateau', when ^{14}C ages show almost constant
1438 values with an overall gradient of <0.3 to <0.5 ^{14}C yr per cal. yr (based on visual
1439 description and/or statistical estimates by means of the 1st derivative of all
1440 downcore changes in the ^{14}C age – calendar age relationship; Sarnthein et al., 2015)
1441 and a variance of less than ± 100 to ± 300 ^{14}C yr, and up to 500 ^{14}C yr prior to 25 cal. ka.
1442 Here ^{14}C ages form a plateau-shaped scatter band with up to 10% outliers, that extends
1443 over more than 300 cal. yr in the Suigetsu record and/or equivalent sections of marine
1444 sediment depth (following rules defined by Sarnthein et al., 2007).

1445

1446 On visual inspection a plateau boundary is assigned to the break point between the low
1447 to zero or reversed slope of a ^{14}C plateau and the normally high regression slope of the
1448 ^{14}C concentration jump that separates two consecutive plateaus (Figs. 1 and S1). More
1449 precisely, a boundary marks the point, where the ^{14}C curve exceeds the scatter band of
1450 the plateau either crossing the upper or lower envelope line. Thus, the boundary is
1451 chosen about halfway between the last ^{14}C age within a plateau band and the next
1452 following age outside the scatter band (Figs. 1 and 2). **On the** U/Th-based model age
1453 scale (Bronk Ramsey et al., 2012) most ^{14}C dates of the Lake Suigetsu section are

1454 spaced at intervals of <10–60 yr from 10 to 15 cal. ka and 20–140 yr between 15 and 29
1455 cal. ka (Fig. 1). Thus the uncertainty of a plateau boundary age assigned halfway
1456 between two ¹⁴C ages nearby inside and outside a plateau's scatter band would, on
1457 average, amount to ±10–±70 cal. yr.

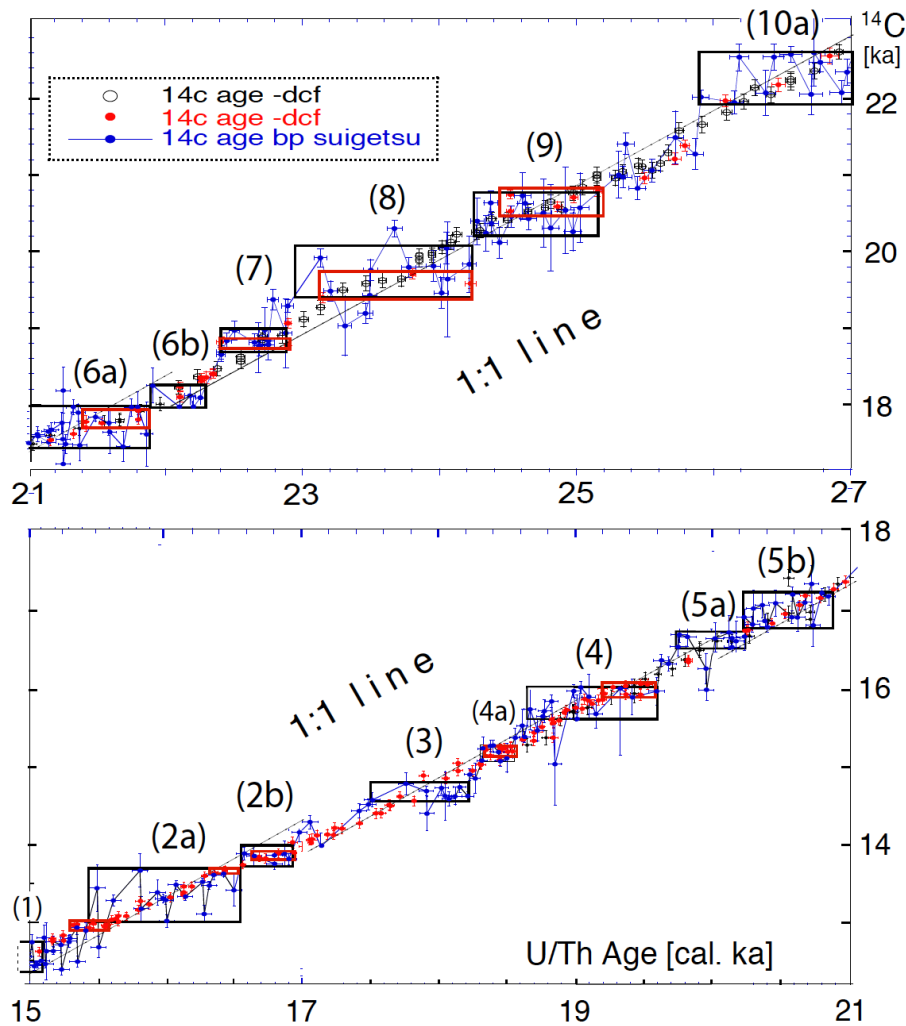
1458

1459 In principle, the calendar age uncertainties of marine ¹⁴C plateau boundaries are treated
1460 likewise: After being tuned to those in the Suigetsu ¹⁴C record, the uncertainties are
1461 deduced for the position of all plateaus of a suite within the uncertainty envelope of the
1462 U/Th model-based age calibration. Hence the estimates of total age uncertainty present
1463 the propagated error of the calibrated age of a Suigetsu plateau boundary plus that of
1464 the pertinent plateau in the marine record, where variable depth spacing of ¹⁴C ages is
1465 converted into average time spans.

1466

1467 SUPPLEMENTARY FIGURE CAPTIONS

1468 √ Fig. S1. Individual atmospheric ¹⁴C ages and error bars of Lake Suigetsu plant
1469 macrofossils vs. U/Th-based model age of 15–21 (bottom) and 21–27 (top) cal. ka (blue
1470 dots; Bronk Ramsey et al., 2012). ¹⁴C plateaus longer than 250 yr are outlined by a
1471 suite of labeled horizontal boxes that envelop scatter bands of largely constant ¹⁴C
1472 ages. Red dots and black circles in Fig. 1a display ¹⁴C ages of Hulu stalagmites. Similar
1473 to ¹⁴C ages of Suigetsu also those of Hulu Cave reveal a suite of ¹⁴C plateaus (red
1474 boxes) tentatively assigned in this figure, plateaus that are shorter than Suigetsu-based
1475 plateaus and occupy slightly different age ranges. The 1:1 line reflects gradient of one
1476 ¹⁴C yr / cal. yr.



1477

1478

1479 √ Fig. S2. Centennial-to-millennial-scale temporal and spatial variations in planktic (pla.)

1480 reservoir (res.) and (raw = uncorrected) apparent (app.) benthic ¹⁴C ventilation (vent.)

1481 ages recorded at 18/20 key sites in the Atlantic (S2a, b, e), Pacific (S2c, d), and Indian

1482 (S2e). Site locations are given in Fig. 7. Stratigraphic units are marked on top of each

1483 diagram: Younger Dryas (YD), Bølling-Allerød (B/A) Heinrich Stadial 1 (HS-1), Last

1484 Glacial Maximum (LGM), and Heinrich Stadial 2 (HS-2).

1485 *Origin and various features characteristic of ¹⁴C records:* About 50% of all planktic and

1486 ('raw') benthic ¹⁴C records **were** already published in Sarnthein et al. (2015). However,

1487 the cal. age of all records originally based on microscopy-based varve counts was now

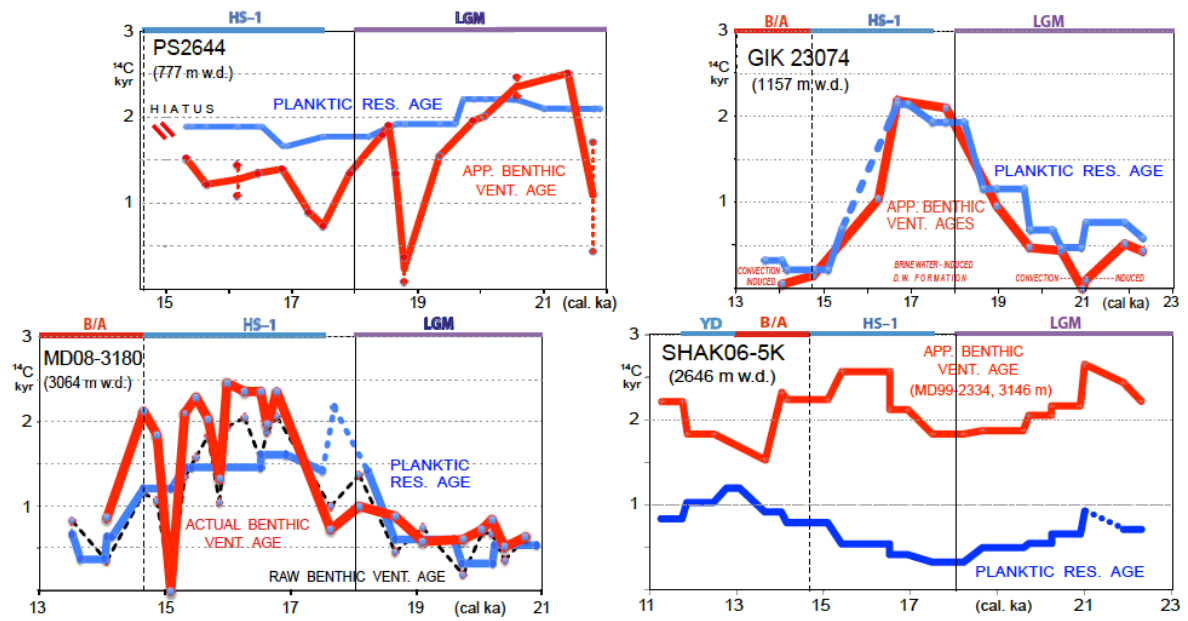
1488 converted into U/Th-based model ages (Bronk-Ramsey et al., 2012). Planktic ¹⁴C

1489 reservoir ages of Core GIK23074 are now supplemented by benthic ventilation ages.
1490 Planktic ^{14}C reservoir ages of SHAK06-5K are detailed in Ausin et al. (2019, unpubl.).
1491 Benthic ventilation ages plotted for SHAK06-5K are matched from neighbor core MD99-
1492 2334K (Skinner et al., 2014) the stratigraphy and ^{14}C reservoir ages of which are closely
1493 correlated by means of narrow-spaced suites of ^{14}C ages. To show an example, 'raw'
1494 benthic ventilation ages in Core MD08-3180 are recalculated into 'actual' ventilation
1495 ages (Balmer and Sarnthein, 2018) that incorporate past changes in atmospheric ^{14}C
1496 concentration between the time of deep-water formation and the local growth of benthic
1497 foraminifers. South Atlantic ^{14}C records GeoB3910, GeoB1711-4, and KNR-159-5-36
1498 (data slightly supplemented) are from Balmer et al. (2016), now however, with cal. ages
1499 converted into U/Th based model ages. The same applies to MD07-3076, where the
1500 continuous planktic and benthic ^{14}C records are from Skinner et al. (2010), corroborated
1501 by three blue bars reflecting the extent of planktic ^{14}C plateaus tuned to atmospheric
1502 plateaus no. 1, 2b, and 4. South Pacific ^{14}C records PS75-104, SO213-76, MD07-3088,
1503 and PS97-137-1 are from Küssner et al., 2018 and **subm.**). Planktic and benthic ^{14}C
1504 records of neighbor cores GIK17940 and SO50-37, PS75-104 and SO213-84, and
1505 ODP893A and MD02-2503 each are plotted on joint graphs, paired records that are
1506 obtained from small-scale sea regions with a common level of planktic ^{14}C reservoir
1507 age. Benthic ^{14}C ages of SO50-37 and SO213-84 are from Ronge et al. (2016), those of
1508 MD07-3088 from Siani et al. (2013).

Fig. S2a. NORTH ATLANTIC AND NORDIC SEA SITES

WEST and CENTER —

— EAST



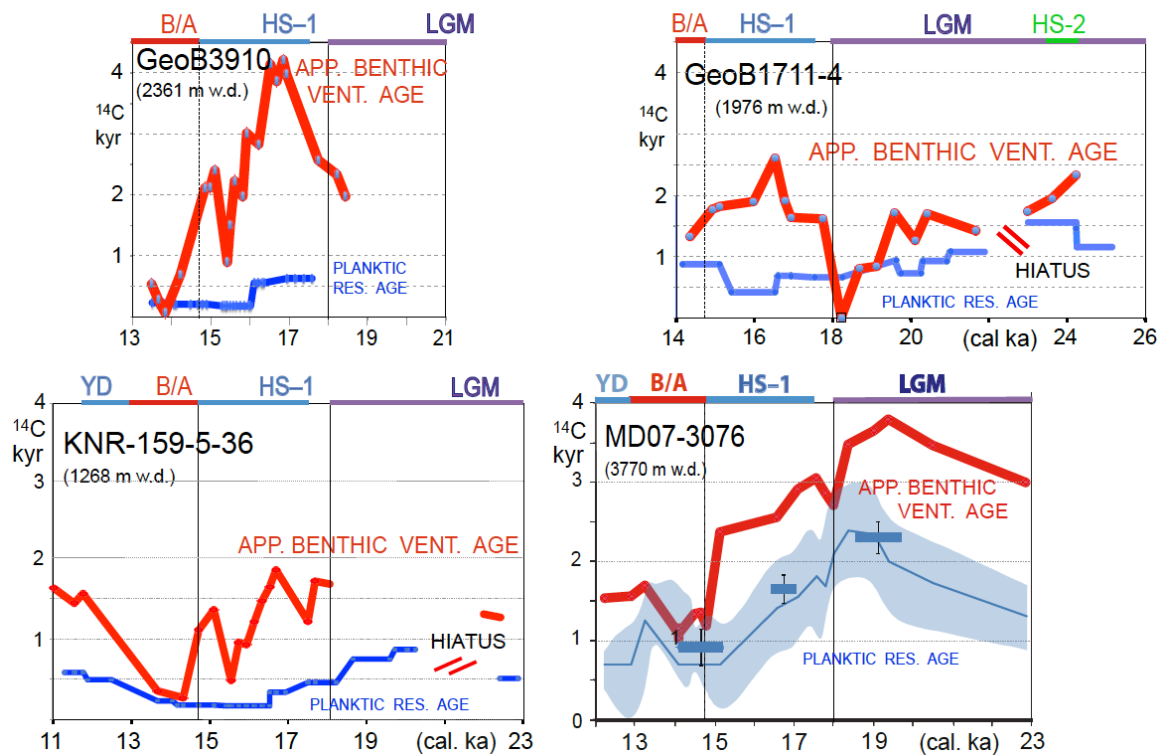
1509

1510

Fig. S2b. SOUTH ATLANTIC SITES

WEST —

— CENTER and EAST



1511

1512

Fig. S2c. SOUTH PACIFIC SITES

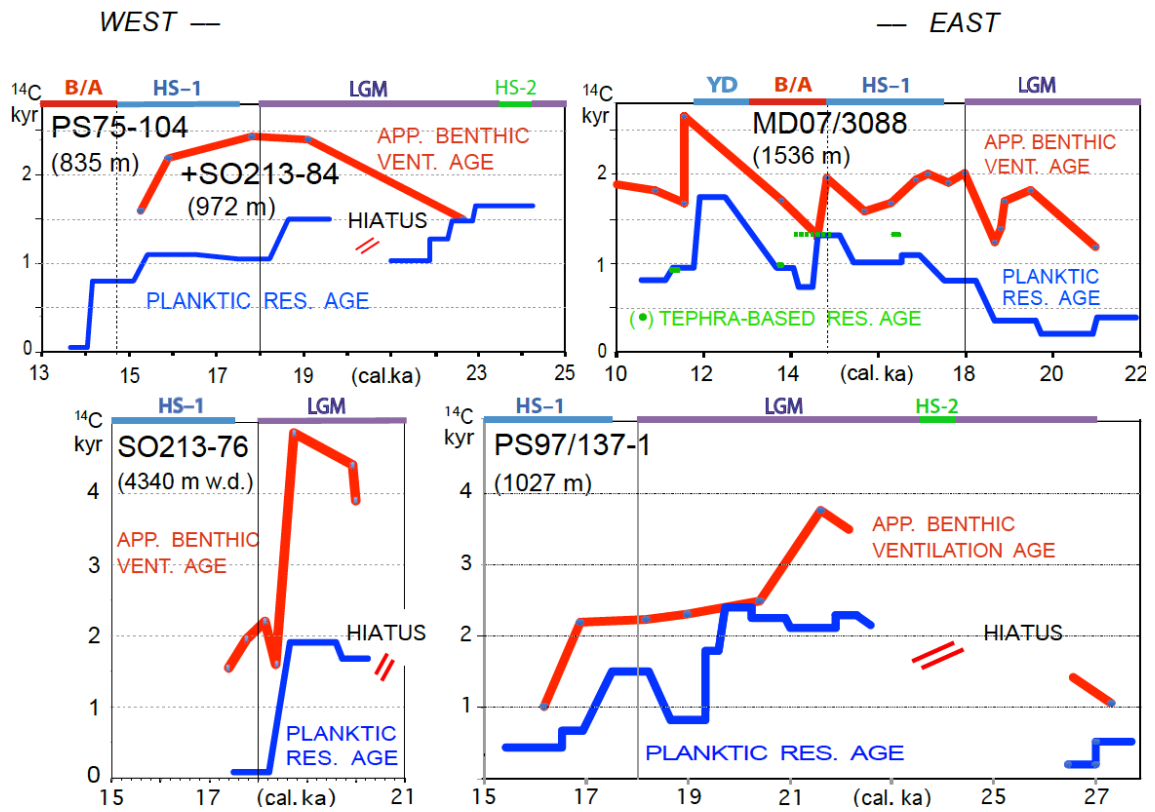
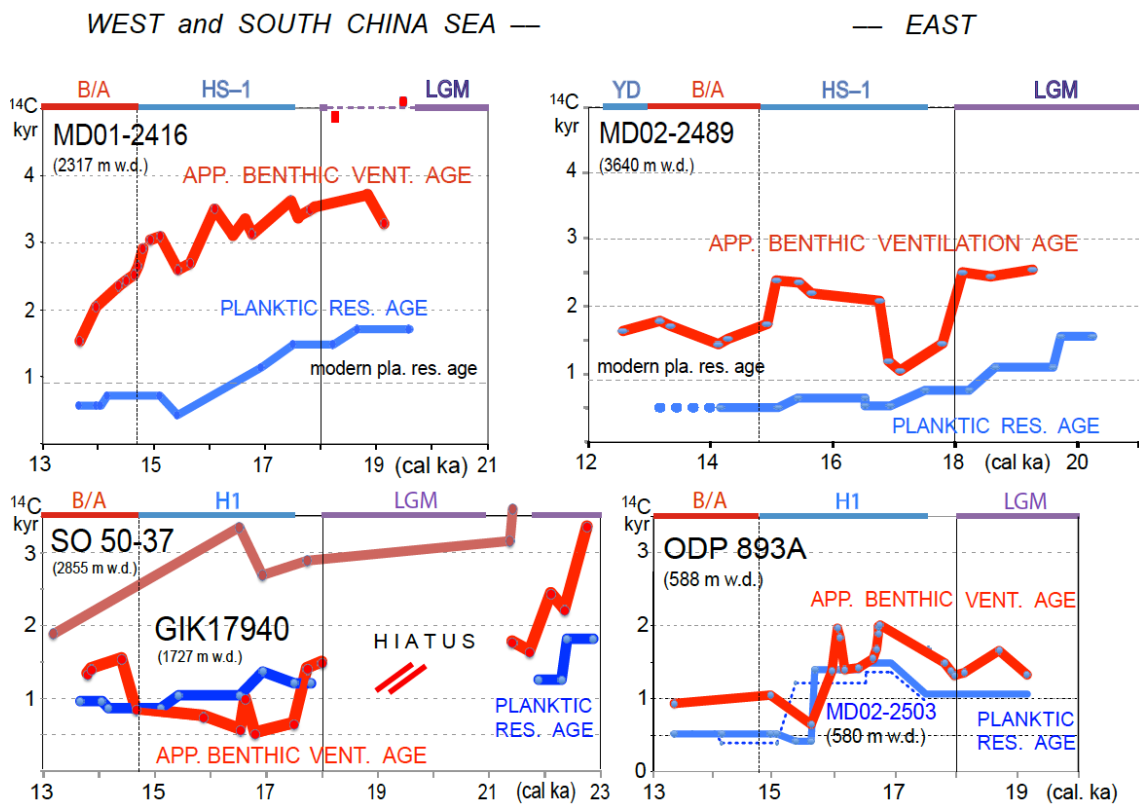


Fig. S2d. NORTH PACIFIC SITES

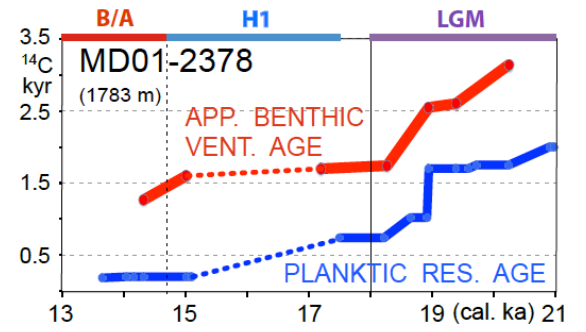
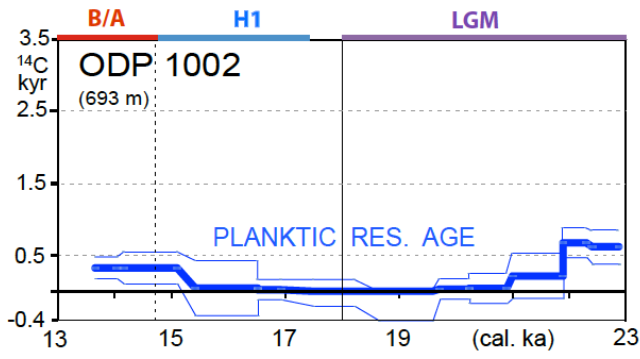


1516

Fig. S2e. SITES in the EQUATORIAL OCEAN

CARIACO BASIN —

— SOUTHERN TIMOR SEA



1517

1518

1519